The Development of a Highly Insulated, Thin Wall Assembly for Canadian Residential Construction

by

Peter Svidler, B.Eng., Dalhousie University, 2019.

A thesis submitted to the Faculty of Graduate and Postdoctoral Affairs in partial fulfillment of the requirements for the degree of

Master Of Applied Science

In

Sustainable Energy Engineering and Policy

Carleton University

Ottawa, Ontario

Abstract

The Canadian buildings sector is responsible for 13% of greenhouse gas emissions in Canada. As such, mandatory and voluntary building codes are becoming increasingly stringent on requirements for highly insulated wall assemblies to reduce building heating loads, thereby reducing emissions. However, traditional means of insulating a wall significantly increase its thickness and in scenarios where the building's footprint is constrained this causes a decrease in indoor living space and a reduction in the home's market value. To address this, this thesis proposes thin, highly insulated wood-frame wall assemblies which incorporate highly performing insulation materials. A variety of such novel wall assembly designs are developed and modelled for thermal performance. Three of these designs are tested using the guarded hot box method described in ASTM C1363. It is found that the proposed wall assembly designs provide sufficient thermal performance with little increase in wall thickness compared to traditional wood-frame walls.

Acknowledgements

I would like to extend my profound thanks for their support on this endeavour to all of my colleagues at Carleton University's Centre for Advanced Building Envelope Research (CABER). In particular, I would like to thank Cynthia Cruickshank, my thesis supervisor, and Christopher Baldwin, CABER's Project Manager, for their steadfast support and commitment to my academic and professional development. I would also like to thank Liam Jones and Tait Seguin, who assisted me throughout the experimental phase of the research, and Mark Carver of Natural Research Canada who supported this project from the very beginning. Thank you also to all those who participated in the charette meetings which culminated in the wall concepts presented here.

I could not accomplish what I have without the infinite support and love I have received from my wife Jen, my family, and my best friends Pipo and Earl Grey.

Table of Contents

List of Tables

List of Figures

Nomenclature

Symbol	Units	Description
A	m^2	Area
E	Wh	Heat Input
h	W/m^2K	Convection Coefficient
k	W/mK	Thermal Conductivity
N	-	Number
R_{eff}	m^2K/W	Effective Thermal Resistance
RSI	m^2K/W	Thermal Resistance
r	mK/W	Thermal Resistivity
T	°C	Temperature
t	h	Time
V	mV	Voltage
x	cm	Wall Thickness

Subscript	Description
avg	Average
C	Cold Surface
eff	Effective
H	Hot Surface

Acronym	Description
ASTM	American Society for Testing and Materials
CJC	Cold Junction Compensation
DAQ	Data Acquisition Device
EPD	Environmental Product Declaration
EPS	Expanded Polystyrene Insulation
GFP	Gas Filled Panel
GPS	Graphite Polystyrene Insulation
GWP	Global Warming Potential
ISO	International Organization for Standardization
SDS	Safety Data Sheet
NBC	National Building Code of Canada
NECB	National Energy Code of Canada for Building
NRCan	Natural Resources Canada
OC	On Centre
OSB	Oriented Strand Board
Polyiso	Polyisocyanurate Insulation
PUR	Polyurethane Insulation
SPF	Spruce-Pine-Fir
TC	Thermocouple
TP	Thermopile
VIP	Vacuum Insulated Panel
XPS	Extruded Polystyrene Insulation

1. Introduction

The following chapter provides an introduction to the research conducted as part of this thesis. This introduction includes the motivation which inspired this research, background knowledge essential to the understanding of the topics discussed throughout the thesis, the underlying objectives which framed the research presented, and an overview of the layout of the thesis as well as the methodology used to reach these objectives.

1.1 Motivation and Background

The underlying motivation for the research presented in this thesis is to resolve an incongruency between the needs of society and the interests of residential construction developers. On the one hand, as a society and a nation, we would like to see a reduction in the greenhouse gas emissions produced by the construction and operation of our homes. On the other hand, developers would like to build homes which maximize the floorspace provided in each housing unit, as it is a significant determinant for the price they are able to charge for each home. In the following two sections, both of these desires are further explained, the apparent incompatibility between them is made clear, and it is shown how high performance, thin walls can help bridge the divide.

1.1.1 Reduction of Residential Building Operational Emissions

Over the past several years, the human-caused climate crisis has become abundantly clear, and impossible to ignore. With environmental disasters like those climate scientists have been warning about occurring increasingly more frequently, and their consequences becoming more painful for many Canadians to bear, there is now broad nation-wide consensus that something must be done to curb national greenhouse emissions [1]. With both federal and provincial politicians attuned to this desire, many roadmaps have been drawn to chart the course towards a state of net-zero

emissions in the coming decades [2]. Given the enormous impact our buildings – the spaces we live, work, and congregate in – have on national emissions, it is unsurprising that reductions in their emissions play a central role in these roadmaps.

Canadian homes play a large role in contributing to national greenhouse gas emissions, with most of these emissions associated with the heating of space [3]. Canada's winters are cold, and adequate space heating in homes is essential for both the wellbeing and the comfort of occupants. Many approaches have been proposed to reduce the emissions associated with space heating in homes while still maintaining adequate indoor temperatures, with several of those approaches discussed in Section 2.1. One essential solution is the improvement of the thermal insulation of homes, which would trap more heat inside, thereby requiring less space heating. This approach has the added benefits of reducing the cost of heating and reducing the amount of cooling needed to maintain a comfortable indoor environment in the summer months.

Although windows, doors, roofs and foundation elements all contribute towards a home's degree of thermal insulation, as the biggest component of a typical home's surface area – and heat transfer being proportional to surface area and insulating level – walls play an enormous role in a home's overall thermal barrier [4]. Any improvement in a wall's thermal resistance value will thus have a consequential effect on reducing the emissions associated with the heating of the home. Such improvements necessarily require the addition of thermal insulation materials to the wall assembly, and these materials most often rely on large volumes to reduce the transmittance of heat; that is, the thicker a wall is, generally, the better it is at keeping indoor heat. For example, adding 10 cm of expanded polystyrene (EPS) insulation to the walls of a typical home in Ottawa whose half of the exterior surface area is made up of walls will reduce that home's heat losses (and thus emissions associated with space heating) by nearly 25%. This simple illustrative example assumes a home

with a whole-envelope thermal resistance value of 4.05 m·K/W (R-23) and EPS insulation with thermal resistivity of 25.0 m^2·K/W [1].

1.1.2 Reduction in Floorspace Loss due to Thick Wall Assemblies

The aforementioned approach may seem like an appealing way to reduce the costs and emissions associated with space heating, especially when considering that EPS insulation only costs about CAD$6.73 per square metre for 2.5 cm thick insulation in June 2022 [5]. Unfortunately, the issue not represented in this assessment is the fact that adding this insulation necessarily increases the thickness of each wall. If the lot that this home is built on is much larger than the space occupied by the building, this would not be an issue; the walls of the home could simply be extended further out, increasing the home's overall size. However, with developers increasingly employing tract building techniques to increase floorspace as much as possible, whereby each home occupies as much area of the lot it sits on as is permitted by local setback by-laws (this is shown illustrated in Figure 1-1), increasing the thickness of the walls would come at the expense of interior floorspace.

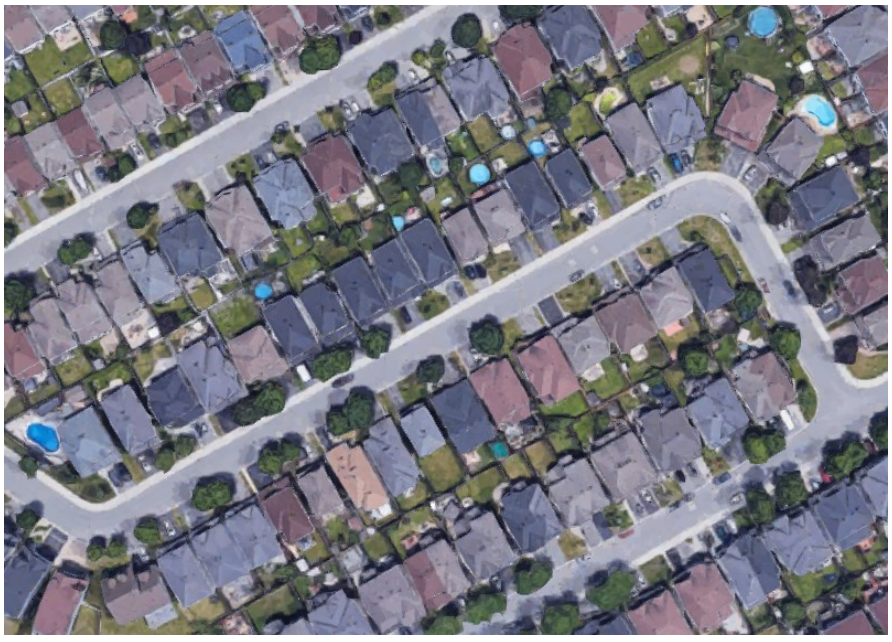

Figure 1-1: Tract Built Homes in Ottawa's Barrhaven Neighbourhood (Photo: Google Maps)

If, for example, the home in question had two storeys and an 8.6 m^2 footprint (and hence 1600 square feet of floorspace, the average for a home in Ottawa [6]), adding 10 cm of insulation to each wall – without increasing the home's external footprint – would reduce the home's floorspace by 7.0 m^2, or 75 square feet. With the cost per square foot of floorspace of single detached homes in Ottawa being CAD$282 in August 2019 [6], this would mean that the value of the home could be reduced by as much as CAD$21,150. Residential construction developers, who presumably aim to maximize their profits from the sale of each home, are thus clearly disincentivized from building walls any thicker than absolutely required by building codes. This often leads to reduced wall insulation, leaving homes which are less capable of retaining interior heat, leading to increased heating requirements and higher emissions.

1.1.3 Maximizing Floorspace While Reducing Heat Loss

A way to reduce heat emissions while maximizing floorspace is to design wall assemblies which are highly thermally insulated but are also as thin as possible. To accomplish this, materials which are highly thermally resistive – that is, their thermal conductivity per unit thickness is very low – must be effectively employed, accomplishing an elimination of thermal bridges while occupying as much of the wall's volume as possible. Simultaneously, the other functions of the wall must still be considered.

In Canada, low-rise residential buildings are most often built with softwood lumber in a practice known as platform framing. An example of a typical Canadian home under construction, showing its lumber framing walls, is shown below in Figure 1-2. These walls, built of many individual lumber framing pieces, must accomplish the structural requirements of the building, including the support of upper floors and of wall cladding features, while also allowing for sufficient space for insulation materials within them. Some approaches to minimizing the volume occupied by these

structural members have been proposed, and they are discussed in more detail in Section 2.3. Due to their widespread use throughout Canada for residential construction applications, wood-frame walls form the focus of the investigation presented in this thesis, and Chapter 4, which focuses on the development of innovative wall assembly designs, builds upon common practices in wall framing in Canada today.

Figure 1-2: Typical Wood-frame Residential Construction in Ottawa (Photo: Jordan McNally)

1.2 Research Objectives

The overarching goal of the research presented in this thesis is to contribute towards the design of a practical wall assembly for Canadian residential wood-frame construction. This wall incorporates nascent, high performance insulation materials and achieves a high degree of thermal performance, thereby reducing the environmental costs associated with the heating and cooling of the home. Such an approach maintains a thin profile which does not appreciably reduce interior floorspace and is thereby attractive for builders and developers.

This overall objective is reached by focusing on a research scope which encompasses the initial design stages of the wall assembly. Within this scope, the following research objectives are met:

- Identify high-performance nascent insulation materials which are suitable for residential construction based on a set of criteria developed in consultation with a group of industry experts including researchers, builders, and materials experts.
- Propose novel wall assembly designs which incorporate these nascent insulation materials and present these wall assemblies to industry experts for their feedback.
- Model the hygrothermal performance of the proposed wall assemblies using common finite element methods to estimate their effective thermal resistances and moisture control capabilities in a variety of Canadian climates.
- Validate the thermal performance of select wall assemblies using an industry-standard experimental procedure. Use the results obtained from the experimental procedure to calibrate the thermal models of the wall assemblies proposed.
- Based on knowledge and experience gained, propose recommendations for future work which will continue to advance the design of thin, high performance wall assemblies until they are able to be incorporated into the construction of homes across the country.

1.3 Thesis Layout and Methodology

This thesis document contains eight chapters which discuss all the work completed. The topic of each chapter is as follows:

- **Chapter 1 – Introduction**

  An outline of the motivations and objectives of the work conducted, as well as background into the relevant fields discussed in this thesis.

- **Chapter 2 – Literature Review**

  A review of important literature and the identification of gaps in research related to the building science topics discussed in this thesis.

- **Chapter 3 – Material Selection**

  A discussion of the work conducted in identifying nascent high-performance insulation materials of interest, how these materials were evaluated for potential integration in residential wood-frame construction applications, and the rationale for selecting three materials for further research.

- **Chapter 4 – Wall Concept Development**

  This chapter outlines how novel wall concepts were developed to incorporate the insulation materials selected in the previous chapter. Each of these wall concepts is described in detail and the rationale for their design is discussed.

- **Chapter 5 – Hygrothermal Performance Modelling**

  Using software tools, the wall concepts developed in the previous chapter are modelled to get a better understanding of their thermal and hygric performance. These software tools are discussed in detail, and the advantages of hygrothermal modelling of building envelopes are discussed.

- **Chapter 6 – Thermal Performance Experimental Validation**

  Three of the wall concepts developed are selected for further experimental testing based on the guidance of a panel of industry experts. The testing conducted is based on ASTM C1363.

- **Chapter 7 – Results and Analysis**

  The results, consequences, and feasibility of the experimental validation experiment are presented and compared to the results of the hygrothermal modelling.

- **Chapter 8 – Conclusion and Further Work**

  Concluding remarks are made regarding the research presented in this thesis, key findings of the research are restated, and recommendations are made for future work to continue based on the research conducted.

The methodology and process followed throughout this research is shown on the following page in Figure 1-3. After a literature review was conducted to identify gaps in knowledge in the field, a charette was conducted with industry experts, including builders, insulation material manufacturers, and members of governmental agencies, to identify key material selection criteria. Based on these selection criteria, insulation materials of interest were identified and rated. Top-performing insulation materials were chosen to be integrated into wall assemblies which were designed and presented at a second design charette. The performance of these assemblies was evaluated using hygrothermal modelling methods, and top-performing assemblies were assembled and undergone thermal testing. The results of these tests were then used to calibrate the hygrothermal models. Based on this process, recommendations are made for future work and development of thin, highly insulated wall assemblies.

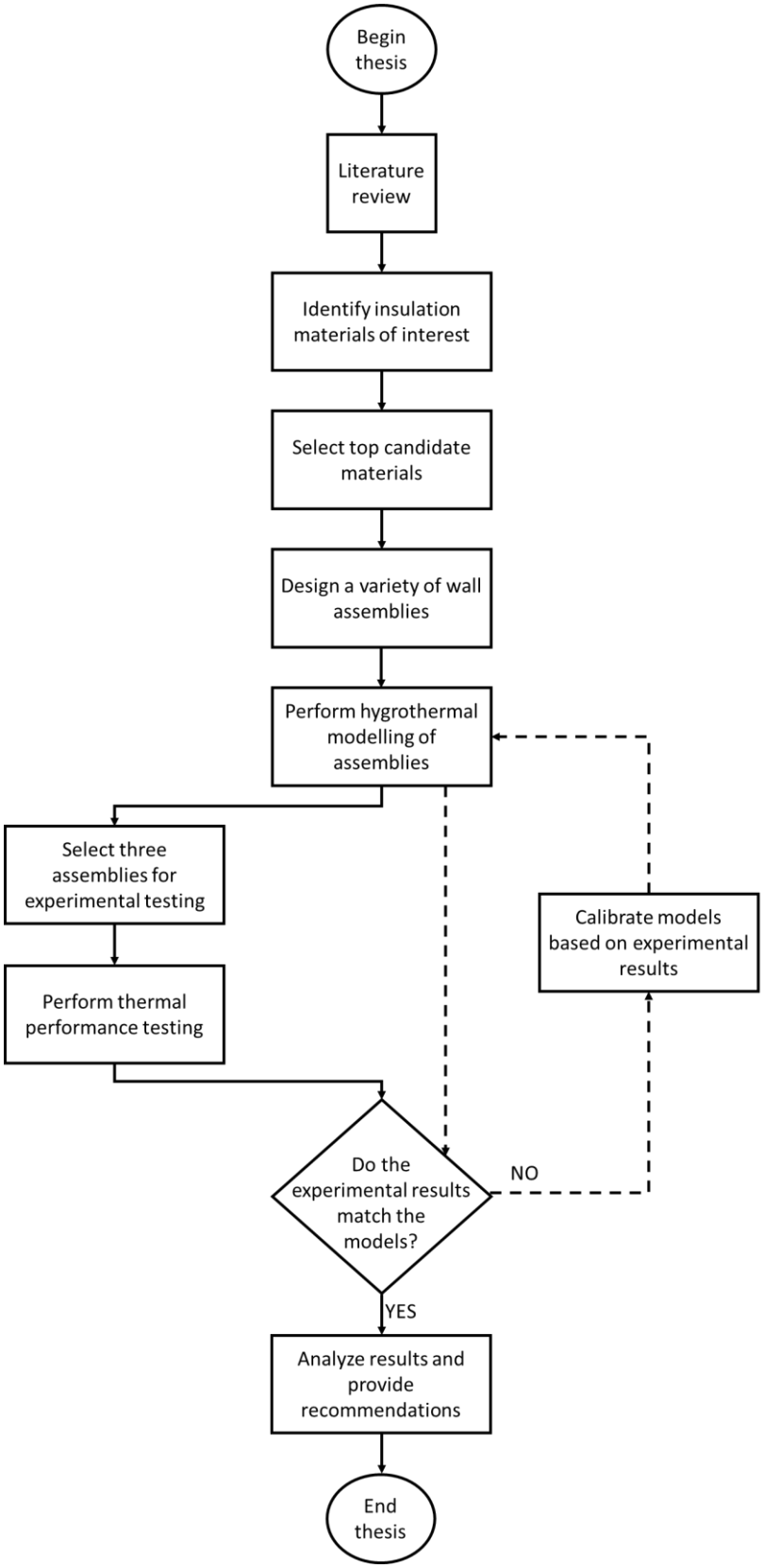

Figure 1-3: Research Methodology and Process

2. Literature Review

The following literature review explores a diverse range of academic and professional work related to the topics discussed in this thesis. It begins with background on the impact which Canadian buildings and their operation have on the ongoing climate crisis, and the role building envelopes play in reducing this impact. The building codes which determine how our buildings are built and to what performance criteria, are then discussed. The focus is then shifted to wood-frame residential buildings in Canada, and what practices and techniques are utilized during their construction. Common wall insulation practices are then discussed, as well as state-of-the-art innovations to these practices. The tools used to model and test innovations in wall assembly design – both numerically and experimentally – are discussed, including the tools used in this work. Finally, based on the information gathered in this literature review, gaps in literature are identified so that they can be addressed in this thesis.

2.1 The Need for More Sustainable Buildings

In recent years, the impact of the buildings sector on global greenhouse gas emissions has received significant attention from industry. It was estimated by the United Nation's Global Alliance for Building and Construction that the construction of buildings and their maintenance account for roughly 37% of overall human-caused greenhouse gas emissions [7]. In Canada, Environment and Climate Change Canada estimates that buildings account for 13% of national emissions, the third largest overall contributor of emissions and behind only the oil & gas and transportation sectors [8]. The success of Canada's goal of reaching net-zero emissions by 2050, as outlined in the 2030 Emissions Reductions Plan [2], is therefore highly dependent on significantly reducing the environmental impact of buildings.

Greenhouse gas emissions associated with the buildings sector can generally be divided into two categories. The first is known as embodied carbon and refers to the greenhouse gas emissions associated with the construction or retrofitting of a building. These emissions are largely due to the manufacturing of the building materials eventually used in construction [9]. The sources of embodied carbon in building materials – and specifically insulation materials – are discussed in Section 3.1.4. The second is known as operational carbon, and it accounts for the emissions associated with the general operation and maintenance of an existing building over its lifetime [10]. In Canada and in the residential context in particular, the largest contributor by far to operational carbon emissions is the heating of indoor space [3].

Reductions in the emissions associated with space heating can be accomplished in one of two broad ways. First, one could focus on improving the method of heating used. This can be accomplished by improving the efficiency of the heating system as has been done in recent decades with high efficiency gas boilers [11], thereby reducing the amount of fossil fuel needed to accomplish an equivalent level of heating. In regions where the electrical system has low emissions intensity, improvements in heating method can also be accomplished by choosing an electric heating system. This is especially true of high efficiency heat pump systems, which employ a thermodynamic heat pump cycle to achieve more heating than electrical energy required [12]. Continuous improvements in heat pump technology, and in particular improvements in their cold weather efficiency, have made them an attractive option for space heating in Canada [12].

The second approach to reducing emissions associated with space heating is by reducing the amount of heating needed altogether. This can be accomplished with smart occupancy controls which use computational technology to assess when and how much heating is really needed [13], or by improving the building envelope by either increasing thermal insulation or by improving

airtightness so that more heat remains in the conditioned space for longer [4]. It is these envelope improvements, and in particular improvements to wall assemblies, which are the focus of this thesis.

2.2 Building Envelopes and Performance-Based Building Codes

A building's envelope refers to all which separates the indoor environment from the outdoor, including windows, doors, walls, roof, and foundation. A building's envelope serves as three different types of barriers between the outdoor and the indoor. First, the envelope serves as an air barrier; undesired mixing of indoor and outdoor air, a large contributor to thermal energy loss in buildings, is reduced by designing airtight envelopes with careful elimination of air infiltration pathways [14]. Second, the envelope serves as a water and moisture barrier, preventing exterior water sources from infiltrating into the home. Beyond just preventing water ingress, building envelopes must also be carefully designed in a manner which reduces the likelihood of the envelope itself being damaged by moisture, whether from the outdoors or indoors [15]. Finally, the building envelope also serves as a thermal barrier, offering insulative properties, which reduce the loss of heat energy from the indoor heated environment to the outdoors during cold weather.

As the primary thermal barrier, as well as a large source of embodied carbon during construction and retrofit [16], the building envelope plays a critical role in achieving reductions in building emissions. This fact has not been ignored by regulatory agencies throughout the world and in Canada, who in recent years began to codify minimum performance criteria for envelope elements within building codes. In Canada, the primary codes document to spearhead improvements in envelope performance is the National Energy Code of Canada for Buildings, or the NECB [17]. First published in 1997 and most recently updated in 2020, the model building code sets out technical requirements for the energy efficient design and construction of new buildings [17]. As

a model code, the NECB has no legal status until it is adopted, in full or with revisions, by jurisdictions across Canada, most notably by the individual provinces and in some cases, specific municipalities.

Although each subsequent revision of the NECB increases the performance requirements for building envelopes, to ensure that new construction remains affordable to build, the code must also balance feasibility. Therefore, the performance requirements prescribed within it are well within what is attainable with regular construction practices. For example, the thermal performance requirement prescribed in the 2020 NECB for above-grade walls in climate zone 6 (4000-4999 heating degree days), the climate zone Ottawa is in, is 4.05 $m^2 \cdot K/W$ (R-23) [17]. This is well below the effective thermal resistance typically achieved by high performance walls, which can exceed 7.04 $m^2 \cdot K/W$ (R-40) [18]. In cases where such high-performance targets are achieved, builders typically follow a voluntary building code.

Several of these voluntary codes apply for residential construction and regularly followed in Canada. These include R-2000, Passive House, and NetZero Ready. R-2000 is a voluntary technical standard developed by Natural Resources Canada (NRCan) and launched in 2013 [19]. It outlines environmental responsibility, air quality, and energy efficiency requirements for new residential construction, and requires builders to undergo regular training and certification to be kept up to date on the continuously evolving standard. Homes certified to the R-2000 standard can expect energy consumption levels lower than 50% of an equivalent code-built home [19]. Passive House, also known as Passivhaus, is an energy-based voluntary standard originally developed in Germany and maintained in Canada by Passive House Canada, a non-profit organization [20]. Considered to be highly rigorous, this standard requires that heating loads for a home must not exceed 15 kWh per metre squared of floorspace, in addition to a stringent air infiltration

standard [20]. Finally, NetZero is a voluntary code currently being developed by NRCan in partnership with industry partners. This code is building upon, and a continuation of the R-2000 program with even more stringent performance-based requirements; homes certified to the NetZero standard can only consume as much energy as can be produced by renewable sources on-site [21].

2.3 Wood-frame Residential Construction

In Canada, the vast majority of single-family homes are built with wood frame construction [22]. These homes are typically built using softwood lumber structural members colloquially known as "sticks". These structural members are typically made of either spruce, pine, or fir wood, hence the material's Canadian Standards Association (CSA) standardization designation – SPF lumber. The CSA also regulates a variety of geometric and material properties for the lumber, to ensure conformity, uniformity, and structural soundness [23]. SPF lumber comes in a variety of sizes, with the most common sizes for residential construction being "two by four", which refers to lumber 38.1 mm thick by 88.9 mm wide, and "two by six", which refers to lumber 38.1 mm thick by 139.7 mm wide.

Modern Canadian wood frame construction adheres to the platform framing method, whereby each floor of a wood frame structure is separately framed (hence, a "platform") and supported by the floors below [22]. Rather than relying on several distinct structural members to support each platform, the walls of each platform are the structural component supporting the platform or roof above it. Therefore, careful consideration must be given during the framing process to ensure that vertical framing members, known as studs, and horizontal framing members, known as plates, are located in a manner that supports the structural integrity of the building. Canada's model building code, the National Building Code of Canada (NBC), describes acceptable solutions for the framing

of wood frame buildings in Part 9, Section 9.23 [24]. The acceptable solutions are based on best practices commonly carried out in the construction industry today. Paragraph 9.23.10. describes the way wall studs must be sized, spaced, and oriented. Any deviation from this prescribed approach must be inspected and approved by a structural engineer, who is to confirm that the deviation meets the load bearing requirements set out in the Code.

In recent years, a set of framing practices known as advanced framing techniques have emerged and grown in popularity as a means of balancing structural building code requirements and increasingly stringent thermal resistance requirements. In essence, these practices promote a reduction in the proportion of the wall volume occupied by framing members, and thus a lower framing ratio. This leaves a higher proportion of the wall volume available to be filled by insulation materials, which have a higher thermal resistivity value than the wooden framing members, thus increasing the effective thermal resistance value of the wall [25]. These practices also have the benefit of reducing the amount of lumber needed to frame a building, thereby reducing the material costs. Advanced framing techniques include increasing the spacing of studs as much as possible (typically increasing spacing from 406 mm on centre to 610 mm on centre), increasing the width of studs to allow for larger stud cavities to be filled with batt insulation, and adjusting the geometry of wall corner framing such that continuous insulation can be accomplished [26]. The overall outcome of employing advanced framing techniques is a reduction of up to 5% in overall heating and cooling loads when compared to an equivalent conventionally framed home [27]. Several of the wall concepts presented in this work have been inspired by the practices of advanced framing techniques [28].

2.4 Integration of Novel Insulation Materials in Wall Assemblies

More important to the thermal performance of a wall assembly than the framing technique employed are the insulation materials used. In Canada, the practice of filling stud cavities with batt insulation such as mineral wool or fiberglass blankets, or blown insulation such as cellulose or polyurethane foam (PUR), is now practically universal, and the practice of installing rigid sheathing insulation, most commonly expanded polystyrene (EPS) or extruded polystyrene (XPS), is becoming common.

Despite limited real-world use, some research has been conducted into the integration of novel, high performance insulation materials into residential wall assemblies. Conley [18] studied the thermal performance of residential wall assemblies incorporating vacuum insulated panels (VIPs) embedded in XPS and found that they offer improved performance over conventional insulation practices, while reducing the risk of panel puncture. Campbell [29] employed long-term in-situ hygrothermal monitoring of a research house to observe the long-term performance of wall systems employing VIPs, and found no risk of mould growth during the testing period. Cuce et al. [30] conducted a comprehensive review of the application of aerogels as building insulation materials and found them to be promising, but still hampered by the materials' very high manufacturing costs, which they predicted will continue to decrease. Finally, Brideau [31] contemplated the use of phenolic foam insulation in Canadian wall insulation applications but found very little literature discussing its use. It is clear, then, that little work has been carried out to analyze the performance of highly insulated, thin wall assemblies incorporating insulation materials other than VIPs.

2.5 Thermal Modelling of Highly Insulated Wall Assemblies

A variety of tools and software can be used for the thermal modelling of wall assemblies. Modelling can take place in one, two, or three dimensions, and the choice between the three approaches typically depends on whether the design of the wall assembly is homogeneous along the horizontal plane. Commonly used two-dimensional modelling tools include THERM and HEAT2, and commonly used three-dimensional modelling tools include ANSYS, ABAQUS, HEAT3, and SIEMENS [32]. When used correctly, these tools enable a modeller to assess the thermal properties of envelope assemblies at a fraction of the cost required to conduct in-situ or steady state testing. However, to ensure that these tools are correctly used, studies must be conducted to validate the modelled results with experimental data, as was done by del Coz Diaz et al. [33] for concrete hollow brick assemblies.

For the purposes of the study presented here, two-dimensional modelling was sufficient to represent the wall assemblies proposed, as their geometry and material properties do not vary in the vertical axis. For this reason, THERM and HEAT2 were chosen to model the assemblies and their operation is described in detail in Section 5.3 and Section 5.4, respectively. The usage of these software tools is broadly popular in the study of building envelopes; for example, Stanescu et al. [34] used HEAT2 to model the walls of a newly-constructed recreation centre in Montreal and demonstrate that nonconformities in the walls' designs did not contribute meaningfully to heat losses from the building, and Sadowska and Bieranowski [35] used THERM to study different modernization methods for balcony slabs in multi-family building retrofits.

2.6 Steady State Testing Methods

A variety of standard testing methods have been described to test the thermal performance both of individual materials, as well as of wall specimen meant to simulate a real wall assembly. The work

presented in this thesis relies on two such testing methods; the first, *ASTM C177: Standard Test Method for Steady-State Heat Flux Measurements and Thermal Transmission Properties by Means of the Guarded-Hot-Plate Apparatus*, is used in the calibration of the guarded hot box by comparison to results obtained using the hot plate method [36]. The application of this test method to this work is described in Section 6.2.3. The second test method used, *ASTM C1363: Standard Test Method for Thermal Performance of Building Materials and Envelope Assemblies by Means of a Hot Box Apparatus* [37] is used to evaluate the thermal performance of the wall assemblies proposed in this work. The application of this test method is described in detail in Section 6.1.

The ASTM C177 test method is a steady state test which makes use of a central guarded hot plate, to which heat addition is metered. On either side of this plate is a specimen sample; it is crucial that both samples are identical in all properties for measurement to be accurate. On the other side of each test sample is a cooled plate, which can be set to a specific temperature. Around the guarded hot plate are auxiliary guard heaters which maintain the surrounding area at the same temperature as the guarded plate; this minimizes any flanking heat losses which would otherwise be unaccounted for in heat flux and thermal conductivity calculations. Figure 2-1 presents a diagram of this apparatus based on ASTM C177 [36]. This method is very commonly used for the heat flux and thermal conductivity testing of both homogeneous building materials (both insulation materials and structural materials) [38]–[40], as well as the testing of simple assemblies and composites [41]–[43]. The guarded hot plate present at Carleton University's facility is configured to test only homogeneous samples.

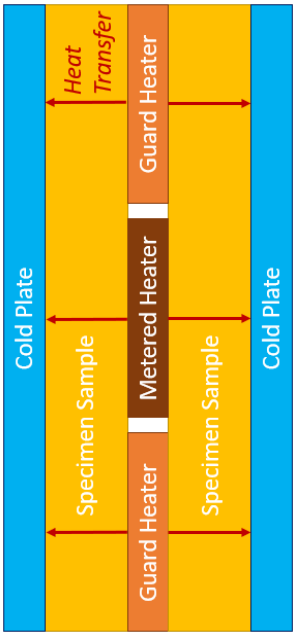

Figure 2-1: A Diagram of the Guarded Hot Plate Apparatus as Described in ASTM C177

There is precedent for the use of the ASTM C177 test procedure as a means of calibration by comparison of other tests. This approach was used by Conley [18] in preparation for the testing of advanced wall systems which incorporate VIP panels in a guarded hot box with test method ASTM C1363. Similarly, Somerford [43] made use of the ASTM C177 test method to evaluate the thermal performance of a novel masonry wall employing an integrated thermal barrier and recommended to validate the results they found by using the ASTM C1363 method. Finally, Kodur et al. [44] compared test method ASTM C177 to test method C1363 in determining the thermal properties of fiber-reinforced polymer composites, finding that the primary practical difference between both approaches is in the size of specimen which can be tested, with the hot plate method allowing for smaller specimens than the hot box method. ASTM C177 is very similar, but not identical, to *ISO 8302 Thermal insulation — Determination of steady-state thermal resistance and related properties — Guarded hot plate apparatus* [45].

The guarded hot box test procedure outlined in ASTM C1363 is very commonly used for the testing of the thermal properties of novel building envelope assemblies, including fenestration items such as windows and doors, as well as opaque wall assemblies. Guarded hot box apparatuses range widely in size, from metering areas in the range of a metre squared such as the one used in testing for this thesis, to tens of metres squared as the guarded hot box recently commissioned at Carleton University's Centre for Advanced Building Envelope Research (CABER) [46]. Although they are typically vertical, some guarded hot box apparatuses can also be rotated to a horizontal position to test the thermal performance properties of roof assemblies [47]. Most commonly in guarded hot box testing, a building envelope assembly is constructed to represent a larger, repeating envelope unit, and installed into the apparatus. The thermal performance results produced are then used to validate models or identify any thermal bridges.

A wide range of literature exists discussing the usage of the guarded hot box apparatus in this manner. Moore et al. [48] used a guarded hot box apparatus to study a metal stud wall incorporating VIP insulation, determine its effective thermal resistance, and identify the thermal bridges present on the edges of the VIP panels. Tarabieh and Aboulmagd [49] used the guarded hot box procedure to characterize the performance of three wall assemblies typical in Egypt to identify areas of potential improvement and to identify the best wall design. Finally, Conti et al. [50] used the guarded hot box apparatus to study the thermal properties of rectangular straw bales, a potential biogenic insulation material, to better understand how it can be incorporated into building envelopes.

2.7 Areas of Limited Research

Based on the foregoing topics discussed, the following research questions were identified which this thesis aims to answer.

- **How can nascent, high performance insulation materials be identified, evaluated and selected for consideration for residential building wall insulation applications?** The properties of many nascent insulation materials are readily available in literature. Some are even used in insulation products in other markets. However, no attempt has been recorded in literature to evaluate how these properties make these materials suitable for a wood-frame residential application.
- **How can these insulation materials be effectively incorporated into residential wood-frame wall assemblies?** To date, little has been written in literature about approaches which should be taken to incorporate new insulation materials into residential wood-frame wall assemblies while minimizing disruption to existing framing practices. Such approaches should incorporate knowledge attained through the practice of advanced framing techniques to further reduce any thermal bridges through structural members.
- **How can such wall assemblies be designed with the explicit purpose of reducing the wall thickness so that interior floorspace is maximized?** Some work has been done to date with the explicit aim of designing a thin profile, highly insulated wall assembly; such work has been carried out by Conley [18]; however, his research focused on the incorporation of VIPs alone, and did not consider additional insulation materials. With the known disadvantages of VIPs and in particular their fragility to damage which may cause them to lose their seal, it is important to identify how other highly insulating materials can be used to reduce the profile of wood-frame walls.

- **How can such wall assemblies be modelled using finite element tools to assess their effective thermal resistances and any potential thermal bridges?** Modelling software which is commonly used for the assessment of the performance of newly proposed wall assemblies and whose usage is regularly cited in literature can bolster confidence in the performance of the wall assemblies presented in this thesis.
- **How can these models be validated against experimental test conducted using the ASTM C1363 standard?** The experimental validation of the numerical models developed in this thesis will contribute towards the validation and calibration of future models incorporating high performance insulation materials in residential wood-frame assemblies, a topic which to date has been scarcely discussed in literature.

3. Material Selection and Assessment

The initial step in the wall design process was the selection of material for the thermal barrier layer. High thermal performance can only be accomplished in a thin wall profile if highly insulating materials are used, and therefore only such materials were considered. A review of commercially available insulating materials identified a variety of materials whose thermal resistivity exceeds 34.7 m·K/W (5.0 $ft^2 \cdot °F \cdot h/BTU \cdot in$), which was decided as the minimum thermal performance for materials to be considered. These materials include vacuum-insulated panels (VIP), extruded polystyrene (XPS), phenolic foam, silica aerogel, carbon aerogel, gas-filled panels (GFP), graphite-infused expanded polystyrene (GPS), polyisocyanurate (PIR), and polyurethane (PUR). The integration of VIPs into thin-profile, highly insulated residential wall assemblies has been previously researched and discussed [18], and they are therefore not considered for further research in this project. Nonetheless, to compare their performance to other insulation materials, VIPs are included in the material selection evaluation process. In this chapter, the process taken to narrow down this list of candidate materials is discussed.

3.1 Selection Criteria

To narrow down the number of prospective insulation materials to be considered for this study, a list of five selection criteria was developed to evaluate the materials and compare them to one another. These selection criteria, which are meant to assess a material's compatibility with conventional Canadian wood-frame construction, were developed in consultation with a panel of subject matter experts during a design charette held on December 15th, 2020. The participants of the charette included two members of Carleton University's CABER, three members of NRCan's CanmetENERGY research centre in Ottawa, a building science engineering consultant based in Vancouver, an engineer with an insulation materials manufacturer based in Quebec, and a home

builder who specializes in construction in Canada's Northern climate. The weighing of each of the selection criteria presented in this thesis was decided during this charette, based on the input of the participants, who were briefed on the goals and objectives of this project. Therefore, the criteria and their weighing presented here are specific to the application discussed in this thesis.

The selection criteria include long-term thermal resistivity, durability, cost, environmental impact, and safety. Greater weight was placed on the long-term resistivity criterion as it was determined to be the most important during the design charette in accomplishing the goals of the research. The performance of insulation materials in each of the criteria was assessed based on a review of data from manufacturers, retailers, academic researchers, and the experience of construction experts. Each of the selection criteria is discussed in detail in the following sections.

3.1.1 Long-term Thermal Resistivity

The thermal resistivity of insulation materials defines the ratio between the material's resistance to conductive heat transfer and the insulation layer's thickness. This relationship is expressed below in Equation (3-1). The unit for this value is mK/W.

$$r = \frac{\mathrm{R_{eff}}}{x} \qquad (3\text{-}1)$$

In other words, materials which have a high thermal resistivity achieve a high degree of thermal insulation over a thinner profile, as is desired by the objectives of this study. Because thermal resistivity values typically vary with temperature, it is important to consider the mean temperature for which the value is cited. For the purposes of this study, thermal resistivity values at a temperature of 0°C will be considered.

The advertised thermal performance of building insulation products commercially available in North America is determined using test method ASTM C518, which cites no requirements for the

minimum age of the test specimen. Because of varying manufacturing processes, many insulation products are generally expected to lose some thermal performance over time. Test methods such as those described in ISO 11561, ASTM C1303 and CAN/ULC-S770 measure the thermal performance of insulation materials after this decrease in performance by subjecting the insulation to an accelerated laboratory-controlled ageing process to produce a value known as the "long-term thermal resistance". Many insulation manufacturers cite the long-term thermal resistance of their products along with thermal performance determined using test method ASTM C518. Because the long-term thermal resistance value better represents the performance of the insulation material over time, where possible it will be this value which is used in the material evaluation.

3.1.2 Perforation Vulnerability and On-site Alteration Capability

In a construction setting, it is advantageous to be able to easily alter the shape and dimensions of insulation materials, both before and after installation. This is both to accommodate the geometric constraints of a particular wall section (for example, to allow for the installation of fenestration) as well as to allow for deviations from the original design. Also in a construction setting, materials are frequently subjected to poor storing conditions and handling. Ideally, the thermal performance of the insulation product should not diminish due to either practice. A notable example of an insulation product which is incapable of being altered on-site nor withstand significant damage without loss of thermal performance is the vacuum insulated panel (VIP). VIPs cannot be cut to size to adapt to deviations in construction from original plans, nor can they be subjected to significant abuse and misuse. This means that integration of VIPs in building plans must be carefully considered before construction, and any labourers which encounter VIPs should be trained in their care. Both considerations may add significant costs to the price of construction.

Thus, in this evaluation, the ability of the various insulation materials to withstand both accidental damage and intentional alteration without degrading in performance is evaluated qualitatively. Those materials which can be both altered and damaged without significant impact are rated favourably, whereas those which experience a significant decrease in performance are rated poorly. Materials which are either difficult to alter on-site or which experience a moderate decrease in performance upon alteration or damage, are rated moderately.

3.1.3 Cost

An important consideration when choosing any construction material is its cost. However, when evaluating the cost of an insulation product, many different factors are considered, including the thermal performance and the material's coverage area. For the purposes of this evaluation, a generalized before tax cost was determined for each of the insulation materials, in Canadian dollars, and normalized based on the thermal resistance of the insulation and material's surface area coverage. Prices presented in this analysis were determined in December 2020. The price for each material is cited in units of Canadian dollars per RSI per m^2. Materials with a lower normalized cost thus perform better in this criterion than those with a higher normalized cost. It is important to note that some of the evaluated materials are not yet commercially available, and others are not widely available in Canada. The costs shown in this evaluation are therefore only estimates, and their sole purpose is to compare between the different materials.

3.1.4 Environmental Impact

In recent years, engineers and architects began to develop an appreciation of not only the technical performance of building materials, but also their environmental impact. Indeed, some researchers have determined that when considering a building's lifetime emissions, the large environmental impact of manufacturing certain high performance insulation materials significantly negates the

reductions in operational emissions the usage of the material enables [51]. To accomplish an overall reduction in environmental impact for a building, it is therefore important to consider the emissions produced when manufacturing the insulation materials.

To take the environmental impact of the various insulation materials into consideration, The environmental product declarations (EPDs) of representative products were considered. These documents, which are typically authored by third party reviewers and voluntarily published by the manufacturer, aim to estimate the environmental impact of a product throughout its life, from manufacturing to disposal. ISO 14025 is one international standard for the authoring and publishing of EPDs. Although environmental impact is dependent on a great number of variables, global warming potential (GWP) is a commonly used metric evaluated in many EPDs to estimate how much the product contributes towards climate change. GWP is a measure of greenhouse gas emissions produced in terms of kilograms of CO_2 gas equivalent.

For the purpose of this evaluation, the environmental impact of the various insulation materials will be estimated using the GWP values associated with the raw material supply, transport, and manufacturing of each product. These values correspond to modules A1, A2 and A3 in the ISO 14025 standard EPD. Only these values are used and values associated with product installation, use and disposal are omitted so that variations in installation and disposal practices across different markets are ignored. To normalize these values across different types of materials, the value is divided by the RSI and the surface area of the product, to produce a value measured in kilograms of CO_2-equivalent per RSI per meter squared. Materials which demonstrate a lower environmental impact will perform better on this criterion than those which demonstrate a higher environmental impact.

3.1.5 Material Handling, Machining and Fire Safety

The final criterion aims to evaluate the overall safety of the insulation material; both for those installing it as well as the future occupants of the building. Safety concerns for each material were evaluated by reviewing the material safety data sheets (MSDS) for representative products. These documents indicate to the installer whether they need to take any safety precautions due to known health and safety issues with the product. In particular, the MSDSs were reviewed for three aspects of product safety: (1) handling safety during installation; (2) any evidence of VOC off-gassing; and (3) performance in fire testing.

Based on these three aspects, each of the materials was given a value of one through five on this criterion, based on the following rubric:

1) Evidence of volatile organic compound (VOC) off-gassing and/or failure to meet fire safety standards.

2) Serious handling concerns which require specific training and personal protective equipment during installation. No evidence of VOC off-gassing, and adequate fire performance.

3) Some handling concerns, no evidence of VOC off-gassing, and adequate fire performance.

4) Minimal handling concerns, no evidence of VOC off-gassing, and adequate fire performance.

5) No handling concerns, no evidence of VOC off-gassing, and excellent fire performance.

3.2 Materials Evaluated

The following insulation materials were identified as potential candidates for further study:

3.2.1 Phenolic Foam

Phenolic foams are synthesized from phenolic resin, which is the product of the condensation reaction between phenol and formaldehyde and is better known for its commercial name, Bakelite; the first synthetic plastic to be created. Phenolic foam can be formulated from Bakelite in a variety of ways to accomplish a diverse range of physical, mechanical, and thermal properties, which are predominately influenced by the foam's cell geometry. In phenolic-foam based insulation products, a closed cell geometry is desired, which is typically accomplished by volatizing a low-boiling point blowing agent in the foam mixture [52]. To maintain a low thermal conductivity, it is desired that this blowing agent remains trapped in the foam cell structure. In the past chlorofluorinated blowing agents were typically used, but those have been largely replaced by pentane [53].

In North America, phenolic foam became a popular roof insulation solution in the 1980s when it was first marketed by Koppers Co. However, issues emerged with the insulation product several years later, when it was discovered that a corrosive reaction would initiate between the phenolic foam and metal roof decks in the presence of moisture. This led to the discontinuation of the roof insulation product, and a large class action lawsuit settlement against the manufacturer in 2000 [54].

While the reputation of phenolic foam as a building insulation product suffered in North America following the lawsuit, the material gained popularity in Europe, where new formulations overcame the corrosion issues first encountered. Today, the material continues to be popular there for a variety of building insulation solutions, with the most common product being Kingspan Insulation's Kooltherm line of products. Modern phenolic foam insulation boards accomplish RSI per metre values of up to 58.9 m·K/W, are fire resistant, moisture resistant, and do not produce

irritative fibers during installation [55]. However, concerns exist about the long-term thermal performance of the boards, as their thermal performance relies in part on the pentane blowing agent which may permeate from the closed cells over time [53].

3.2.2 Silica Aerogel

Aerogels are materials produced by extracting the liquid constituent of a gel through freeze-drying or supercritical drying [30]. This process allows the gel's liquid content to be replaced with a gas without the collapse of the gel structure, leaving a unique cross-linked molecular structure whose volume is primarily made of many small air-filled pores, ranging in size from 10 to 100 nm [56]. This structure leads to aerogels' physical properties, including their extraordinarily light weight and exceptionally low thermal conductivity. It is this low thermal conductivity which makes aerogels a compelling material for building insulation applications [30].

Silica aerogel is the most common and best studied type of aerogel, and the most commonly used type in building insulation applications [30]. Like other aerogels, silica aerogel is highly brittle, limiting its usability as an insulation material in its pure form. However, silica aerogel can be impregnated into fibrous reinforcement to form a flexible and highly thermally insulative blanket. One commercially available building insulation product which incorporates a silica aerogel blanket product is Aspen Aerogels' Spaceloft, which is marketed primarily for scenarios where a high degree of thermal insulation is desired without a significant impact on wall thickness, such as in the retrofit of architecturally significant buildings [57]. Despite silica aerogel's exceptional thermal performance, its introduction into the building insulation market has been limited due to its significant cost.

3.2.3 Carbon Aerogel

Carbon aerogel, also known as organic aerogel, was first synthesized in 1989 via high-temperature pyrolysis of polymerized resorcinol and formaldehyde [58]. A variety of processes have since developed for the synthesis of carbon aerogels. Like silica aerogel, carbon aerogel is highly brittle, light, and has extraordinarily low thermal conductivity, having a molecular structure full of nanopores of air [59]. Since it was first synthesized, carbon aerogel has attracted significant attention for potential insulation applications, and in particular high temperature insulation, due to the material's extraordinarily high temperature resistance; carbon aerogel retains its low thermal conductivity up to 2800°C [60]. To date, the commercialization of carbon aerogel remains limited [61], and little consideration has been given to it as a potential building insulation material, likely due to its large manufacturing cost and low mechanical strength [62]. Nonetheless, as with many carbon-based "super materials", enthusiasm remains for the applications of carbon aerogel.

3.2.4 Gas Filled Panels (GFP)

GFPs are insulating panels filled with either air or a low-conductivity gas such as argon or krypton, and composed of layers of aluminum foil honeycombs and enveloped in a sealed barrier. GFPs can either ship inflated, or be inflated on-site [63]. By shipping the GFP uninflated, the packaged size of insulated panels is significantly smaller than the volume being insulated, thereby reducing shipping costs. This makes GFPs an attractive option for applications where the transport of building materials makes up a significant proportion of the overall cost of construction, such as in military applications or in remote regions [64]. Predictably, GFPs cannot be cut to shape or significantly altered, making them more appropriate in prefabricated construction. Nonetheless, GFPs do not seem to be readily commercially available in Canada.

3.2.5 Graphite Polystyrene (GPS)

Expanded polystyrene (EPS), a closed cell, air-blown material commonly referred to in North America by the genericized trademark Styrofoam, has been a ubiquitous building insulation material throughout the world since the 1950s [65]. Although it is still commonly used in a variety of applications, the thermal performance of EPS has been surpassed by a variety of foam insulation products, including chemically similar extruded polystyrene (XPS). As a means of improving the thermal performance of EPS, graphite dust is added during the expansion of the polystyrene beads in the manufacturing process, producing graphite-infused expanded polystyrene, or GPS. Although it is otherwise identical to EPS, the addition of graphite to GPS reduces the thermal conductivity across the material by reflecting radiant heat energy [66] and gives GPS its distinct grey colour. The resulting material demonstrates mechanical properties nearly identical to those of EPS, but thermal performance comparable to that of XPS [67].

In Canada, GPS is used in a variety of commercially available building insulation products, including Plasti-Fab DuroSpan, Amvic Building System SilveRboard Graphite, Halo Exterra, and BASF Neopor.

3.2.6 Polyisocyanurate (Polyiso)

Polyisocyanurate, commonly known in North American construction parlance as polyiso, is a thermoset plastic produced from the reaction between methylene diphenyl diisocyanate and polyol and expanded with a blowing agent. Polyiso is commonly used as an insulation material in rigid insulation panels. It is chemically identical to polyurethane (PUR), but manufactured in different reaction conditions. Although polyiso is more common in warmer climates, the material's unique characteristic of decreased thermal resistance with decreasing temperature (meaning its performance degrades with colder temperatures) [68], as well as issues associated with material

shrinkage [69], have limited its use as a construction insulation material in Canada. Nonetheless, it is commercially available under a variety of brand names, including IKO EnerFoil and Soprema SOPRA-ISO.

3.2.7 Polyurethane (PUR)

Polyurethane foam, like polyiso, is synthesized from the reaction between methylene diphenyl diisocyanate and polyol, and mixed with a blowing agent. Unlike polyiso, however, the reactants which form PUR foam are kept separate until they are sprayed on the surface which is to be insulated, reacting on contact. In commercial insulation applications, the two reactants are typically stored in separate containers labelled A and B, with container A typically comprised of methylene diphenyl diisocyanate [70], and container B comprised of polyol, blowing agents, flame retardants, a surfactant, and reaction catalysts [71]. In smaller spray can applications, such as the consumer product Great Stuff Insulating Foam Sealant, the two reactants are kept pressurized in separate sections of the same container until they are released [72]. PUR foam insulation is very commonly used in building construction in Canada, both as the primary thermal insulation layer in opaque assemblies, as well as a sealant foam to fill gaps and cracks surrounding other wall components and fenestration. The insulation material's popularity is thanks to its ability to expand to fill the space it is being sprayed into and provide effective coverage easily.

3.3 Material Performance against Selection Criteria

The following sections summarize the relevant results for each insulation material in each of the evaluation criteria.

3.3.1 Long-term Thermal Resistivity

Table 3-1 below is a summary of thermal resistivities for the evaluated insulation materials. Wherever possible, an aged thermal conductivity value is quoted, representing the thermal

performance of the material years into its use. Most of the values cited here were tested to ISO 11561:1999 Ageing of thermal insulation materials — Determination of the long-term change in thermal resistance of closed-cell plastics (accelerated laboratory test methods).

Table 3-1: Material Long-term Thermal Resistance Performance Summary

Material	R-value / inch [$ft^2 \cdot °F \cdot h/BTU \cdot in$]	RSI / m [$m \cdot K/W$]	Notes	Ref.
VIP	20.6 – 36.0 Compromised: 7.2	142.8 – 249.6 Compromised: 49.9		[73]
XPS	4.5 – 5.0	31.2 – 34.7		[74]
Phenolic Foam	6.6 – 8.5	45.8 – 58.9	Kingspan Kooltherm R-values are supposedly aged R-values, representing the long-term thermal performance of phenolic foam, and thermal performance is guaranteed for the life of the building.	[75]–[77]
Silica Aerogel	9.6	66.6	Thermal conductivity of silica aerogel blanket. Research has shown a negligible effect on the thermal conductivity of silica aerogel blankets due to accelerated aging.	[78]–[80]
Carbon Aerogel	6.3	43.7	Very limited research.	[81]
Gas-filled Panel	5.0 – 11.0	34.7 – 76.3		[63], [64]
GPS	5.0	34.7		[82], [83]
PIR	5.6 – 7.2	38.8 – 49.9	The thermal performance of PIR insulation is reduced in temperatures below 5°C.	[68]
PUR	5.2	36.1	Sprayed PUR insulation.	[84]

3.3.2 Perforation Vulnerability and On-site Alteration Capability

Table 3-2 presents a summary of results in the Perforation Vulnerability and On-site Alteration Capability criterion, a single criterion which represents the fragility of an insulation material in handling. Materials whose thermal performance is completely compromised due to perforation, and which cannot be cut to size on site were given a high impact score. Materials whose thermal performance is somewhat diminished when perforated or cut were given a moderate impact score.

Finally, materials which are designed to be cut to shape and whose thermal performance is unaffected by perforation were given a low impact score.

Table 3-2: Material Perforation Vulnerability Performance Summary

Material	Impact of Perforation and Alteration	Notes
VIP	High	The perforation of a VIP panel compromises its thermal performance.
XPS	Low	XPS insulation can be cut to shape without reduction in thermal performance.
Phenolic Foam	Moderate	No research found which discusses the impact of board damage on the thermal performance of phenolic foam insulation. However, as a closed cell insulation which contains a blowing agent (often pentane), it is reasonable to assume that compromising a phenolic foam board's gas-tight foil would diminish its performance somewhat.
Silica Aerogel	Low	Silica aerogel blankets employ air trapped in a nano-porous matrix to achieve their thermal performance. Damaging the blanket is therefore not expected to compromise the performance of the insulation.
Carbon Aerogel	Low	Carbon aerogel insulation employs air trapped in a nano-porous matrix to achieve its thermal performance. Damaging the blanket is therefore not expected to compromise the performance of the insulation.
Gas-filled Panel	High	As with VIPs, a perforation in the foil of a gas-filled panel would cause irreversible damage to the panel's thermal performance.
GPS	Low	GPS insulation can be cut to shape without reduction in thermal performance.
PIR	Moderate	As a closed cell insulation which contains a blowing agent, it is reasonable to assume that compromising a PIR panel's gas-tight foil would diminish its performance somewhat.
PUR	Low	PUR insulation is blown, poured, or spray-applied, and perforations in the insulation are not expected to cause an impact on thermal performance.

3.3.3 Cost

Wherever possible, Canadian estimated costs were cited in Table 3-3 below. Bulk pricing is not considered. Prices for carbon aerogel insulation were not determined as the material is not yet commercially available, and prices for gas-filled panels were not determined as they could not be reliably established.

Table 3-3: Material Cost Performance Summary

Material	**Cost per R per ft^2 [CAD$]**	**Cost per RSI per m^2 [CAD$]**	**Reference**
VIP	0.36 – 1.26	22.0 – 77.0	[31]
XPS	0.15	9.17	[85]
Phenolic Foam	0.50	30.56	[31]
Silica Aerogel	1.58 – 1.85	96.57 – 113.07	[31]
Carbon Aerogel	N/A	N/A	Not commercially available.
Gas-filled Panel	N/A	N/A	Could not be determined.
GPS	0.11	6.72	[86]
PIR	0.20	12.22	[87]
PUR	0.18	11.00	[88]

3.3.4 Environmental Impact

Table 3-4 below presents a summary of results for the global warming potential for each insulation material, in units of kilograms of CO_2 gas equivalent per RSI per metre squared of coverage. Representative product EPDs were used to assess the environmental impact of each insulation material type.

Table 3-4: Material Environmental Impact Performance Summary

Material	Global Warming Potential [kg CO_2 eq / RSI / m^2]	Notes
VIP	6.7 – 12.2	Lower threshold is based on 43.89 kg CO_2 eq per m^2 for 25 mm thickness panel with a rated thermal conductivity of 0.004 W/mK, equivalent to R-35 [89]. Higher threshold utilizes the specified calculation value for thermal conductivity, 0.007 W/mK.
XPS	23.8	21.9 kg CO_2 eq per m^2 for an HFC-blown panel with a thickness that provides for an R-5.68 [90]. HFO-blown XPS panels with a significantly lower GWP than existing XPS products are entering the market in the coming years; however, an EPD for such a product could not be found at the time of writing.
Phenolic Foam	1.8	7.71 kg CO_2 eq per m^2 for 100 mm thickness, equivalent to R-28.4 [91].
Silica Aerogel	18.3	12.3 kg CO_2 eq per m^2 for 10 mm thick blanket, equivalent to R-3.79 [92].
Carbon Aerogel	N/A	No representative products exist. It is important to note however that because a biogenic feed-in material is used in the production of carbon aerogel, it is likely to have a lesser environmental impact than silica aerogel.
Gas-filled Panel	N/A	No EPDs for existing products found.
GPS	1.8	1.73 kg CO_2 eq per m^2 for a panel with a thickness that provides for an R-5.68 [93].
PIR	2.4	2.67 kg CO_2 eq per m^2 for a panel with a thickness that provides for an R-5.68 [94].
PUR	2.4	2.67 kg CO_2 eq per m^2 for a panel with a thickness that provides for an R-5.68 [94].

3.3.5 Material Handling, Machining, and Fire Safety

Representative product Safety Data Sheets (SDS) and product specification sheets were used to assess the handling and machining safety of the selected materials. In particular, three aspects of product safety were assessed: (1) handling safety during installation; (2) any evidence of VOC off-

gassing; and (3) performance in fire testing. Table 3-5 below presents a summary of these results for the insulation materials assessed.

Table 3-5: Material Handling, Machining and Fire Safety Performance Summary

Material	Handling & Safety Score	Notes
VIP	5	• No special handling instructions specified. • No evidence of off-gassing of VOCs in commercially available products. • VIPs have been found to perform well in fire testing, increasing time-to-failure when compared to EPS [95].
XPS	3	• Product MSDS recommend limiting exposure to XPS boards and their dust to eight hours daily [96]. • XPS insulation contains no VOCs as defined by the U.S. Environmental Protection Agency. Nonetheless, DBDPE, a flame retardant not harmful to human health but which is harmful to organisms in the environment [97] has been recorded in XPS insulation boards [98]. • Flame retarded XPS insulation is classified as Euroclass E, indicating that it highly contributes to fire.
Phenolic Foam	5	• MSDS indicates that dust is non-hazardous, the panels are skin non-sensitising, and there are no exposure limits prescribed [55]. • No evidence of off-gassing of VOCs in commercially available products. • Phenolic foam is classified as Euroclass C, S2, D0, indicating that it has limited contribution to fire, contributes some to smoke development, and does not cause production of flaming droplets [55].
Silica Aerogel	5	MSDS indicates that dust may cause eye irritation; however, no special precautions are required in handling [99]. • No evidence of off-gassing of VOCs in commercially available products. • Aspen Aerogels Spaceloft is classified as Euroclass C, S1, D0, indicating that it has limited contribution to fire, does not emit smoke, and does not cause production of flaming droplets [100].
Carbon Aerogel	N/A	The material is not yet commercially available, and its handling safety has not yet been assessed.
Gas-filled Panel	N/A	Insufficient safety data found.

GPS	3	• The MSDS for BASF Neopor prescribes specific handling instructions to avoid exposure to vapors. Ventilation and/or respiratory equipment is required. Three materials in the GPS composition have occupational exposure limits: graphite, isopentane, and pentane [101]. • VOC off-gassing emissions testing proved to be below limits for any countries with VOC limits [93]. • BASF Neopor is classified as Euroclass E, indicating that it highly contributes to fire.
PIR	5	• MSDS indicates that dust is non-hazardous, the panels are skin non-sensitising, and there are no exposure limits prescribed [102]. • No evidence of off-gassing of VOCs in commercially available products. • Kingspan PIR Isolation is classified as Euroclass C, S1, D0, indicating that it has limited contribution to fire, does not emit smoke, and does not cause production of flaming droplets.
PUR	2	• The MSDS for PUR spray foam insulation requires special PPE when handling the product. It also indicates that the insulation is carcinogenic, demonstrates specific target organ toxicity from both single and repeated exposure, and is acutely toxic [70], [71]. • No evidence of off-gassing of VOCs when PUR spray foam is correctly applied. • Flame retarded PUR insulation is classified as Euroclass E, indicating that it highly contributes to fire. The curing process for PUR insulation is exothermic, and if applied too thick can spontaneously combust [70], [71].

3.4 Evaluation Results

To assess the overall ranking of each insulation material compared to the others assessed, an evaluation matrix was developed. The performance of each insulating material in each criterion of the five outlined above, other than thermal resistivity and safety, was scored out of 1, with the best-performing material in a particular category receiving a score of 1, the worst a score of 0, and all others being scored proportional to their performance on the criteria. To evaluate safety, scores out of 1 were determined proportional to the safety score the material received. To evaluate thermal resistance, a score of 1 was set to represent the thermal resistivity of air at 5°C and 1 atm. Materials

were given a score proportional to their performance relative to air (for example, the average thermal resistance of a VIP panel is about 4.73 times higher than that of air).

The sum of the scores in each evaluation criterion is the overall score the material received in the evaluation. Table 3-6 below presents a summary of the results for each of the insulation materials. Note that because carbon aerogel and GFPs each had insufficient data to complete their evaluation (in particular, their cost, environmental impact and safety could not be established), their overall total score cannot be compared to the scores of the other materials, and they are omitted from further consideration.

Table 3-6: Material Evaluation Results

Material	Thermal Resistivity	Cost	Handling	Enviro. Impact	Safety	TOTAL
VIP	4.73	0.08	0.00	0.13	1.00	5.94
XPS	0.84	0.72	1.00	0.00	0.60	3.16
Phenolic Foam	1.30	0.17	0.50	1.00	1.00	3.97
Silica Aerogel	1.73	0.00	1.00	0.03	1.00	3.76
Carbon Aerogel	1.13	N/A	1.00	N/A	N/A	*2.13*
Gas-filled Panel	1.73	N/A	0.00	N/A	N/A	*1.73*
GPS	0.90	1.00	1.00	1.00	0.60	4.50
PIR	1.15	0.52	0.50	0.73	1.00	3.90
PUR	0.93	0.58	1.00	0.73	0.40	3.64

Based on these evaluation criteria results, phenolic foam, GPS and silica aerogel insulation materials are chosen for further consideration in the subsequent steps of this research. Despite performing better in the evaluation than silica aerogel, PIR insulation was not chosen for further consideration due to its tendency to decrease in thermal performance with decreased temperature, rendering inappropriate for Canadian climate where winter outdoor temperatures routinely drop below 0°C.

4. Wall Concept Development

With the insulation materials to be used identified, the next step of the research was the development of innovative wall concepts which incorporate the three identified materials. In this chapter, the design considerations used in the design of the concepts are discussed, as well as the five unique concepts which were developed.

4.1 Design Considerations

Four design considerations are used in developing the five wall concepts presented below. These considerations were created to ensure that the concepts developed achieve the objectives of the research. In no specific order, these are the considerations:

- Achieve an effective RSI of at least 5.28 $m^2 \cdot K/W$ (30 $ft^2 \cdot °F \cdot h/BTU$): although voluntary building codes such as Passive House and NetZero require higher values for the effective thermal resistance of above grade wall assemblies, to date most provincial building codes and the 2015 NECB require at most a minimum effective RSI value of 4.76 $m^2 \cdot K/W$ (27 $ft^2 \cdot °F \cdot h/BTU$) for nearly all residential construction outside of climate zone 8 (heating degree days exceeding 7000) [103]. Setting the desired effective RSI value at 5.28 ensures that the wall concepts developed here exceed the current code-required performance nearly everywhere in Canada. In addition, for most of the wall concepts presented here, the overall effective thermal resistance of the assembly can be easily increased by simply increasing the thickness of the thermal insulation layer by the requisite amount; this would go against the goals of this project, however the wall thickness accomplished would still be lesser than typical assemblies.

- Reduce wall thickness as much as possible: the impetus for this research is the reduction of the wall thickness to increase the livable space within a new building as much as possible, to make increased performance wall assemblies more attractive for building developers, who look to increase value for occupants.
- Concepts are to be appropriate for new residential construction: as much as possible, the proposed wall concepts should comply with Division B, Section 9.23. of the 2015 NBC. This section outlines acceptable solutions for wood-frame construction in Canada, and any wall concepts which cannot follow the solutions listed in this section are considered an "alternative solution". When an alternative solution is proposed, it must be demonstrated that the solution addresses the same issues as the applicable acceptable solution, and that it meets the same attributed objectives and functional statements. Clause 1.2.1.1.(1)(b) of the 2015 NBC outlines how an alternative solution can demonstrate compliance with the Code. Alternative solutions therefore would incur higher engineering costs and should be avoided.
- Comply with existing wood frame construction techniques as much as possible: to reduce the costs associated with construction, the proposed wall concepts should not deviate significantly in required construction steps from typical Canadian wood frame construction. Any significant deviation will require additional training of contractors and labourers and increase the possibility that the wall will not be correctly assembled, potentially risking reduced hygrothermal performance.

As a means of ensuring these design considerations are met, the design approach undertaken in developing the wall concepts started with considering a base case wood frame wall assembly, shown in Figure 4-1. This wall concept consists of a 13 mm (0.5 inches) gypsum board layer on

the interior, followed by 38 mm by 89 mm (2 by 4 inches nominal) wooden structural members spaced 406 mm (16 inches) on centre (OC) apart. 2 by 4 structural members were selected for consideration as they provide more flexibility to develop thin walls. The cavities formed by these structural members, which are 368 mm (14.5 inches) wide, are occupied by mineral wool insulation. Attached to the outboard side of the structural members is a 13 mm (0.5 inches) structural sheathing layer formed of oriented strand boards (OSB). Outboard of the structural sheathing is a rainscreen cavity and cladding. Effort is made to ensure each proposed wall concept deviates as little as possible from this conventional wall design, to reduce the chance of the design being considered an alternative solution or requiring additional training for construction personnel.

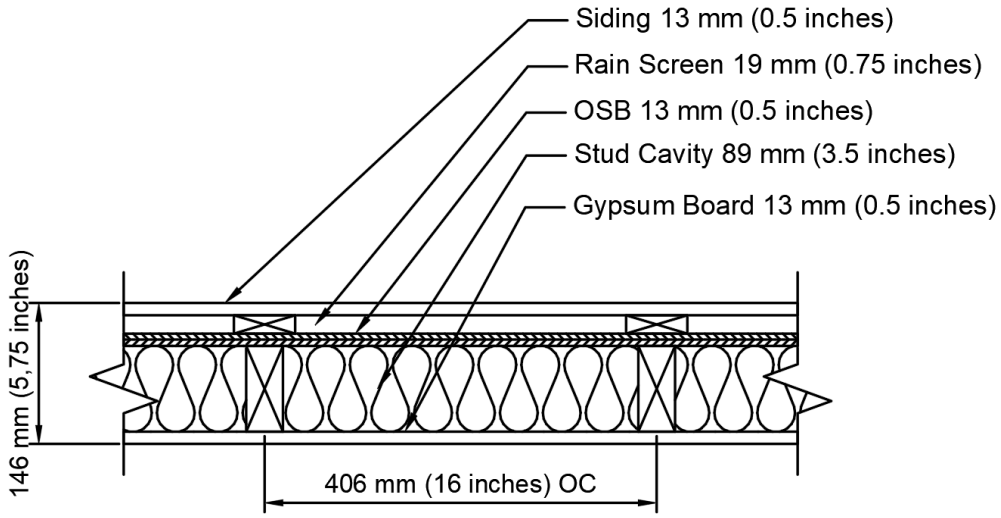

Figure 4-1: Simple Base Case Wood Frame Wall Assembly

4.2 Concepts Developed

The following sections describe the designs of the proposed wall concepts.

4.2.1 Rigid Exterior Insulation

The first wall concept employs an existing industry practice of installing continuous rigid insulation on the exterior face of the wall, on the outboard surface of the plywood or OSB sheathing

layer. This is also known as insulation sheathing. At times, the layer of rigid exterior insulation has been used to replace the wood sheathing layer altogether with the interior gypsum board layer providing structural bracing to meet lateral load requirements. However, this practice is uncommon in Canadian wood frame construction [104] and for the purposes of this research, the layer of rigid insulation is modelled as an additional layer between the wood sheathing and the rain screen. Figure 4-2 shows an illustration of a continuous section of this wall concept. The required thickness of the insulation layer depends on the thermal resistivity of the insulation material, the effective thermal resistance of the other wall components, and the assumed film coefficients on the interior and exterior faces of the wall. Using the Isothermal Planes Method, the required thickness of the insulation layer is determined for phenolic foam, silica aerogel, and GPS as the insulation material in Section 5.2.

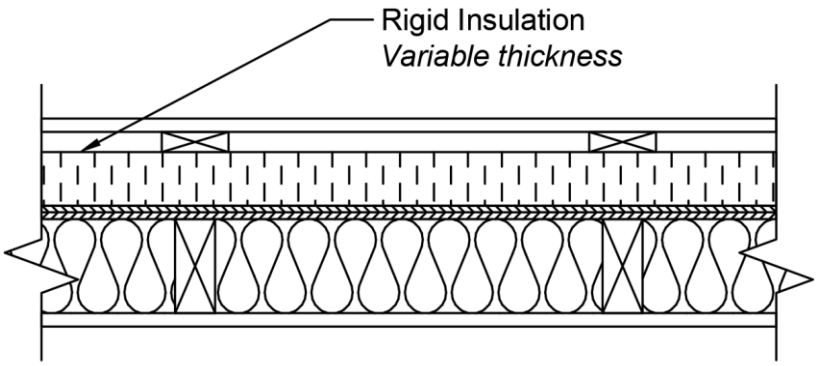

Figure 4-2: Rigid Exterior Insulation Concept Diagram

4.2.2 Thermal Break Insulation

A significant design constraint in improving the thermal performance of wood frame walls is thermal bridging across the studs which constitute the structural frame of the wall. As a means of reducing the thermal bridging across the studs while minimizing additional material costs and added wall thickness, this wall concept adds a single thin layer of insulation on the exterior face of the studs as a thermal break. The thickness of this insulation strip is set to 10 mm (0.4 inches),

a popular material thickness for high-performance silica aerogel insulation. A continuous rigid insulation layer outboard of the structural sheathing would still be required, the thickness of which is determined based on the desired insulation material in Section 5.2. The thermal break insulation concept is shown in Figure 4 below.

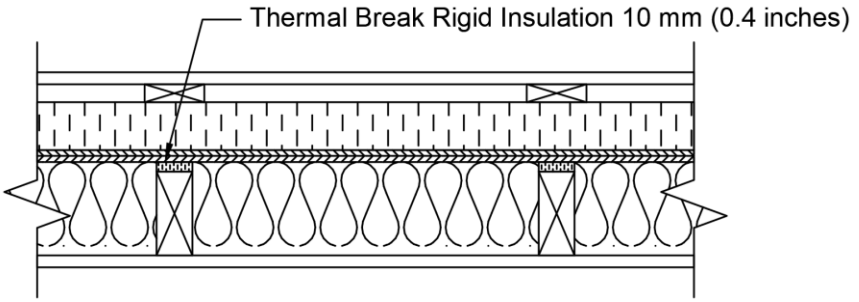

Figure 4-3: Thermal Break Insulation Concept Diagram

The approach proposed here to mitigate the thermal bridging across structural members is not novel. Advanced Insulations Inc. manufactures a product by the name of Proloft, which is a 10 mm thick strip of silica aerogel insulation with an adhesive on one side. This product is advertised for use with metal studs.

4.2.3 Rigid Insulation with Stud Grooves

Under current wall insulation practices, stud cavities are typically insulated with rock or glass fibre batt insulation blankets, which achieve a typical RSI of about 24.3 per meter (R-value of 3.5 per inch). Replacing this insulation with a higher performance rigid insulation would increase the overall thermal performance of the wall. An approach to extend the rigid insulation layer into the stud cavity is by making use of rigid insulation designed with appropriately spaced grooves for studs. One such approach is presented in Figure 4-4 below, where the layer of rigid insulation protrudes into the stud cavity by 25 mm (1 inch), leaving a 64 mm (2.5-inch) cavity to be filled by batt insulation. The remainder of the rigid insulation thickness is determined based on the

insulation material of choice to accomplish the desired effective R-value for the wall assembly. In this approach, some batt insulation remains to allow for wire passage and the installation of electrical junction boxes. This is thermally preferable to leaving a large air cavity between the rigid insulation layer and the gypsum board.

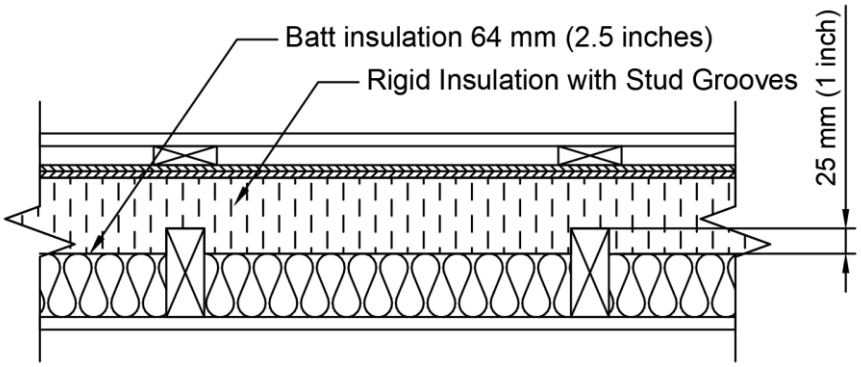

Figure 4-4: Rigid Insulation with Stud Grooves Concept Diagram

A similar design of rigid insulation is offered by Styro Rail, under the brand name SR.2X4. Offered in both EPS and GPS options, this design of rigid insulation is intended to be used to insulate foundation walls, with structural studs embedded into the rigid insulation layer.

4.2.4 Offset-framed Wall with L-shaped Rigid Insulation

In a departure from existing framing practices, this concept proposes to frame 48 x 98 mm (2 x 4-inch nominal) studs on 148 mm (6-inch nominal) plates, with stud members alternating between being flush with the interior and exterior faces of the plate in a practice known as offset framing. Stud spacing will be 406 mm (16-inch) OC. The remaining space between the studs will be occupied entirely by repeating L-shaped rigid foam insulation blocks, as shown in Figure 4-5 below. The repeating stud-insulation block pattern would create a continuous, air-tight thermal insulation layer. Unlike the previous concepts, this design's thermal performance is constrained by the thermal performance of the insulation material used, as the thickness of insulation cannot be increased.

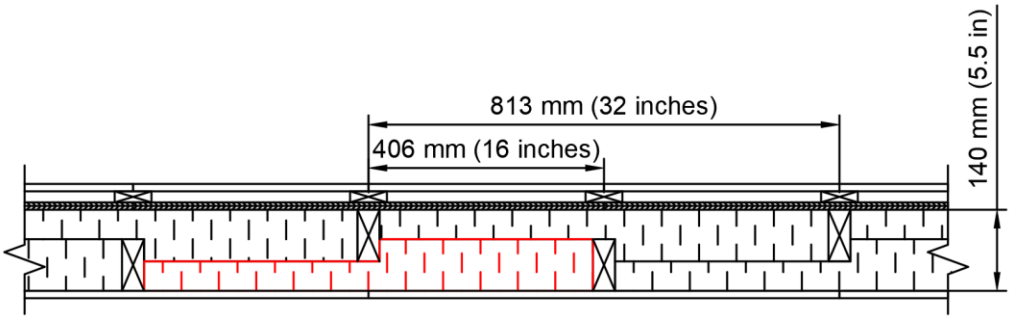

Figure 4-5: Offset-framed Wall with L-shaped Rigid Insulation Concept Diagram

This proposed concept relies on good compliance between the rigid insulation blocks and the studs, meaning that engineered wood studs may be required for this design. Alternatively, the faces of the rigid insulation which interface with stud faces could be trimmed, and replaced with a thin layer of soft, compliant insulation blanket, which would better fit potential dimensional imperfections in sawn lumber. Alternatively, gaps between structural members and rigid insulation could be filled with spray foam insulation. A second issue identified with this concept is the fact that the top and bottom 148 mm (6-inch) plates are not thermally broken, necessitating additional thought into how this thermal bridging can be addressed.

4.2.5 Continuous Aerogel Layer Insulation

The final wall concept considered incorporates two wall studs attached parallel to one another, on either face of an 89 mm (4-inch nominal) plate, with a 13 mm (0.5 inch) gap left between the studs. This 13 mm gap is filled with a continuous layer of silica aerogel blanket insulation, serving as a continuous thermal barrier. The stud cavities on either side of the aerogel layer are filled with batt insulation. Two variations of this design are proposed: one with a 406 mm (16-inch) OC stud spacing shown illustrated in Figure 4-6, and one with a 610 mm (24-inch) OC stud spacing shown illustrated in Figure 4-7. A 610 mm (24-inch) option can be considered for this wall concept as the number of structural members is effectively doubled. Increasing the stud spacing is predicted to

increase the thermal performance of the wall, as a higher volume of the wall will be occupied by insulation. For either option, an additional rigid external insulation layer is required to achieve the desired effective RSI of 5.28 m2·K/W.

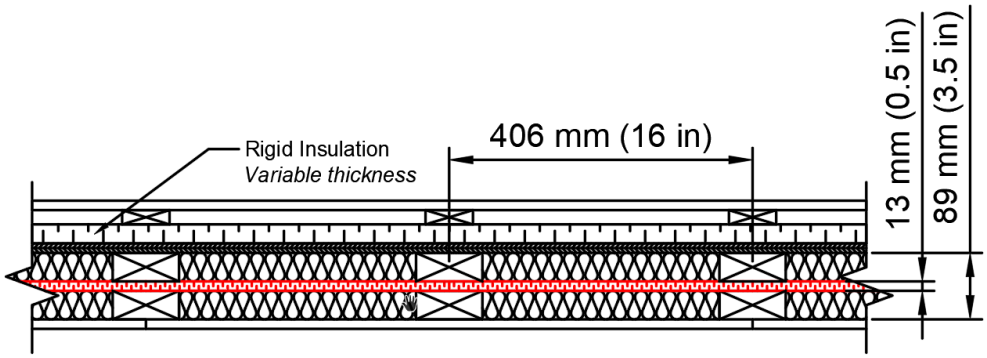

Figure 4-6: Continuous Aerogel Layer Insulation, 406 mm (16-inch) OC

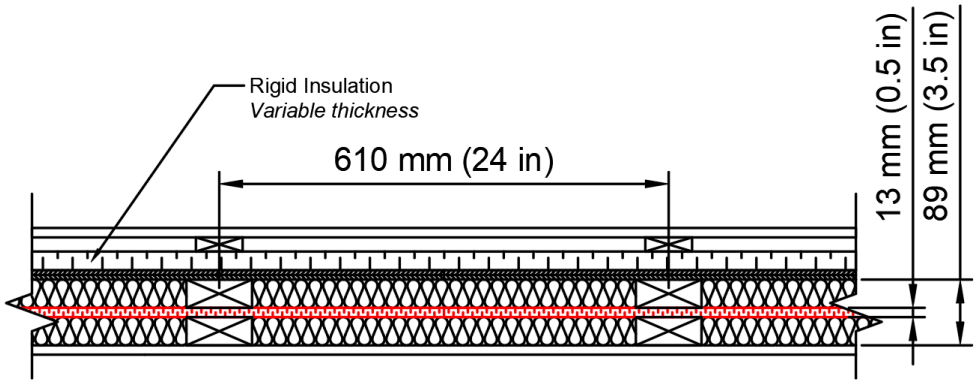

Figure 4-7: Continuous Aerogel Layer Insulation, 610 mm (24-inch) OC

With these proposed wall concepts refined, each is to be modelled using a range of thermal and hygrothermal methods to assess their performance and suitability for a range of Canadian climatic typologies.

5. Hygrothermal Performance Modelling

In this chapter, the models developed to assess both the thermal performance and the hygric performance of the wall concepts are discussed. Three different approaches were used for the determination of thermal performance; the isothermal planes method was used to determine the thermal resistance in one dimension across the wall concepts, whereas THERM and HEAT2 were used to determine the thermal resistance, heat fluxes and temperature gradients across the wall concepts in two dimensions. WUFI Pro was used to assess the hygric performance of the wall assemblies in one dimension.

5.1 Summary of Assumptions

In developing both thermal and hygric models, assumptions must be made about the hygrothermal properties of all materials included, as well as the boundary conditions of any surfaces in the models. Table 5-1 below presents the assumed thermal resistances used in the models. For the novel insulation materials being investigated in this research, the thermal resistance was taken as the average value of the ranges shown in Table 3-1. For the other materials which constitute the wall assembly, including the gypsum board, the OSB, the soft wood lumber which makes up the studs, and the mineral wool batt insulation, the thermal resistances used were obtained from NRCan [105]. To simplify the models, it is assumed that the thermal resistances of all the materials do not vary with temperature, although it is known that most materials see an increase in thermal resistance with decreasing temperatures.

Table 5-1: Assumed R-values for Materials for Modelling

Material	RSI / m	R-value / inch
Gypsum Board	6.2	0.90
Oriented Strand Board (OSB)	8.7	1.25
Soft Wood Lumber (stud material)	8.7	1.25
Batt Insulation	24.3	3.50
GPS	34.7	5.00
Phenolic Foam	52.0	7.50
Silica Aerogel	66.6	9.60

When assessing the effective thermal resistance of a wall assembly, the film coefficient is an important consideration. This value defines the convective heat transfer between the solid surface of the wall on either side, and the air making contact with the wall. The higher the film coefficient, the more heat transfer takes place through convection. The value of the film coefficient is dependent on multiple variables, including the air flow velocity around the wall, the air temperature, the surface finish of the wall, etc. A variety of empirical correlations between these conditions and the film coefficient have been proposed [106], however, they are beyond the scope of this research. For the purposes of estimating the performance of the wall assemblies, average film coefficients for the exterior and interior surfaces of the wall were based from NRCan estimates [105], and are shown in Table 5-2. The adjacent surfaces in each model were assumed to be adiabatic; this assumption is based on the idea that the wall section being analyzed is a part of a continuous, repeating envelope with identical features.

Table 5-2: Assumed Boundary Conditions Used in Thermal Modelling

Surface	Temperature (C)	H_c (W/m^2-K)
Interior	21.0	8.33
Exterior	-5.0	33.33
Adjacent surfaces	Adiabatic	

5.2 Isothermal Planes Method Calculations

The isothermal planes method for calculating the effective thermal resistance of wall assemblies is a simple approach to determining a one-dimensional approximation of a wall's overall performance. Also known as the series-parallel method, this approach divides the layers of a wall assembly into two types; (i) homogeneous, continuous material layers the thermal resistance of which can be added in series, and (ii) layers made up of materials of differing thermal resistance through which there will be parallel heat flow. The isothermal planes method is the method prescribed by NRCan for the calculation of the effective thermal resistances of opaque assemblies in ENERGY STAR certified homes [105].

A diagram describing the isothermal planes method is shown below, in Figure 5-1. In this diagram, a simplified wall assembly made of three layers is shown and compared to a thermal circuit. The first and third layers are homogeneous with a thermal resistance of R_1, whereas the middle layer is made up of two materials of dissimilar thermal resistances, R_2 and R_3. In this second layer, the material with thermal resistance R_3 makes up ¾ of the surface area of the wall, with the other material occupying the remainder.

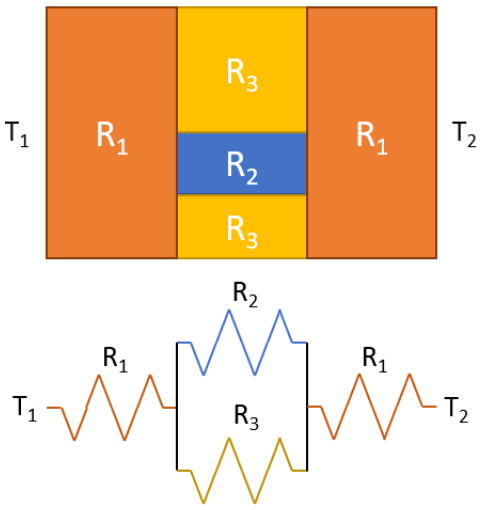

Figure 5-1: An Illustration of the Isothermal Planes Method

To calculate the effective thermal resistance of the overall wall assembly, the thermal resistance of each layer is added; this is simple for the first and third layers, but in calculating the thermal resistance of the second layer, one must take into account the fact that heat flow will take place to different degrees across both materials in parallel. This can be done by adding the reciprocal of the thermal resistances of the constituent materials (multiplied by the ratio of the surface area each material occupies), and then adding the reciprocal of this operation. The overall effective thermal resistance of this operation for the simple wall shown in Figure 5-1 is shown in the expanded form in Equation (5-1) and simplified in Equation (5-2).

$$R_{\text{eff}} = \mathrm{R}_1 + \frac{1}{\frac{3}{4}\frac{1}{\mathrm{R}_3} + \frac{1}{4}\frac{1}{\mathrm{R}_2}} + \mathrm{R}_1 \qquad (5\text{-}1)$$

$$\mathrm{R}_{\text{eff}} = 2\mathrm{R}_1 + \frac{4\mathrm{R}_3\mathrm{R}_2}{3\mathrm{R}_2 + \mathrm{R}_3} \qquad (5\text{-}2)$$

This approach is undertaken to determine the effective thermal resistances of the wall concepts proposed in Chapter 4. Where the effective thermal resistance of the proposed wall is dependent on the thickness of an insulation layer, the thickness of the layer is determined using the isothermal planes method to accomplish an effective thermal resistance for the wall of 5.28 $m^2 \cdot K/W$ (R-30). The work carried out to make these calculations is presented in Appendix A, and the results are presented and compared to the other thermal modelling methods in Table 5-3.

5.3 THERM Thermal Modelling

THERM is a free-to-use computer software developed by the Windows and Envelope Group in the Energy Technologies Area at the Lawrence Berkley National Laboratory [107]. Although it was originally developed for the purpose of assessing the thermal performance of glazing systems, the software is now commonly used in industry to assess two-dimensional steady-state heat

transfer across a variety of building components, including walls, windows, doors, foundations, and roofs. The software is particularly useful in the quick identification of possible issues of thermal bridging; such issues can be easily identified by reviewing the graphical results of a THERM model, where temperature distribution and heat flux distribution plots can be transposed over the model's geometry.

When creating a THERM model, one makes use of a simple graphic user interface which allows the user to draw a scale geometric model based on polygons. Each area enclosed by polygons must be assigned a material model, which defines the thermal properties of that particular area. Material properties can be drawn from THERM's library or created by the user. With the geometric model drawn and material properties assigned, all that is left for the user to do is to define the boundary conditions present on the outer edges of the geometric model. These conditions describe the heat transfer parameters between the surface of the model and its theoretical surroundings.

With the geometric model drawn, material properties assigned, and boundary conditions established, THERM solves the model by first creating a finite element mesh and determining the temperature and heat flux for each element. These results then undergo an error energy norm check, and if this check is failed, a finer mesh is used. Once a set of solutions meets the check, THERM's post-processor displays the results as a colour gradient and determines overall thermal conductivity (U-factor) between two predetermined points of interest. The underlying algorithm behind THERM's operation is based on *ISO 15099: Thermal performance of windows, doors and shading devices - Detailed calculations*, a standards document which describes a procedure for the calculation of thermal and optical transmission through both opaque and transparent fenestration [107].

The proposed wall concepts discussed in Chapter 4 were modelled to scale in THERM with the assumptions presented in Table 5-1 and Table 5-2 and their overall thermal resistance was determined and presented in Table 5-3. The graphical results produced by THERM displaying the temperature and heat flux gradients for each wall assembly are presented in Appendix B. Where the effective thermal resistance of the proposed wall is dependent on the thickness of an insulation layer, the thickness of the insulation layer found using the isothermal planes method was used in the THERM model.

5.4 HEAT2 Thermal Modelling

Like THERM, HEAT2 is a computer software commonly used in the building industry for the assessment of thermal performance of various assemblies and components. HEAT2, along with its three-dimensional counterpart HEAT3, were developed by the Lund Group for Computational Building Physics at Lund University in Sweden. AB. Unlike THERM which can only model steady state, HEAT2 can be used for the simulation of transient systems, and temperature-dependant properties such as thermal conductivity can be modelled to vary with temperature. Nonetheless, the graphical user interface for HEAT2 is not unlike that of THERM, and a similar procedure applies for the establishment of the model geometry, material properties, and boundary conditions. Just like THERM, HEAT2 solves the simulation by developing a finite element mesh, determining the temperature and heat flux for each element, and using these results to establish the overall thermal conductivity across the model. HEAT2 has been validated against *ISO 10211 Thermal bridges in building construction – Heat flows and surface temperatures – Detailed calculations*, and the underlying algorithm for the software has been described in [108].

The proposed wall concepts discussed in Chapter 4 were modelled to scale in HEAT2 with the assumptions presented in Table 5-1 and Table 5-2 and their overall thermal resistance was

determined and presented in Table 5-3. Where the effective thermal resistance of the proposed wall is dependent on the thickness of an insulation layer, the thickness of the insulation layer found using the isothermal planes method was used in the HEAT2 model.

5.5 Comparison of Thermal Modelling Results

The results presented in Table 5-3 compare the overall effective thermal resistances and thicknesses of each of the wall concepts presented in Chapter 4, as well as the thermal resistance per centimetre. The wall concept column describes which concept is being analyzed, and how thick the primary insulation layer is. The thermal performance per centimetre column is based on an average of the three different models' thermal resistances. In general, there is good agreement between each of the modelling methods, with most thermal resistance values being within 0.2 $m^2 \cdot K/W$ of the average for each concept. The exception of this is the offset-framed L-shaped phenolic insulation concept, for which the isothermal planes method underestimated the overall thermal resistance by 0.61 $m^2 \cdot K/W$ when compared to the results produced by the THERM and HEAT2 models. This discrepancy may be attributed to the fact that the isothermal planes method does not consider the effective prevention of thermal bridges which this concept accomplishes by insulation each structural member. The THERM and HEAT2 models do take this into account by assessing the properties of each individual element in the mesh.

Table 5-3: Summary of Thermal Modelling Results

	RSI, $m^2 \cdot K/W$				
Wall Concept	**IPM**	**THERM**	**HEAT2**	**Wall Thick., cm**	**RSI/cm**
Exterior Insulation, 64 mm Phenolic	5.37	5.55	5.32	21.6	0.25
Groove Insulation, 85 mm GPS	5.28	5.39	5.35	23.1	0.23
Groove Insulation, 51 mm Phenolic	5.20	5.43	5.39	19.7	0.27
L-shaped Phenolic Insulation	5.97	6.55	6.61	19.7	0.32
Cont. Aerogel: 406 mm OC, 51 mm Phenolic Ins.	5.15	5.31	5.32	19.7	0.27
Cont. Aerogel: 610 mm OC, 51 mm Phenolic Ins.	5.29	5.43	5.44	19.7	0.27

5.6 WUFI Pro Hygric Modelling

WUFI, which stands for "Wärme Und Feuchte Instationär", meaning "heat and moisture transiency", is a suite of software products which enable the modelling of transient heat and moisture transfer through building components. WUFI Pro, the suite's original and most popular software, allows moisture transport and vapour diffusion modelling in one dimension. WUFI is a popular tool in the building science industry and is the most commonly used tool for hygrothermal modelling of building assemblies. WUFI was first developed as a more robust, transient substitute to the Glaser method, a steady-state approach for the assessment of moisture in building components described in the German standard DIN 4108. It allows designers and engineers to identify potential moisture issues in their building designs before construction commences, rather than rely on the dated "build and monitor" approach, which refers to the practice of monitoring building envelope assemblies for signs of failure.

In North America, the usage of hygrothermal modelling for the assessment of moisture risk was codified in *ASHRAE Standard 160: Criteria for Moisture-Control Design Analysis in Buildings*.

In this standard, the moisture-control performance of an envelope is assessed based on the envelope's resistance to the promotion of mould growth. In its first 1996 iteration, the standard set out a high benchmark: to pass, the 30-day average relative humidity of any surface within an envelope assembly cannot exceed 80% between temperatures of 5°C and 40°C, irrespective of the surface material. Subsequent research showed that mould growth is far more nuanced, and in 2016 ASHRAE 160 adopted the Viitanen model of mould growth [109], which describes 6 distinct degrees of mould growth, known as the Mould Index [110]. In the new iteration of the standard, envelope assemblies are deemed as passing if they do not reach or exceed a sustained Mould Index of 3.

To assess the hygric performance of the wall concepts presented here, 1-dimensional WUFI Pro models were created for the four wall concepts. These models, which simulated the performance of the entire wall from the cladding to the gypsum layer, were subjected to 3-year long transient simulations of climate conditions in four select cities which are meant to represent a wide variety of Canadian climates. The simulations made use of The American Society of Heating, Refrigerating and Air-Conditioning Engineers (ASHRAE) Year 2 climate files [111] for St. John's (NL), Ottawa (ON), Calgary (AB), and Vancouver (BC). The climate zones for these cities are 7A, 6, 6 and 5 respectively, with a large variation in annual precipitation across the four cities. Assumptions used in the simulation are presented in Appendix C.

As a means of comparing the concepts, the mould growth indexes on the exterior and interior surfaces of the sheathing layer in each concept were determined. The sheathing layer was selected for examination as it is generally known to be of highest risk for mould growth in wood-frame construction. Any assembly which exceeded a mould growth value of 3 or presented persistent increase in the index at either surface at the end of three years was considered failed. In those

assemblies which failed this test, additional consideration is needed in the design of the vapour layers to improve the drying potential or to reposition sensitive layers within the assembly. Table 5-4 summarizes the results of the WUFI Pro hygric modelling of the wall concepts across the four selected Canadian cities.

Table 5-4: WUFI Simulation Results

Assembly	St. John's	Ottawa	Calgary	Vancouver
Base Wall	✘	✓	✓	✘
Rigid Exterior, Phenolic	✓	✓	✓	✓
Stud Grooves, GPS	✘	✓	✓	✘
L-shaped, Phenolic	✘	✓	✓	✘
Continuous Aerogel	✓	✓	✓	✓

These results show that all wall concepts pass the MI test in the Ottawa (ON) and Calgary (AB) climate regions. However, the stud grooves and L-shaped concepts failed the test in St. Johns (NL) and Vancouver (BC). Both of these regions see significant rainfall throughout the year, which makes hygrothermal design more challenging. The two concepts which failed do not incorporate any insulation layers outboard of the sheathing layer, failing to protect the inner surface of the plywood sheathing from developing condensation when its surface reaches the dew point. To overcome this, the walls should be designed in such a manner such that the sheathing layer is ventilated, to allow it to dry after water exposure.

The other concepts which did pass the MI test may still present hygrothermal challenges in the climate regions which see significant rainfall if the interior surfaces are not properly dried before the installation of exterior insulation. This is because the insulation materials proposed in this

thesis are strong moisture retardants, which may prevent interior wall components from drying to the exterior, leading to trapped moisture which would promote the growth of mould.

6. Thermal Performance Experimental Validation

In this chapter, the approach undertaken to validate the thermal performance of the proposed wall concepts is discussed, including descriptions of the equipment used, the calibration steps taken, and the means undertaken to overcome supply shortages in insulation materials arising due to the COVID-19 pandemic.

6.1 Guarded Hot Box

The guarded hot box test method for the evaluation of building envelope assemblies is a well-defined and commonly used approach for assessing the thermal resistance of large building envelope samples. ASTM International describes the test method in standard *ASTM C1363: Standard Test Method for Thermal Performance of Building Materials and Envelope Assemblies by Means of a Hot Box Apparatus* [37]. At Carleton University, a guarded hot box device compliant with ASTM C1363 has been used to test experimental thin wall assemblies since 2013, when it was constructed, instrumented and calibrated. The Carleton University guarded hot box is shown below in Figure 6-1. Visible in the photograph are the three frames which constitute the apparatus; the left frame houses the metering and guard chambers, the middle frame secures a wall sample in place, and the right frame houses the climate chamber.

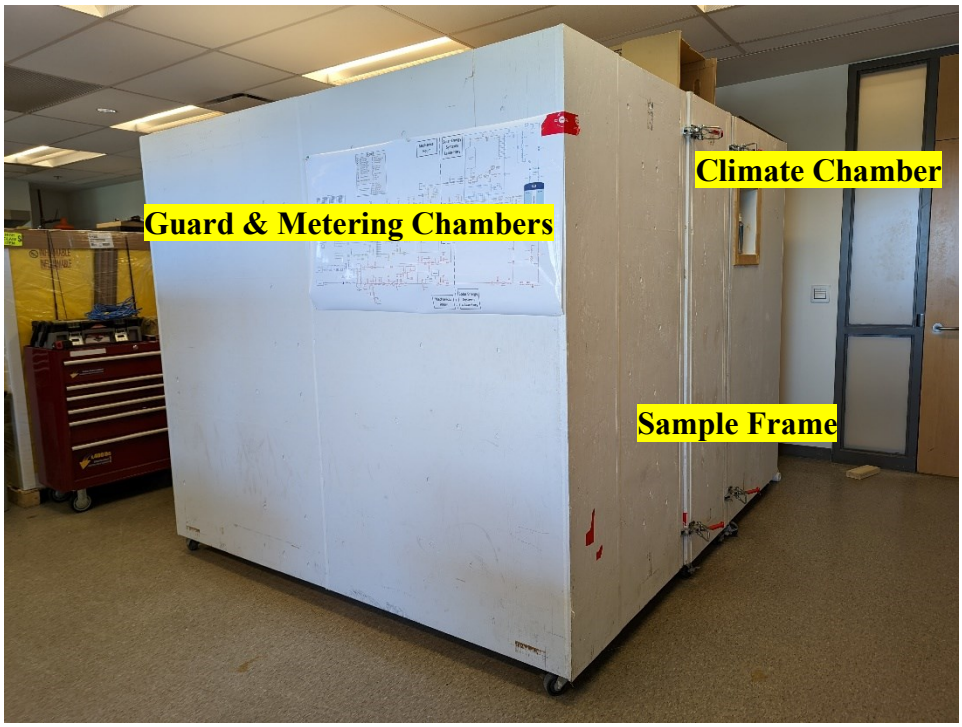

Figure 6-1: Carleton University's Guarded Hot Box Apparatus

The guarded hot box apparatus accomplishes an assessment of the steady state thermal resistance of envelope assemblies by creating a temperature gradient across the wall sample. The climate chamber maintains a constant low temperature meant to represent the outdoors, while the guard and metering chambers are kept near room temperature, and the energy required to maintain the metering chamber temperature at that level is metered. The temperature difference between the metering and climate surfaces, the specimen metering surface area, and the heat energy input into the metering chamber, are sufficient to determine the sample's thermal resistance. A simplified schematic of the guarded hot box apparatus is shown in Figure 6-2. The three distinct chambers which constitute the apparatus are shown colour coded; the guard chamber is shown in grey, the metering chamber within the guard chamber is shown in brown, and the climate chamber is shown in blue. The wall specimen, which separates the guard and metering chambers from the climate chambers, is shown in orange. The black arrows in the figure represent the primary energy flows

within the apparatus. In the sections that follow, each of the three chambers is discussed in detail, as well the general operation of the guarded hot box.

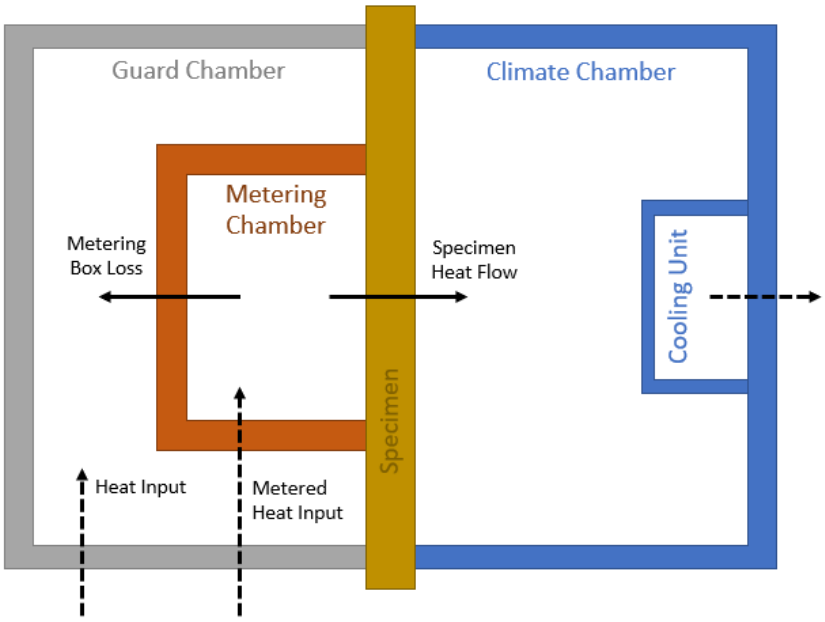

Figure 6-2: Simplified Diagram of a Guarded Hot Box Apparatus

6.1.1 Climate Chamber

The purpose of the climate chamber is to simulate exterior conditions on the outer surface of the wall specimen. This is accomplished by a large cooling unit capable of maintaining the chamber air temperature as low as -35°C by providing as much as 1500 W of cooling. A baffle in the form of a plastic sheet creates a barrier between the cooling unit and its fan, to prevent the incidence of cold spots on the surface of the wall specimen. The cold air within the climate chamber is circulated along the surface by a bank of five fans above the baffle; the fan bank draws air towards the cooling unit, this air is cooled, and is pushed back at the specimen at the bottom underneath the baffle.

The climate chamber also contains instrumentation in the form of permanently installed thermocouples, thermocouple quick connect adaptors, thermopile leads, and a relative humidity sensor. The permanently installed thermocouples measure the temperature of the specimen exterior

surface (both within and outside the metering area), as well as the air temperature in the chamber. The thermocouple quick connectors, of which there are 34, allow thermocouples embedded within the wall assembly to be connected to the data acquisition system. The 12 thermopile leads are used to assess the temperature difference between the metering area surface on the climate side with the metering area surface on the metering side. Finally, the relative humidity sensor data is used in the control of the guarded hot box. The climate chamber is 2.3 m wide and 2.0 m tall. A photograph of the climate chamber is shown below in Figure 6-3.

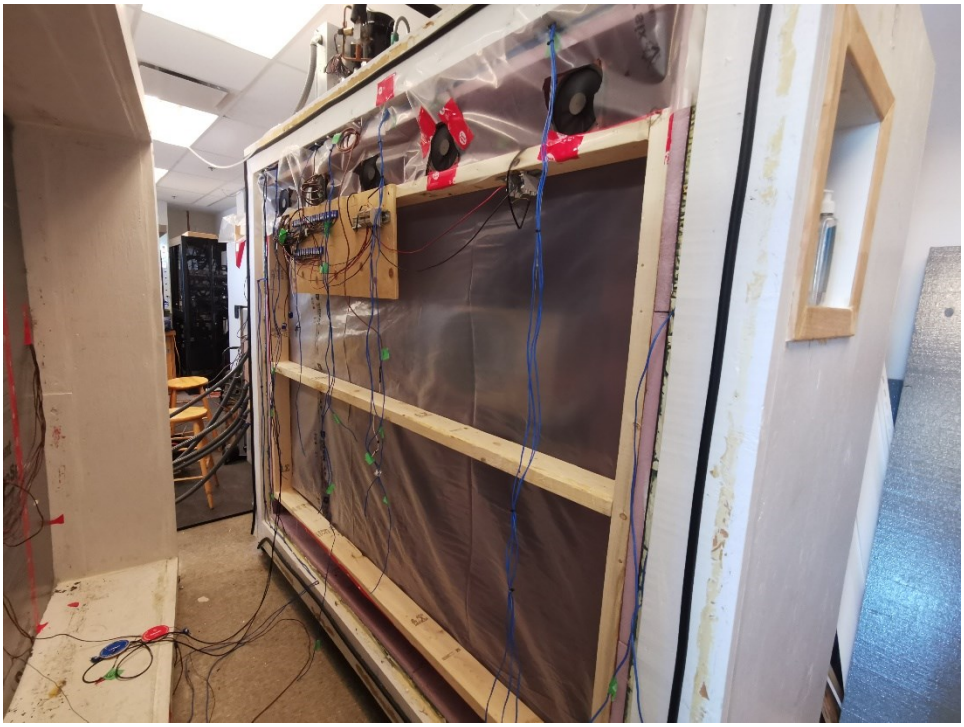

Figure 6-3: The Guarded Hot Box Climate Chamber

6.1.2 Metering Chamber

The metering chamber, a small chamber enclosed inside the guard chamber, defines the surface area of the wall specimen which is being evaluated. The metering chamber is kept at a constant temperature near, but slightly higher than, room temperature. The metering chamber is kept at this temperature using a 500 W electrical coil heater, with the power input of the heater recorded. The

temperature is higher than room temperature to enable better control of the chamber temperature, as there is no means of instantaneously reducing the temperature. Also within the metering chamber is a bank of small fans and a baffle; as with the climate chamber, these ensure that heat is distributed homogeneously throughout the metering chamber, and that convection conditions closely resemble those of a typical indoor environment. The heating coil and metering chamber fan bank are shown below in Figure 6-4.

Figure 6-4: Fan Bank and Heating Coil in the Metering Chamber

The walls of the metering chamber, which separate it from the guard chamber, are insulated with a continuous 25 mm layer of XPS foam. This, in addition to the guard chamber being kept near the same temperature as the metering chamber, ensures that there is very little heat loss (or gain) from the metering chamber to the guard chamber, and that instead all the heat produced by the metered heater inside the metering chamber travels across the specimen towards the colder climate chamber. Nonetheless, some discrepancy between the metering and guard chambers temperatures

may exist, and this discrepancy is taken into account in thermal resistance calculations by knowing the thermal resistance of the XPS foam insulation, the surface area of the metering chamber walls, and the surface temperatures on either side of the metering chamber wall, which are monitored using 5 thermocouples on either surface.

The metering chamber is heavily instrumented, and beside the 5 thermocouples attached to the inside surfaces of the metering chamber's walls, it also contains 12 thermocouples and thermopile leads to monitor the specimen's surface temperature relative to the climate chamber surface temperature, 6 thermocouples to monitor the air curtain temperature 10 cm away from the specimen surface, a relative humidity sensor to assist in the control of the guarded hot box, and a power monitor to measure the heat energy input from the electric coil heater. Figure 6-5 below shows a photograph of the interior of the metering chamber.

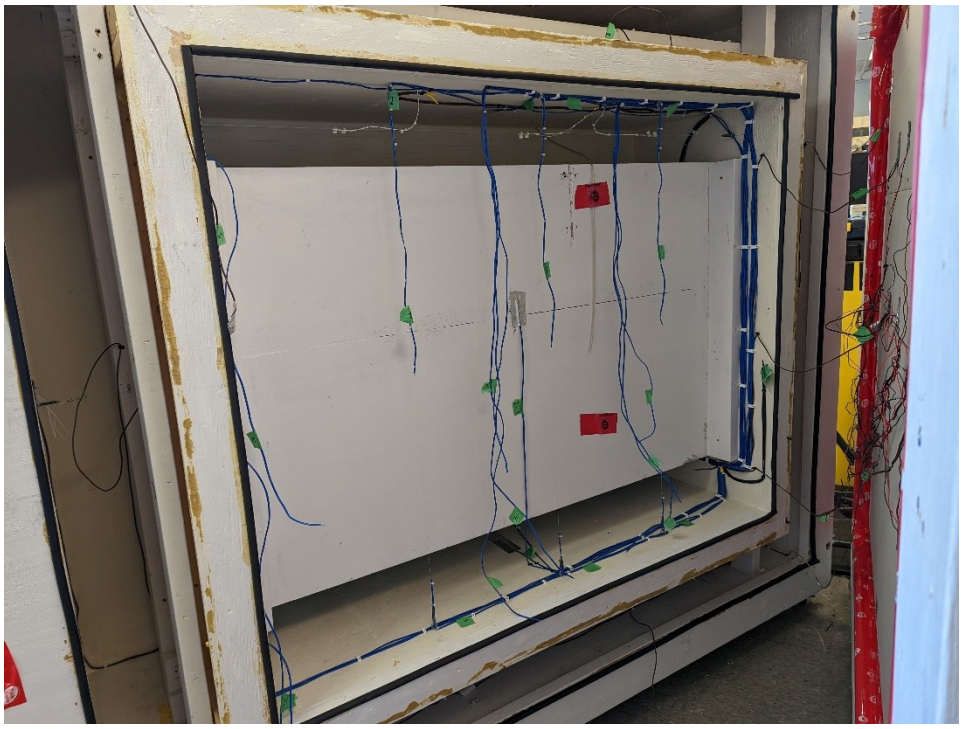

Figure 6-5: The Guarded Hot Box Metering Chamber

6.1.3 Guard Chamber

The third chamber which constitutes the guarded hot box apparatus is the guard chamber. The guard chamber encloses the metering chamber, and its only purpose is to ensure that the heat transfer between the surroundings and the metering chamber is minimized. This is accomplished using a non-monitored 500 W electric coil heater and thermocouples which continuously measure the surface temperature of the exterior walls of the metering chamber to ensure it matches that of the interior surface. In addition to these thermocouples, the guard chamber also has thermocouples which attach to the surface of the specimen exterior to the metering area. The data from these thermocouples is compared to the data from the surface thermocouples interior to metering chamber, and general agreement between the values suggests minimal impact from flanking losses; heat transfer interior of but parallel to the specimen. The guard chamber's dimensions are identical to those of the climate chamber, at 2.3 m wide by 2.0 m tall.

6.1.4 Guarded Hot Box Data Acquisition and Control

Two independent systems were used to control the guarded hot box apparatus and record the data it produced. A Delta controller was used to regulate the experimental conditions in each of the three chambers by controlling the heating and cooling systems present. The logic used in the control program for the guarded hot box is described by Baldwin [112]. Input into the Delta control system was conducted using a simplified ORCAview graphical user interface application, where one can toggle the guarded hot box on or off, input the setpoints for each of the chambers, or activate the climate chamber's manual defrost cycle, which was used whenever accumulated frozen condensate was present. Specific inputs, such as the on/off status of the fans in each of the chambers, could be made to override the inputs into the application. A screenshot of the ORCAview interface is shown below in Figure 6-6.

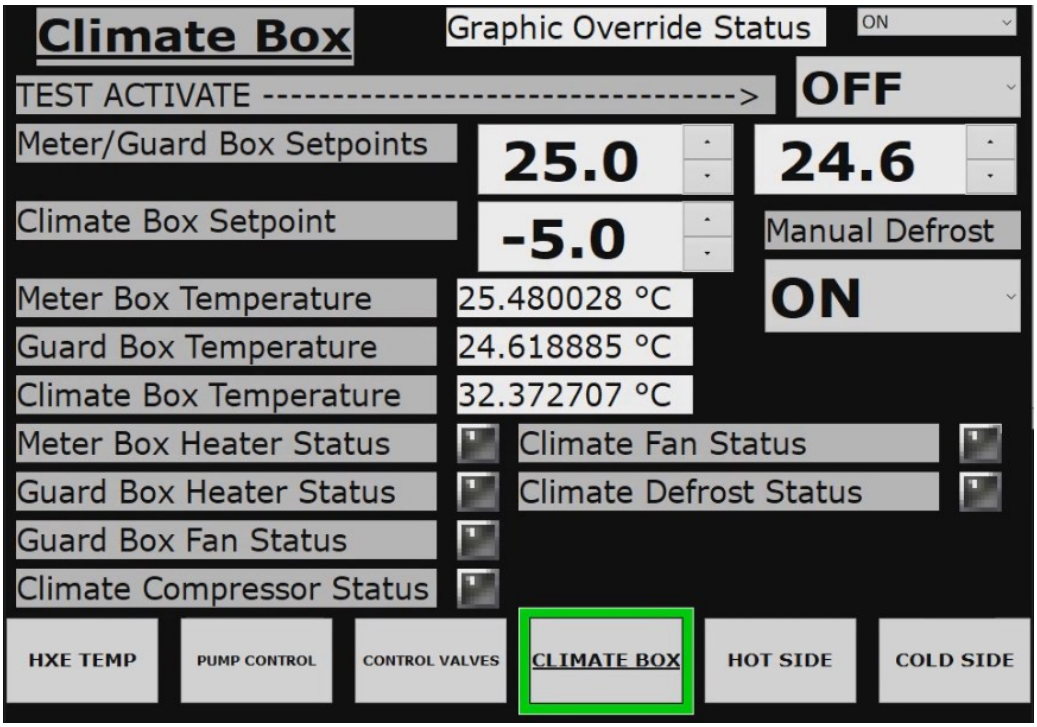

Figure 6-6: ORCAview Graphical User Interface for the Guarded Hot Box

Data acquisition for the experiment was carried out using a National Instruments CompactDAQ NI-cDAQ9188, an 8-card data acquisition chassis. The CompactDAQ receives any analogue data transmitted from the thermocouples, thermopiles and power meter in the form of a voltage, current or pulse, and relays this data through an Ethernet cable to a computer loaded with National Instruments LabView software. On the computer, a LabVIEW VI program interprets these signals, and converts them to practical units: degrees Celsius for the thermocouples and thermopiles, and Watt-hours for the power monitor. The conversion to these units is carried out by a calibrated sensitivity provided by the manufacturer, as is the case for the power monitor, or by using an equation developed through a calibration procedure, as is the case for the thermocouples and thermopiles. As the LabVIEW program records this data (at an interval and for check-lengths decided by the user), it is also continuously monitoring whether the conditions required by ASTM C1363 for steady state are met; these steady state conditions are discussed further in Section 6.1.5.

Upon the steady state criterion having been met, or once terminated by the user, the LabView software automatically saves all data recorded for the duration of the trial into an .XLSX Excel file. A screenshot of the LabVIEW VI graphical user interface is shown below in Figure 6-7.

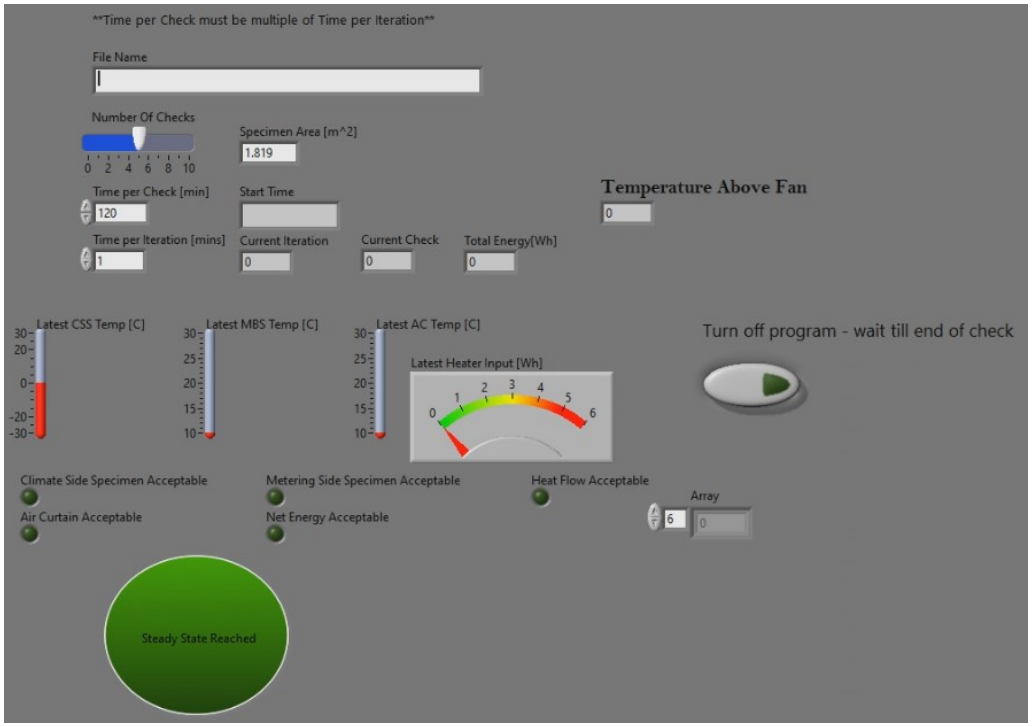

Figure 6-7: LabVIEW VI for Guarded Hot Box Data Acquisition

6.1.5 Steady State Conditions

The guarded hot box apparatus is used to determine the steady state thermal resistance of wall specimen, and the conditions requisite to establish steady state are not trivial. Fortunately, ASTM C1363 outlines the conditions required, as well as their duration, before recording of data can be made. Specifically, ASTM C1363 section 10.11 prescribes that the test is complete when, for a duration of five data acquisition runs, each measured variable does not vary from its mean over those five runs by more than the uncertainty of that variable. Further, each data acquisition run cannot be shorter than 30 minutes, meaning that steady state conditions must persist for at least 2.5 hours. These conditions are monitored for by the LabVIEW application, which automatically

terminates data recording when the conditions are met. Specifically for the Carleton University guarded hot box, and based on the uncertainties of the equipment used within the apparatus, the following five criteria constitute steady state:

- Climate side specimen surface temperature: the average temperature across the 12 thermocouples which monitor the surface temperature of the specimen on the climate side does not vary by more than 0.25°C in any given data acquisition run from the mean over the past five data acquisition runs.
- Metering side specimen surface temperature: the average temperature across the 12 thermocouples which monitor the surface temperature of the specimen on the metering side does not vary by more than 0.25°C in any given data acquisition run from the mean over the past five data acquisition runs.
- Air curtain temperature: the average temperature across the 6 thermocouples which monitor the air curtain temperature on the metering side does not vary by more than 0.25°C in any given data acquisition run from the mean over the past five data acquisition runs.
- Heat flow: in any given data acquisition run, the heat flow across the walls of the metering wall does not exceed 1% of the total heat delivered by the metered electric heating coil.
- Net energy: the net power delivered by the metered electric heating coil in any given data acquisition run does not vary from the mean power delivered across the past five data acquisition runs by more than 1%.

To ensure that steady state conditions are observed for a meaningful duration of time, the data acquisition run duration for the tests is set at 120 minutes. Each data acquisition run is the mean of 120 discrete data points; in other words, the conditions of the test are recorded at a one-minute interval.

6.2 Calibration and Validation

6.2.1 Thermocouple Calibration

Thermocouples, a relatively simple temperature measurement device, are crucial in a variety of experimental applications for the precise, continuous monitoring of temperature. In essence, a thermocouple is simply a cable composed of two sleeved wires of dissimilar material. This cable can be cut to length to accommodate the distance between the data acquisition terminal, and the location where the temperature is to be measured. At this sensor end, the thermocouple is terminated by soldering the two wires together. Due to the Seebeck effect, a voltage potential can be measured across this simple circuit at the data acquisition terminal, and this voltage correlates to the temperature at the sensor end. However, knowledge of the voltage potential is not sufficient; the reference junction temperature – the temperature at the end of the thermocouple cable – must also be known to calculate the sensor temperature. The relationship between these variables can thus be summarized with the following equation:

$$T_{sense} = T_{ref} + f(V_0) \qquad (6\text{-}1)$$

where T_{sense} represents the temperature at the sensor end, T_{ref} represents the reference junction temperature, and $f(V_0)$ represents the function which correlates the measured voltage potential to a temperature difference. A diagram which represents a typical thermocouple arrangement is shown below in Figure 6-8.

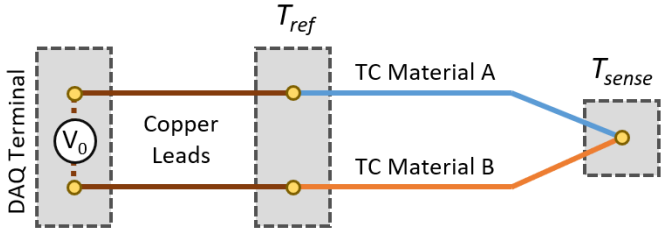

Figure 6-8: Simplified Diagram of a Thermocouple

The function which correlates voltage to temperature is dependent on the type of thermocouple used (which in turn depends on the two metals used in its manufacturing) and can be influenced by small deviations in manufacturing conditions. Manufacturers of thermocouple spools typically provide this function, but greater accuracy as well as a smaller uncertainty can be accomplished if the thermocouple spool is calibrated on-site. This is accomplished at the CABER lab using an automated calibration by comparison technique modified from the procedure described in ASTM E220, whereby the correlation function is determined by using thermal baths and highly sensitive platinum-resistance thermal detectors. In this procedure, the reference junction of a thermocouple sample is submersed into a thermal bath which is held at a constant temperature. The sensor end of the thermocouple is submersed into a second bath, which cycles its temperature across the range of temperatures the thermocouple is expected to operate in, between -30°C and 75°C in 5°C increments. The voltage recorded by a DAQ card at each discrete temperature is used to determine a third order polynomial relationship between the temperature and the thermocouple voltage. This operation repeats at four distinct reference junction temperatures (15°C, 20°C, 25°C and 30°C), allowing an interpolation process to be used to accurately determine the measured temperature of the thermocouple's sensor end based on the reference junction temperature, which is typically at room temperature.

Figure 6-9 below shows a thermocouple calibration procedure in process; the right thermal bath maintains the reference junction at a constant temperature, and the left thermal bath cycles the sensor end of the thermocouple across a range of temperatures. The thermocouple is attached to the CompactDAQ in the centre, which records the voltage potential generated. This process, which takes several days to complete, must be repeated for each new thermocouple spool. Type T thermocouples are used in this experiment.

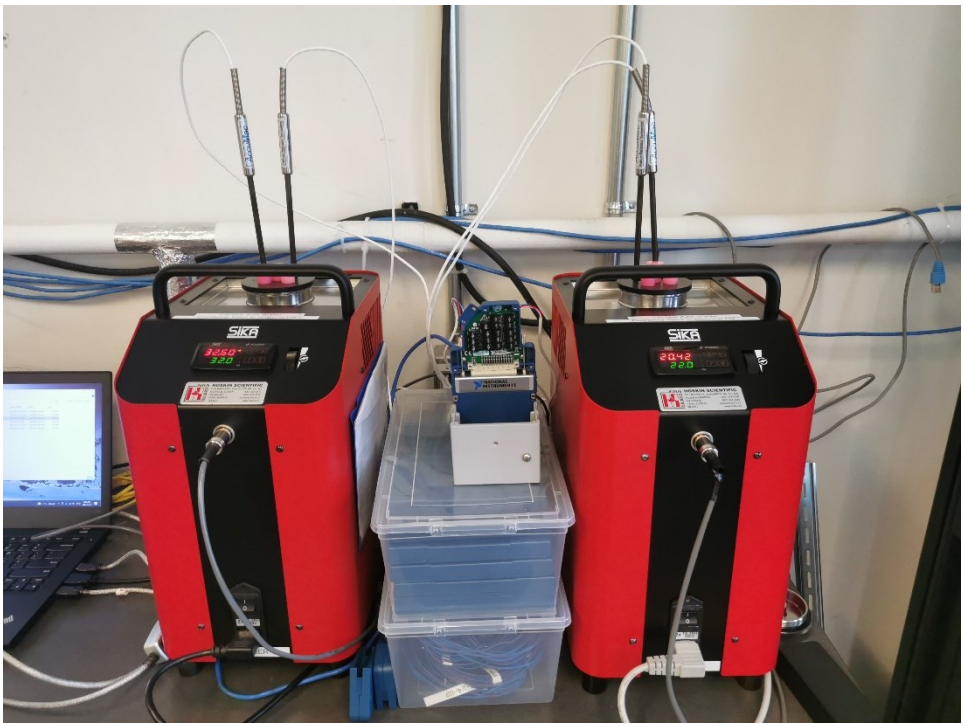

Figure 6-9: Thermal Baths Used in the Calibration of Thermocouples and Thermopiles

6.2.2 Thermopile Calibration

While thermocouples are effective at accurately measuring the temperature at a location, the inclusion of the reference junction temperature is responsible for a significant portion of the uncertainty on the final measurement. When the actual temperature is not as important as the temperature difference across two points, a thermopile can measure this difference more precisely, by effectively making one side of the temperature gradient the reference junction. This is accomplished by wiring multiple thermocouples from the same spool in series, with alternating wire material. Each node where two dissimilar materials are soldered together becomes a lead, and as long as the leads alternate on either side of the temperature gradient, the voltage measured across this circuit will correlate to the temperature difference. If there are multiple leads on each side of the temperature gradient, the average temperature between the leads is determined. A larger number of thermopiles further decrease the uncertainty in the temperature difference measurement,

as the voltage signal scales proportional to the number of leads, and therefore the impact of the voltage reading error from the DAQ decreases. A simplified diagram of a 6-lead thermopile (that is, a thermopile with 6 leads on either side of the temperature gradient) is shown in Figure 6-10.

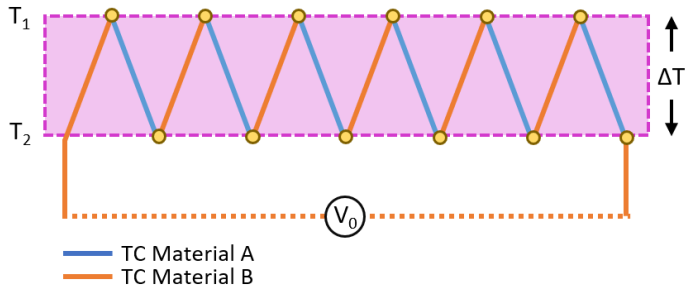

Figure 6-10: Simplified Diagram of a 6-Lead Thermopile

As with thermocouples, the relationship between voltage potential measured and temperature difference can be determined experimentally and modelled using a third-order polynomial. This can also be accomplished using a calibration by comparison technique, with the leads on one side of the thermopile submersed into one thermal bath, and the leads from the other side submersed in the other. The difference in temperatures between the two baths creates a voltage difference, which is measured using CompactDAQ. Unlike thermocouples, manufacturers do not typically provide the voltage-temperature relationship for thermopiles (as it varies with the number of leads wired), and thus the relationship must be determined experimentally.

6.2.3 Guarded Hot Box Validation

Before commencing with the testing of the proposed wall concepts, it was necessary to ensure that the thermal resistance results produced by the guarded hot box reliably and accurately reflect the real performance of the walls. To this end, the values of thermal resistance recorded by the guarded hot box needed to be compared to the results developed by a different method. This was accomplished by using a guarded hot plate apparatus that is validated to the ASTM C177 standard. The Carleton University guarded hot plate is shown below, in Figure 6-11.

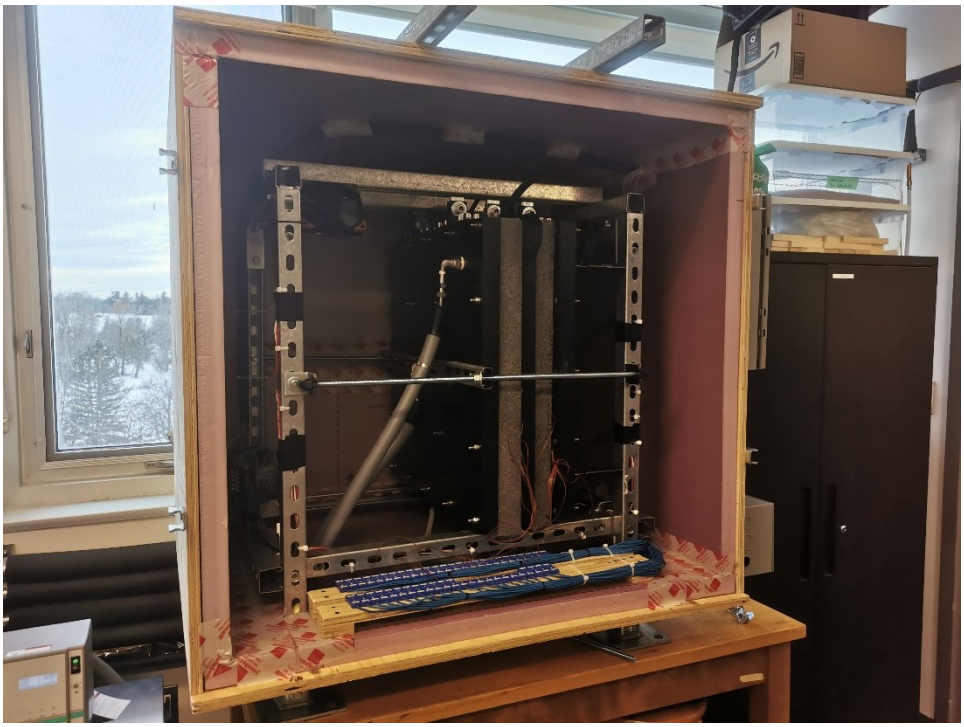

Figure 6-11: The Guarded Hot Plate Apparatus

The guarded hot plate can be used to determine the thermal conductivity through small samples of insulation material with great accuracy. This apparatus was used to measure the thermal conductivity of a sample of GPS foam with a thickness of 5.08 cm (2 inches), and the results were compared with those produced by the guarded hot box when installed with a “calibration wall sample”; a continuous layer of GPS insulation that is 10.16 cm (4 inches) thick (representing two layers of rigid insulation – doubling the thickness of insulation increases the effective thermal resistance and improves the accuracy of the result). Panels of insulation were attached together using sheathing tape. The calibration wall sample is shown installed in the guarded hot box and ready for testing below in Figure 6-12.

Figure 6-12: The Calibration Wall Sample Installed in the Guarded Hot Box

The measured thermal resistance per metre of insulation from each method is shown calculated below in Table 6-1. The thermal resistivity of most materials, including GPS insulation, is dependent on the average temperature across the material. Because there was a discrepancy between the average temperature of the plates in the guarded hot plate apparatus, and the average temperature between the chambers in the guarded hot box apparatus, the RSI value at the average temperature of the GHB in the guarded hot plate was determined by linearly interpolating between two different temperature setpoints for the GHP data to the average temperature between the guarded hot box chambers, 1.35°C.

Table 6-1: Comparison of Results between the Guarded Hot Plate and Guarded Hot Box

Measurement Method	Effective RSI [K·m^2/W]	Effective RSI / m [K·m/W]
Guarded Hot Plate	1.86 ± 0.13	34.5 ± 2.5
Guarded Hot Box	3.89 ± 0.28	36.0 ± 2.5
GHB, film coef. correction	3.74 ± 0.28	34.6 ± 2.5

The discrepancy observed between the results is thus 1.51 K·m/W, or 4.2%. This discrepancy can largely be attributed to the film effect which occurs during convective heat transfer, which effectively increases the thermal resistance of the sample in the guarded hot box. This effect does not apply in the guarded hot plate because heat transfer occurs through conduction. When the assumed film coefficients presented in Table 5-2 are taken into consideration by subtracting their reciprocals from the effective RSI value for the guarded hot box, the effective RSI per metre value is adjusted to 34.65 K·m/W, only 0.12 K·m/W or 0.35% higher than the result determined using the guarded hot plate. It was decided that this level of uncertainty is satisfactory for the purposes of this experiment.

6.3 Experimental Approach

Three wall concepts outlined in Chapter 4 were selected for further experimental testing: (1) the rigid external insulation concept; (2) the rigid insulation with stud grooves concept, and; (3) the offset-framed wall with L-shaped insulation concept. These wall concepts were selected by vote by a panel of industry experts during a second design charette held on September 28th, 2021. The participants of the charette, which included the same guests as the first charette described in Section 3.1, voted on the designs based on their modelled thermal performance, their constructability, and their suitability for the residential sector. The selected concepts were considered for applications involving their construction on-site, as well as prefabricated applications; for example, it was identified that the offset-framed concept may be more suitable if it is assembled in a highly controlled setting using engineered lumber, which may be more compliant with dimensioning and tolerancing, and hence reduce the risk of air cavities between structural members and elements of the rigid insulation.

6.3.1 Rigid External Insulation Concept

The first wall concept assembled is the rigid external insulation concept. To build the concept, first, a stud frame was assembled using "two by four" structural members of spruce-pine-fir (SPF) class lumber. This type of lumber is the most commonly used in wood frame construction across Canada. Although nails are far more common in typical construction because they are quicker to insert, the framing members were assembled together using wood screws to allow for easy disassembly. The stud spacing used, shown illustrated in Figure 6-13, was chosen to ensure that the boundaries of the metering box (shown in the illustration in red) overlaps with the studs. In this manner, the results of the experiment better represent the framing ratio of a typical wall. The outer dimensions of the wall assembly were chosen such that they allow for 2 cm of clearance between the specimen and the walls of the guarded hot box specimen mount; this ensured that the specimen can be easily installed using regular screws and sealed against the edges of the frame using sheathing tape.

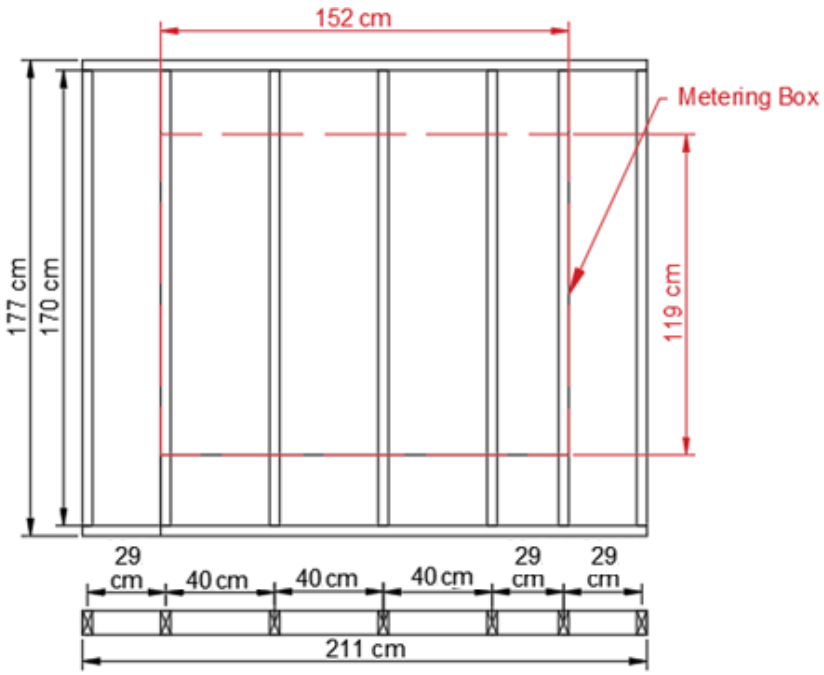

Figure 6-13: Stud Spacing Diagram for Assembled Concepts

On the outboard surface of the framing members, a 127 mm (1/2-in) thick plywood sheathing layer was attached using wood screws. Two equally sized, vertically installed sheets of sheathing were used to ensure full coverage of the specimen surface. To abate air leakage through the gap between the two plywood sheets, it was filled with spray foam insulation and the foam was subsequently trimmed and covered with sheathing tape. After the sheathing was installed, blankets of Rockwool mineral wool batt insulation were used to insulate the stud cavities on the interior of the wall assembly. The wall frame with batt insulation installed is shown in Figure 6-14. After the installation of the batt insulation, a layer of 6-mil polyethylene sheeting was installed over the insulation. This sheet is commonly used in Canadian wood frame construction as the primary vapour barrier. A 127 cm (1/2-in) thick gypsum board was then installed over the polyethylene sheeting over the entire surface area of the wall specimen; this layer is used as the finishing surface of a typical Canadian wood frame wall, and it doubles as a fire-retardant layer.

Figure 6-14: Rigid External Insulation Concept During Assembly

Finally, the external rigid insulation layer was installed to the outboard surface of the plywood sheathing layer. Although phenolic foam was the preferred insulation material for use in this wall concept, supply chain issues associated with the COVID-19 pandemic have severely constrained the supply of phenolic foam insulation boards in North America, making them impossible to source for a reasonable cost and within the timeframe allocated to this project. For this reason, more readily available GPS insulation boards were used in the assembly of this wall concept. Two 508 mm (2 inch) GPS boards were installed, one over the other, and secured against the plywood sheathing using 6-inch wood screws and large washers. With the wall specimen now fully assembled, it was transferred into the guarded hot box middle frame, where it was secured using wood screws and sheathing tape.

Throughout the assembly process, 16 thermocouples were embedded into the specimen. The thermocouples were installed at 4 locations across the surface of the wall, with each location having 4 thermocouples, one at each distinct layer of the wall assembly. Two of the 4 locations represented sites which interface with stud locations, and the other two were at the centre of stud cavities. A diagram showing the locations of the thermocouples is shown below in Figure 6-15; the red crosses represent the locations in these profile and top views of the assembly. The purpose of these embedded thermocouples is to observe the temperature gradient across the wall specimen, so that it can be compared with the steady state results produced by the modeling methods. On the outboard and inboard surfaces of the wall specimen, 12 thermocouples and 12 thermopile leads were arranged in a grid pattern within the metering area; both TCs and TPs were used simultaneously so that the TPs could produce an accurate temperature difference across the specimen value for the evaluation of the thermal resistance and the TCs could be used to assess the temperature grid across the surfaces.

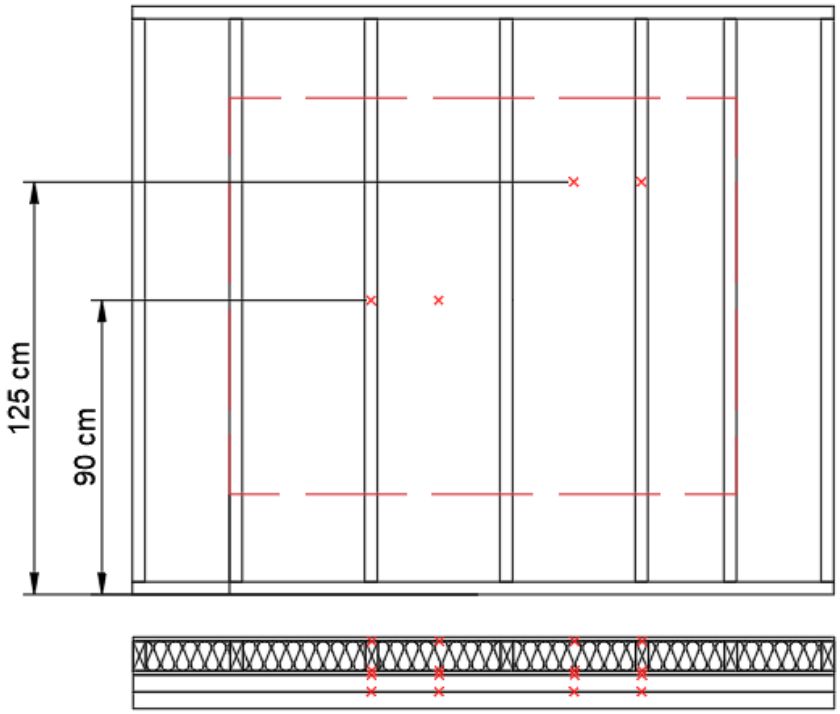

Figure 6-15: The Locations of Embedded Thermocouples in the Wall Assemblies

After being assembled and installed into the guarded hot box, the wall specimen underwent three separate runs with temperature setpoints of -25°C in the climate chamber, and 25°C in the metering chamber. Other climate chamber setpoints were also attempted (-15°C and -5°C), but reliable, repeatable results could not be produced, likely due to flanking heat losses across the specimen. Each experimental run was carried out with an iteration duration of one minute (that is, the conditions in the specimen were sampled once every minute), with check durations of 120 minutes. Each test run would conclude once the steady state criteria outlined in Section 6.1.5 were met for a duration of 5 checks (or in other words, 10 hours). During testing, it would typically take the specimen about 10-15 hours to reach steady state from room conditions, meaning that each test run would take about 20-25 hours to complete.

Occasionally, test runs had trouble meeting the *Net Energy* criterion, which required each check's net energy delivered to the metering chamber's heating coil not to vary by more than 1% from

previous checks. This typically occurred when heat energy was delivered to the coil immediately before the end of a check, or at the very beginning of a new check. This would cause a larger perceived heat input variation between the checks. Averaging these heat input across the two checks they border would typically allow this steady state criterion to be met. When such instances were identified, the test would be manually turned off, and the run would be considered to have reached steady state. This could have been avoided if a longer test period was used; however, issues of freezing which are discussed below prevented the guarded hot box from running for prolonged periods of time.

6.3.2 Rigid Insulation with Stud Grooves Concept

Upon the completion of testing for the rigid exterior insulation concept, the wall specimen was removed from the guarded hot box and disassembled down to the framing. The framing, a diagram for which is shown in Figure 6-13, was also reused for the rigid insulation with stud grooves concept. This was done to reduce the cost and waste associated with the testing, and to reduce the variability in the wall specimens' material properties. To assemble the rigid insulation with stud grooves concept, 254 mm (1 inch) thick GPS insulation panels were cut to size and installed into the frame stud cavities. These panels were secured in place to the outboard face of the framing members using sheathing tape, and this is shown in Figure 6-16. Two layers of GPS insulation, each 508 mm (2 inch) thick, were then installed over top of the stud cavity GPS insulation, and a 127 mm (0.5 inch) thick layer of plywood sheathing was installed over those. The sheathing was attached to the framing using long 6-in wood screws, which also secured the insulation layers in place with compression.

Figure 6-16: GPS Insulation Installed Inside the Stud Cavities

On the interior side, 6.35 cm (2.5 inch) thick Rockwool mineral wool insulation blankets were installed to fill up the remainder of the stud cavity volume. A polyethylene sheet was then installed over the mineral wool insulation and framing members, before being covered by a 1.27 cm (0.5 inch) thick gypsum board, which was attached to the framing using drywall screws. As with the first wall concept, 16 thermocouples were embedded across the layers of the wall assembly (in locations identical to those shown in Figure 6-15), and both thermocouples and thermopiles were used on the surfaces of the wall specimen. Data collection for this wall concept was carried out in a manner identical to that described for the previous wall concept, with three runs having been carried out with temperature setpoints of -25°C in the climate chamber, and 25°C in the metering chamber.

6.3.3 Offset-framed Wall with L-shaped Rigid Insulation Concept

The final wall concept experimentally tested was the offset-framed wall with L-shaped rigid insulation. For this concept, a new structural frame had to be assembled using new SPF lumber. "Two by six" (510 mm by 152 mm nominally) studs were used as top and bottom plates, between which "two by four" (51 mm by 102 mm nominally) studs were attached, with each stud alternating its location between being flush with the inboard and outboard surfaces of the wall. As with the other two concepts, the framing arrangement was designed so that studs are located at the interface points with the boundaries of the metering area. The framing plan for the concept is shown below in Figure 6-17.

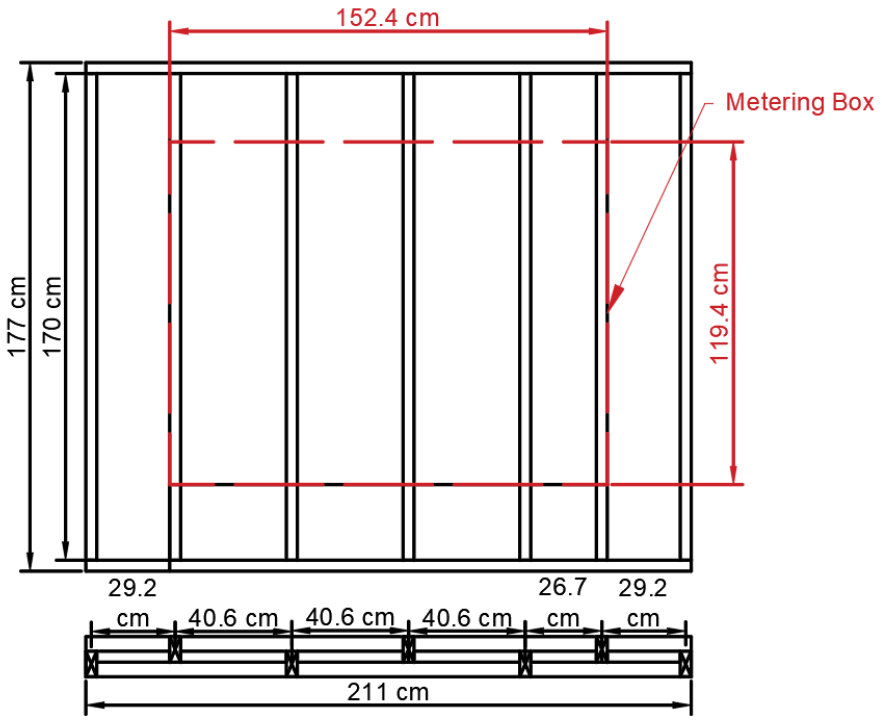

Figure 6-17: Framing Plan for the Offset-framed Wall Concept

A photograph of the assembled framing for the wall concept is shown below in Figure 6-18. Wood screws were used in the assembly of the frame instead of the more ubiquitous framing nails to increase the ease of disassembling the specimen after testing.

Figure 6-18: Assembled Framing for the Offset-framed Wall Concept

After the framing was assembled, 510 mm (2 inch) and 380 cm (1.5 inch) thick XPS insulation panels were cut to size such that they occupy the entire volume between studs. XPS insulation was used instead of the preferred insulation material, phenolic foam, due to supply issues associated with the COVID-19 pandemic. The 510 mm-thick insulation pieces were installed in line with the framing members, along the edges of the wall surfaces, whereas the 380 mm-thick pieces occupied the interstitial volume in the middle. In this manner, the entire wall assembly volume was either occupied by rigid XPS insulation, or structural members. The insulation panels were secured in place with wood screws against the framing members. Finally, due to the structural members not being perfectly straight, upon installation some air cavities remained between the insulation panels and framing members; these air cavities were filled using PUR spray foam insulation. This reduced the likelihood of air leakage across the wall specimen. Figure 6-19 shows the offset-framed wall concept at this stage of construction.

Figure 6-19: The Offset-framed Wall Concept with Insulation Installed

After the spray foam insulation dried and any excess was cut with a utility knife, the inboard surface was covered with polyethylene sheeting and a 127 mm (0.5 inch) thick gypsum board, which was attached to the framing using drywall screws. On the outboard surface, a 127 mm (0.5 inch) thick plywood sheathing layer was installed using wood screws. Throughout the construction of this wall specimen, thermocouples were embedded to assess the temperature gradient across the wall in a manner similar to that of the two previous wall concepts, and both thermocouples and thermopile leads were attached to the surfaces of the wall. Upon completion of the construction, this wall specimen was tested in a manner identical to the other wall concepts, by conducting three testing runs, with temperature setpoints of -25°C in the climate chamber, and 25°C in the metering chamber.

7. Results and Analysis

The thermal performance validation experiment described in detail in Chapter 6 was conducted on the three wall assemblies. In this chapter, these results are analyzed, and their uncertainties are determined, and the results are subsequently used to calibrate and validate THERM numerical models for each wall. A discussion follows based on these results and the experience of building each wall assembly to determine the suitability of each in integration in conventional wood-frame residential construction.

7.1 Experimental Testing Results

Table 7-1 below presents the thermal resistance results of the experimental testing conducted on the wall specimens assembled. Each wall specimen was assembled to the specifications described in Section 6.3 and installed into the guarded hot box. Each was then subjected to setpoints of -25°C in the climate chamber and 25°C in the metering chamber. These setpoints remained constant for 24 hours, until each wall specimen reached steady state as identified by the parameters outlined in Section 6.1.5. The five checks – each two hours long with samples taken every minute – which constitute the period of time during which the specimen was at steady state were then averaged to determine the RSI values presented in the results.

Table 7-1: Experimental Testing Thermal Resistance Results

Wall Assembly	Trial 1 $K \cdot m^2/W$	Trial 2 $K \cdot m^2/W$	Average $K \cdot m^2/W$
Rigid External Insulation	5.23	5.22	5.23
Rigid Insulation with Stud Grooves	5.97	5.83	5.90
Offset-framed Wall with L-shaped Rigid Insulation	4.65	4.68	4.66

To calculate these results, a total of five data points was needed: the temperature difference across the first thermopile, the temperature difference across the second thermopile, the temperature

difference across the walls of the metering chamber, the energy input into the metering chamber's heater over the period of recording, and the metering surface area. The thermal resistances were then calculated using Equation (7-1):

$$\mathrm{RSI} = \frac{\Delta \mathrm{T} * \mathrm{A}}{\mathrm{E} - \mathrm{E_{loss}}} \qquad (7\text{-}1)$$

where ΔT is the average of the temperature differences across the thermopiles, A is the metering surface area, E is the heater input, and E_{loss} is the energy loss across the walls of the metering chamber to the guard chamber, which in turn is calculated as shown in Equation (7-2):

$$\mathrm{E_{loss}} = \frac{\Delta \mathrm{T_{MWall}} * \mathrm{A_{MWall}}}{\mathrm{R_{MWall}}} \qquad (7\text{-}2)$$

where ΔT_{MWall} is the measured temperature difference between the interior and exterior of the metering wall, A_{MWall} is the interior surface area of the metering wall, and R_{MWall} is the thermal resistance of the walls of the metering chamber.

These results demonstrate that all three wall concepts tested accomplish a thermal resistance per unit thickness of wall of at least 5.23 K·m^2/W, with the offset-framed concept accomplishing the highest thermal resistance per thickness, at 28.24 K·m/W. The rigid exterior insulation concept and the rigid insulation with stud groove concept accomplished a resistivity of 24.22 K·m/W and 27.33 K·m/W, respectively. In comparison, a typical wall framed with "2 by 6" studs and insulated with batt cavity insulation would achieve a thermal resistance per thickness of 19.14 K·m/W.

The following are the results of the embedded thermocouple readouts which will be used in combination with the temperature gradients produced by THERM to calibrate the thermal performance models. TC locations along the thickness of the wall are depicted in Figure 7-1; it is good to note that TC locations 1 and 4 are in-line with structural framing members, whereas

locations 2 and 3 are situated in the middle of stud cavities. The numerated wall locations represent the positions along the thickness of the wall, with location 0 representing the interior surface, location 1 behind the drywall, location 2 behind the stud or stud cavity, location 3 behind the sheathing, and location 4 representing the exterior surface.

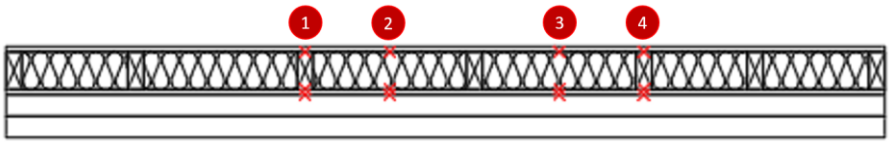

Figure 7-1: Locations of Embedded TCs in the Rigid Exterior Insulation Concept

Table 7-2 presents the embedded TC temperature results for the rigid exterior insulation concept. These temperatures are the product of averaging across the five checks which represent the steady state of the test.

Table 7-2: Temperatures of Embedded Thermocouples, Rigid Exterior Insulation Concept

Wall Location	TC Location 1	TC Location 2	TC Location 3	TC Location 4
0	23.54	23.54	23.54	23.54
1.27	21.92	23.37	23.39	22.89
10.16	9.06	7.29	8.55	9.38
11.43	5.12	4.92	6.56	6.90
21.59	-18.13	-18.13	-18.13	-18.13

The aforementioned results for the rigid exterior insulation concept are represented below in Figure 7-2 to better graphically illustrate trends in the temperature gradient across the thickness of the wall.

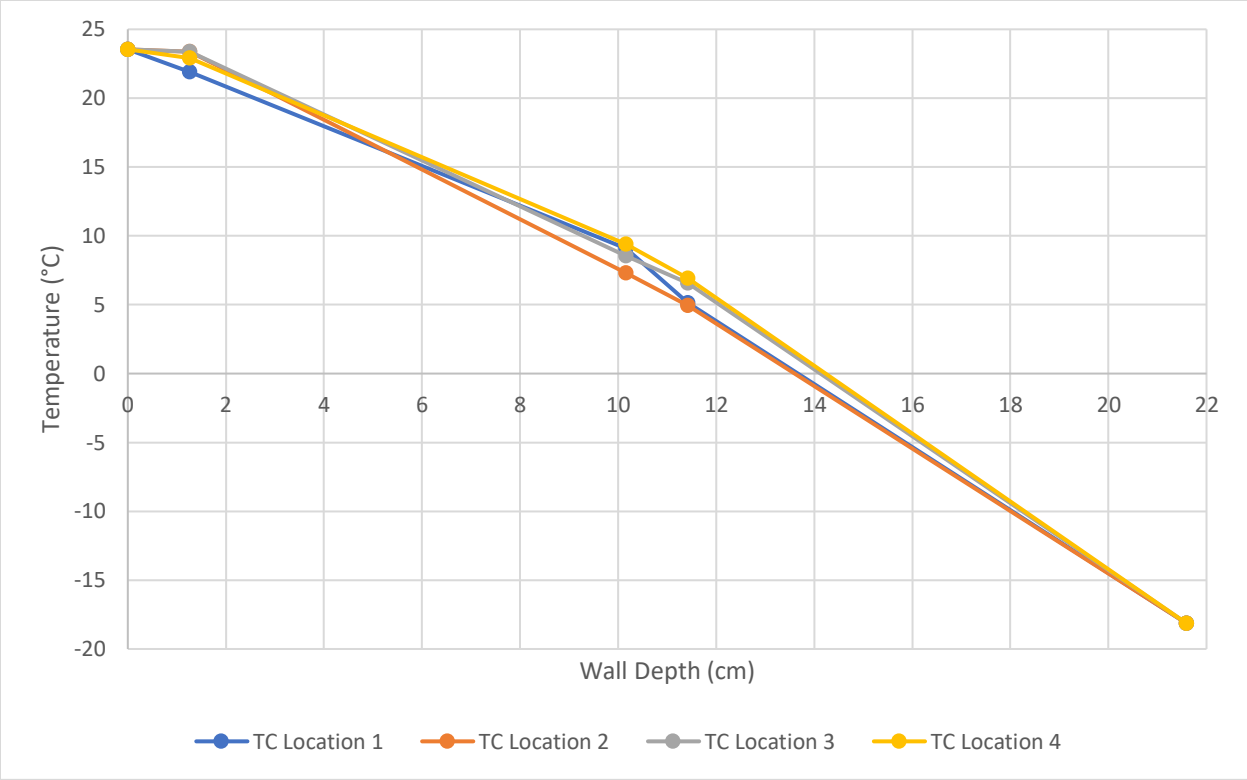

Figure 7-2: Temperatures of Embedded Thermocouples, Rigid Exterior Insulation Concept

The results for the embedded TC temperatures for the stud groove rigid insulation concept are presented below in Table 7-4. As with the previous concept, TC locations 1 and 4 represent locations which interface with the structural framing members, whereas locations 2 and 3 represent the centres of stud cavities; the locations along the thickness of the wall are identical to those presented in Figure 7-1 for the rigid exterior insulation concept.

Table 7-3: Temperatures of Embedded Thermocouples, Stud Groove Rigid Insulation Concept

Wall Depth [cm]	TC Location 1 [°C]	TC Location 2 [°C]	TC Location 3 [°C]	TC Location 4 [°C]
0	23.74	23.74	23.74	23.74
1.3	23.24	22.91	23.64	23.11
10.2	8.54	12.37	7.99	11.61
20.3	-15.66	-15.37	-15.46	-15.58
21.6	-18.04	-18.04	-18.04	-18.04

Figure 7-3 below is a scatterplot of the results presented in Table 7-3 for the stud groove rigid insulation concept.

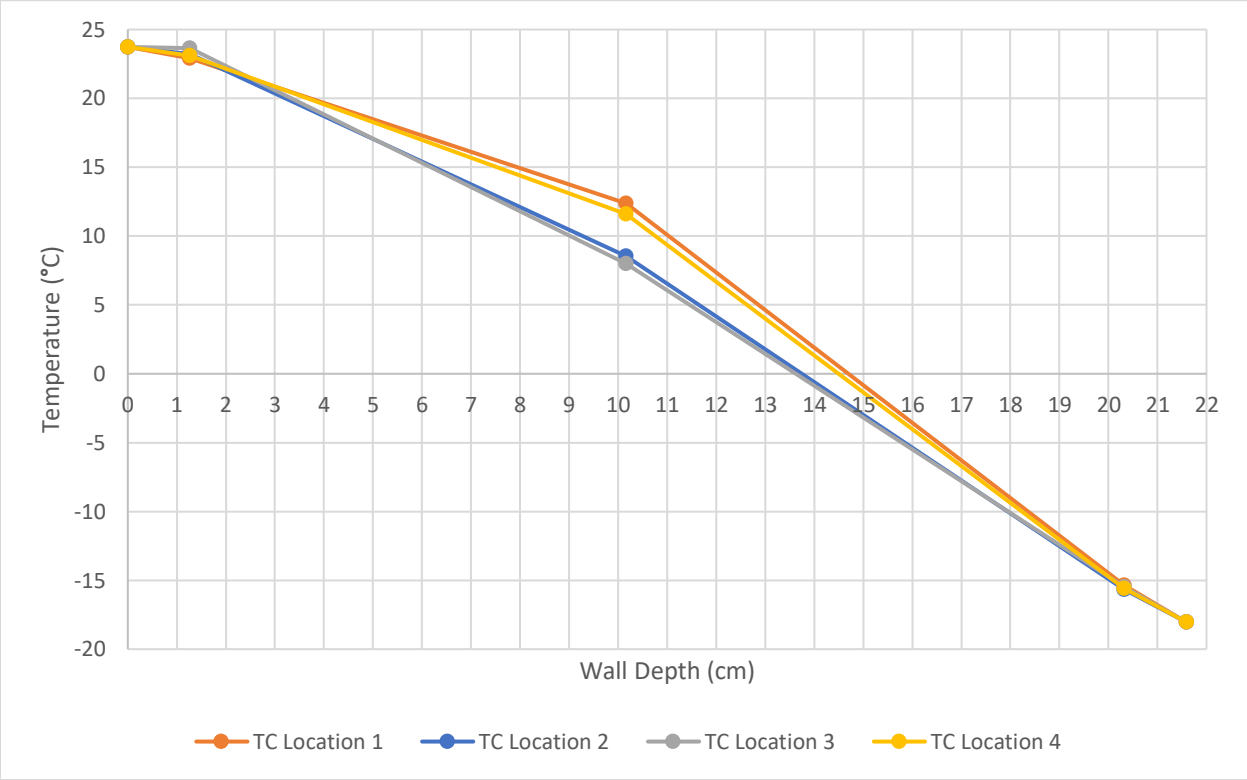

Figure 7-3: Temperatures of Embedded Thermocouples, Stud Groove Rigid Insulation

Only three TC locations were selected along the cross-section of the offset-framed L-shape insulation concept, with up to 6 TCs at each location; the positions of these TCs is as follows: wall location 0 corresponds to the interior surface, wall location 1 is behind the drywall, wall location 2 is behind the first 5.08 cm (2-in) layer of insulation, wall location 3 is behind the second 3.81 cm (1.5-in) layer of insulation or behind the interior-facing stud, wall location 4 is behind the third 5.08 cm (2-in) layer of insulation or behind the exterior-facing stud, and wall location 5 is on the exterior surface of the wall. The positions are illustrated in Figure 7-4.

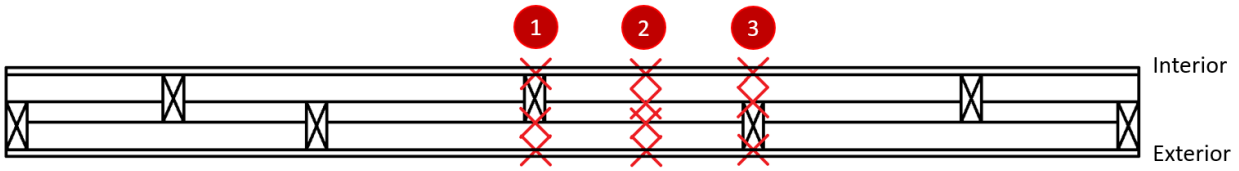

Figure 7-4: Locations of Embedded TCs in the Offset-framed L-shaped Insulation

Table 7-4 below presents the temperatures recorded by the TCs embedded in the offset-framed L-shape insulation concept. Note that TC location 1, wall location 2, and TC location 3, wall location 3 do not have temperature readings as the wall planes of these points intersect with the interior of the framing member and are therefore not instrumented.

Table 7-4: Temperatures of Embedded Thermocouples, Offset L-shape Insulation Concept

Wall Depth (cm)	TC Location 1 [°C]	TC Location 2 [°C]	TC Location 3 [°C]
0	23.29	23.29	23.29
1.3	22.92	23.26	23.16
6.3	-	9.34	6.64
10.2	4.75	-1.68	-
15.2	-13.88	-15.24	-14.67
16.5	-18.01	-18.01	-18.01

Finally, Figure 7-5 graphically illustrates the results presented for the offset-framed L-shape insulation concept in Table 7-4.

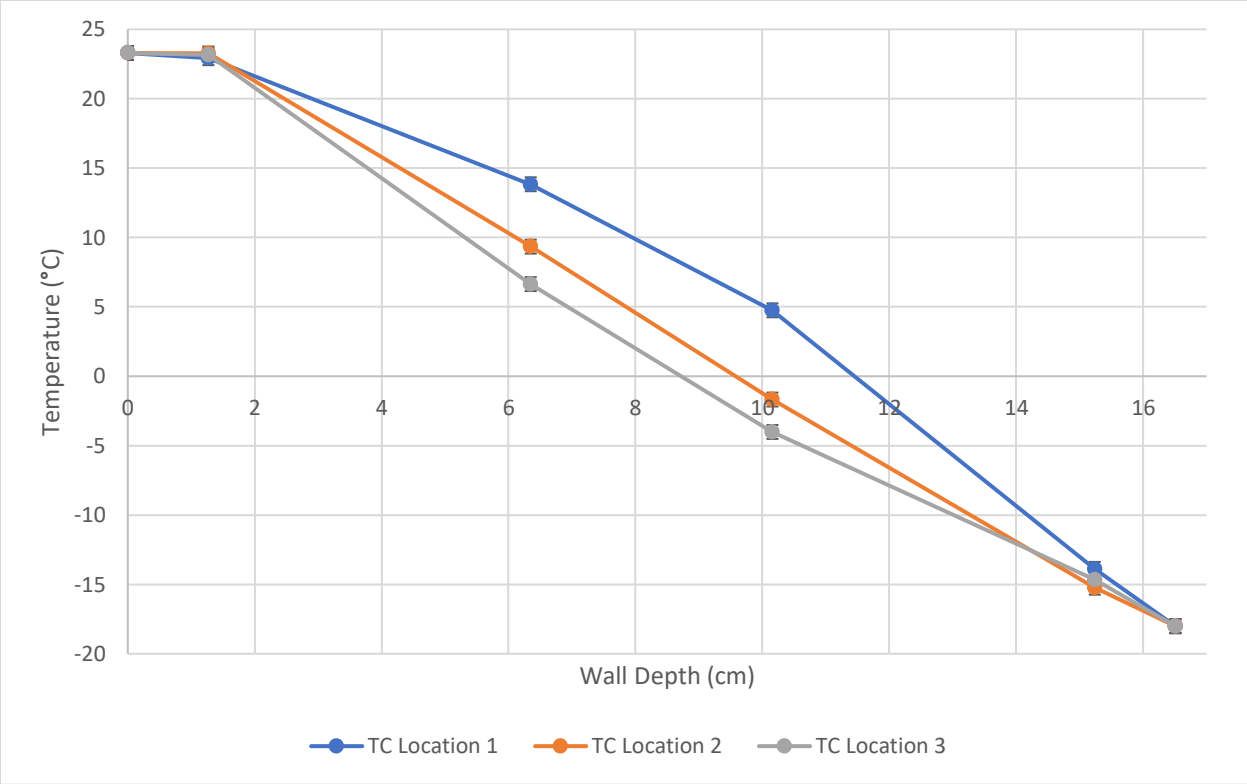

Figure 7-5: Temperatures of Embedded Thermocouples, Offset L-shape Insulation

7.2 Uncertainty Analysis

In this section, the uncertainty associated with the effective thermal resistance results determined using equations (7-1) and (7-2) is calculated using the data obtained during experimental testing. Taken into account for the uncertainty determination are both the quantity of data measured, as well as the quality of the instruments used to measure the data. A 99% confidence interval based on the acquired steady state for thermopile temperature difference and surface and embedded temperature measurements was used. A total of 3 measured values are included in the effective thermal resistance measurement, including the temperature difference across the specimen, the heat input into the metering chamber, and the temperature difference across the walls of the metering chamber.

To determine the uncertainty in the measurement of the temperature difference across the specimen as recorded by the thermopiles, equation (7-3) is used, as shown below. In this equation, the uncertainty of a temperature reading by one of the thermopiles, $U_{\Delta T_i}$, is determined using the bias of the thermopiles used, $B_{\Delta T}$, which is equal to 0.27 ˚C, and the precision of measurement based on a 99% confidence interval, $B_{\Delta T_i}$.

$$U_{\Delta T_i} = \sqrt{B_{\Delta T}^2 + P_{\Delta T_i}^2} \qquad (7\text{-}3)$$

The total uncertainty in the temperature difference reading, $U_{\Delta T}$, is determined using equation (*7-4*), whereby the sum of the squares of the individual uncertainties is evaluated based on the use of two individual thermopiles.

$$U_{\Delta T} = \sqrt{\sum_{i=1}^{N} \left(\frac{U_{\Delta T_i}}{N}\right)^2} \qquad (7\text{-}4)$$

Based on this approach, the uncertainties in the temperature difference across the specimen for each wall assembly are ± 0.28 ˚C, ± 0.28 ˚C and ± 0.46 ˚C for the first, second, and third wall assemblies, respectively. The lower uncertainty values for the first two wall assemblies reflect a low degree of temperature variation on the surfaces of the specimen, with the instrument bias being the predominant source of uncertainty. The third wall assembly saw greater variation in surface temperature, and the total uncertainty value reflects this.

To evaluate the error associated with the metering chamber heater input, equation (7-5) is used. Here, *E* represents the measured energy input, *a* is the power meter's nominal accuracy of 0.5%, and *b* is the value of a single pulse increment, 0.375 Wh.

$$U_E = aE + b \quad (7\text{-}5)$$

The total uncertainty associated with the measurement of the power input over the course of each test is thus calculated to be ± 0.5 Wh for each of the three wall assemblies.

Finally, the uncertainty in the energy loss through the walls of the metering chamber must be assessed using the uncertainty in the temperature readings for the exterior and interior surfaces of the metering chamber. There are 5 thermocouples measuring temperatures on the interior surface and 5 on the exterior surface of the metering box, with the temperature each set of five thermocouples records averaged for each check, and the total temperature difference determined by finding the difference between the exterior and interior surface temperatures. Using equations (7-3) and (7-4) adjusted to the biases and precisions associated with the readings of these thermocouples, the total uncertainty in temperature difference is equal to ± 0.27 ˚C, and since only the temperature difference affects the uncertainty in E_{loss}, the proportional uncertainty in E_{loss} is ±0.15 Wh.

To calculate the total uncertainty in the effective thermal resistance for each wall assembly, equation (7-6) is used, where the uncertainty is equal to the root square sum of the partial derivatives of each of the relevant variables with respect to effective thermal resistance.

$$\mathrm{U_{R_{eff}}} = \sqrt{\left(\frac{\partial \mathrm{R_{eff}}}{\partial \mathrm{E}}\mathrm{U_E}\right)^2 + \left(\frac{\partial \mathrm{R_{eff}}}{\partial \Delta \mathrm{T}}\mathrm{U_{\Delta T}}\right)^2 + \left(\frac{\partial \mathrm{R_{eff}}}{\partial \mathrm{E_{loss}}}\mathrm{U_{E_{loss}}}\right)^2}$$

$$\mathrm{U_{R_{eff}}} = \sqrt{\left(\frac{\Delta \mathrm{TAU_E}}{\mathrm{E^2 - E_{loss}}}\right)^2 + \left(\frac{\mathrm{AU_{\Delta T}}}{\mathrm{E^2 - E_{loss}}}\right)^2 + \left(\frac{\Delta \mathrm{TAU_{E_{loss}}}}{\mathrm{E - E_{loss}^2}}\right)^2} \quad (7\text{-}6)$$

When solving equation (7-6) for the three wall assemblies, the determined uncertainty for the effective thermal resistance of each wall assembly are ± 0.38 K·m^2/W, ± 0.38 K·m^2/W, and ± 0.35 K·m^2/W for the first, second, and third wall assemblies, respectively. The predominant proportion of the uncertainty calculated is associated with the determination of energy losses through the walls of the metering chamber; this is due to the relatively very small temperature differences determined across the walls, and the fact that thermocouples are used in finding the temperature difference instead of thermopiles, which tend to introduce a lesser degree of uncertainty. Nonetheless, each uncertainty value corresponds to no more than 7.3% of the total determined effective resistance for each wall.

7.3 THERM Model Calibration and Validation

By using the results of the experimental procedure presented previously, and in particular the results presented in Table 7-1, Table 7-3, and Table 7-4 with the temperature gradients produced by THERM and shown in *Appendix B: THERM Temperature Gradients*, the THERM models could be calibrated to better reflect the measured performance of the wall assemblies. This was carried out by fine-tuning the material profiles and geometric features of the models such that the overall temperature gradient across the cross section of the modelled wall matches the embedded TC temperatures. After performing this operation, the overall effective thermal resistance values calculated by THERM for each of the wall assemblies were determined, and these are presented and compared to the experimental results below in Table 7-5.

Table 7-5: Comparison of Calibrated THERM Results and Experimental Results

	Wall 1 R_{eff} [K·m^2/W]	**Wall 2 R_{eff} [K·m^2/W]**	**Wall 3 R_{eff} [K·m^2/W]**
THERM	5.69	5.89	4.53
Experimental	5.23 ± 0.38	5.90 ± 0.38	4.66 ± 0.35
% Difference	8.1%	-0.0%	-2.3%

Very good agreement is found between the THERM models and the experimental results for both the stud groove rigid insulation and the offset-framed L-shaped insulation concepts, with the THERM models predicting the effective thermal resistance for both wall assemblies to within the experimental uncertainty. However, no such agreement existence between the model and the experimental results for the rigid exterior insulation concept. This may at first appear to invalidate the THERM models altogether; however, closer examination of the experimental results for this wall specimen reveals that an issue which occurred during testing may have resulted in inaccurate results for the overall effective thermal resistance of the specimen. This issue is readily visible when plotting the temperature difference between the faces of the wall assembly over the course of the test, as was done below in Figure 7-6.

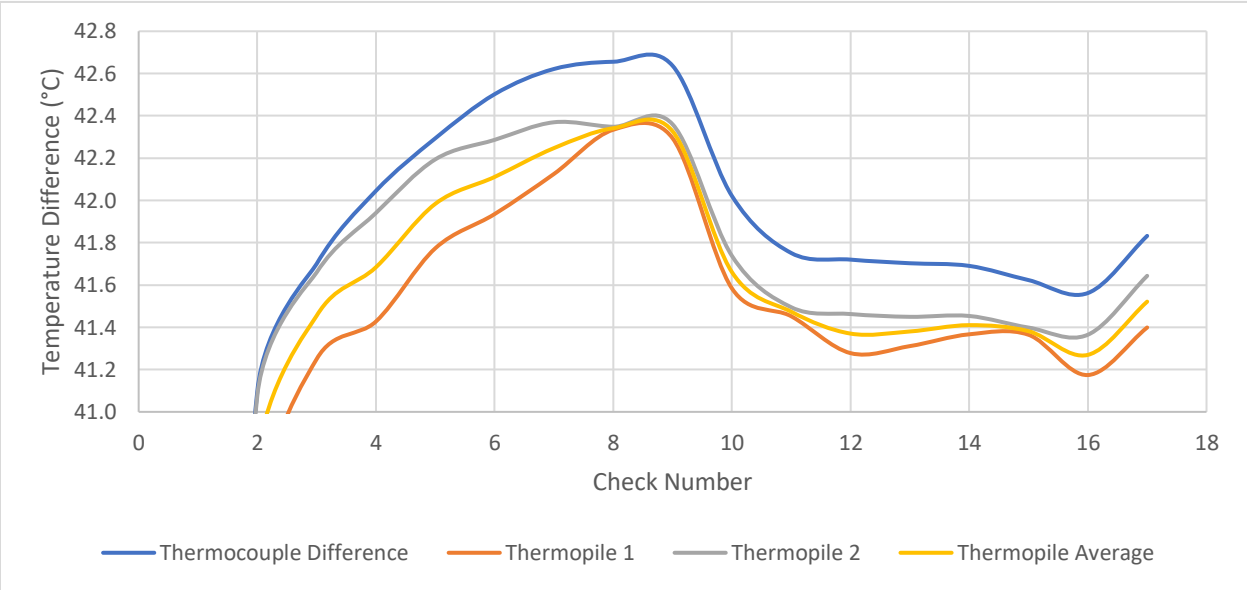

Figure 7-6: Temperature Difference vs. Check Number: Rigid Exterior

In this plot, it can be readily observed that up until check number 9 (that is, 18 hours into the test), the wall assembly was approaching thermal equilibrium, which would be seen as the temperature difference changing only negligibly over 5 or more checks. Instead, after the 10th check, a relatively significant decrease in temperature difference was measured, at which point the

temperature difference levelled. This can be compared with the temperature difference for a different wall specimen, shown below in Figure 7-7, where thermal equilibrium was clearly achieved between checks 5 and 9.

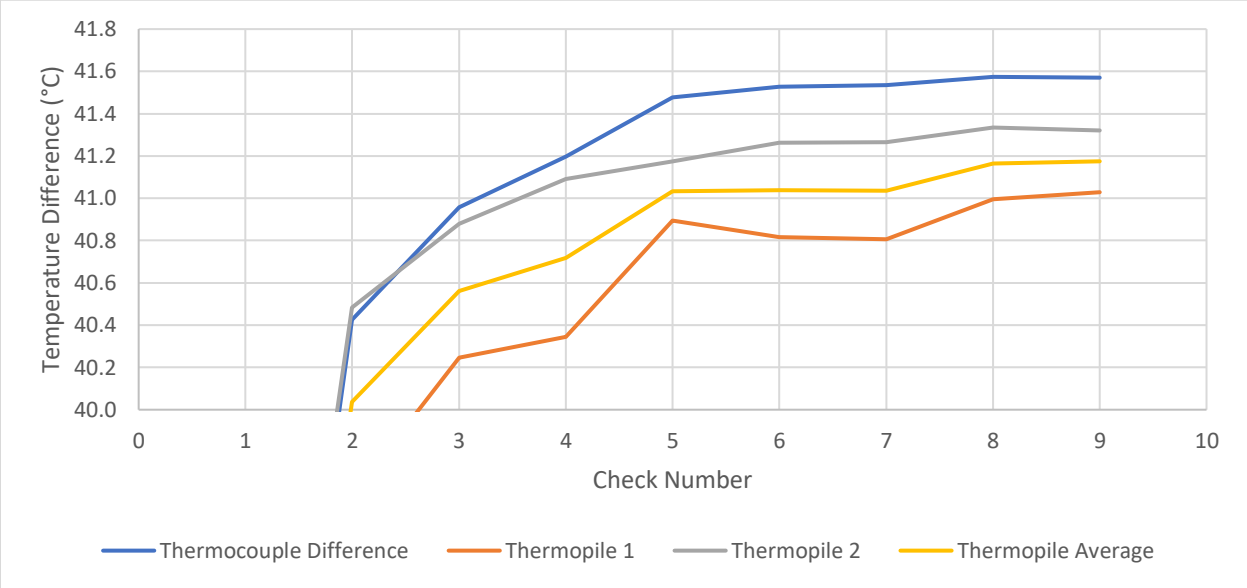

Figure 7-7: Temperature Difference vs. Check Number: Offset Wall with L-shape

After some troubleshooting, it was found that the cause for the sudden drop in temperature difference observed in Figure 7-6 was an accumulation of frozen condensate on the cooling unit's evaporator in the climate chamber. This deteriorated the cooling unit's performance, preventing it from accomplishing the desired climate chamber temperature until the test was stopped, and frozen condensate was allowed to melt. Unfortunately, this issue was only addressed after testing on the rigid exterior insulation concept was completed and the wall specimen disassembled, so testing could not be repeated. This issue is caused by ambient air moisture present in the lab space freezing against the cold components of the climate chamber after prolonged testing; because the relative humidity of the lab cannot be effectively reduced, the prevalence of this issue can only be reduced by either reducing the amount of time the guarded hot box continuously operates for, or by better insulating any components on which moisture condensates.

8. Conclusion and Further Work

Based on the experiences developed over the course of conducting the research presented in this thesis, it was found that novel wood-frame wall assemblies incorporating high performing nascent thermal insulation materials could serve as a suitable approach to reducing the environmental impact of heating newly built Canadian homes, while simultaneously being attractive to developers who wish to reduce the profile of the wall and thereby maximize indoor floorspace. It was found that the existing practice of using exterior sheathing insulation continues to be an effective approach to efficiently insulating a wall without significantly altering the traditional method of framing a wood-frame wall. However, using a higher performance insulation material such as phenolic foam instead of existing incumbent materials such as XPS will result in either a better insulated wall, or an equally well-insulated wall with a thinner profile. Based on the results of this work, it is recommended that additional research be conducted into the incorporation of phenolic foam insulation panels into Canadian residential construction.

Novel wall assemblies such as the offset-framed wall with L-shaped insulation panels, which require a reimagination of how a wall is framed, were shown to achieve a higher degree of thermal resistance per unit thickness of the wall, especially when incorporating highly thermally resistant nascent insulation materials. However, the construction of such a wall does entail several additional steps which increase the time required for framing, and additional training would be required of framers to ensure the assembly procedure is correctly carried out. These two factors may significantly increase the cost of such an implementation, negating the benefits of reduced floorspace loss. Additional cost benefit analysis should be carried out to assess the return on investment of such an approach.

Due to its relatively complicated geometry, the offset-framed wall assembly may be more appropriate for applications where a prefabrication of the wall assembly is possible. This would allow the framed and insulated wall to be simply transported and installed on-site after being built elsewhere. Prefabrication would allow for a tighter control of tolerances in framing, reducing or eliminating the chance of air gaps which reduce the wall's thermal performance. This would also eliminate the need for specially trained framers on site for the construction of the wall, and with sufficient automation of the assembly process, the time it takes to frame the offset wall can also be reduced to more closely match the length of construction for a conventionally framed wall.

8.1 Contributions to the Field of Research

The work presented in this thesis has contributed to the field of building envelope research in a variety of ways. These contributions are listed and described below.

- Development of an evaluation system for nascent, high performance insulation materials: based on the input of industry experts during a design charette, an approach to the evaluation and comparison of innovative insulation materials was developed for the purposes of the research presented in this thesis. This approach, outlined in full in Chapter 3, may be replicated to evaluate and compare different sets of insulations materials for a variety of applications beyond those discussed here.
- Development of an approach to estimating and comparing the environmental toll of different insulation materials: the approach undertaken to estimating the environmental cost of each insulation material based on its global warming potential as calculated in environmental product declarations and normalizing it to the material's thermal resistivity is novel, and may be replicated to compare other insulation materials, as well as different manufacturing approaches for the same material. This approach allows the direct

comparison of different materials and the consequences of their use on the environment. In future research, this approach can be adapted to assess the real cost of using a certain material over another by incorporating estimates for the financial costs associated with pollution, such as carbon taxes.

- Development of a variety of innovative, thin, and highly insulated wall assemblies: a diverse range of wall assembly designs has been presented in this research, which employ a variety of nascent approaches to the assembly of wood-frame walls. These approaches can be modified to meet the requirements of building codes, as well as project constraints and requirements, to achieve real improvements in the thermal performance of walls.
- Development of a modelling approach to the evaluation of thin, highly insulated wall assemblies, and the calibration of this approach using experimentally derived data: although the modelling approach presented here was developed for a specific use-case, its application can foreseeably be expanded to evaluate the performance of other designs of wood-frame wall assemblies, especially those which employ novel materials. The calibration parameters developed in this research can subsequently be used to develop more accurate models.
- The selection of promising wall assembly designs which merit additional research and testing: the wall assemblies which were selected to undergo further experimental testing in this thesis have shown promising results, and their assembly was not substantially more difficult than that of wall designs currently employed. These designs should undergo further research and testing to better understand how they can be employed in the Canadian market to reduce the environmental impact of newly-built homes.

8.2 Further Work

In addition to the aforementioned topics, the following is a list of additional inquiries which would contribute to the development of highly insulated thin walls.

- Integration of the investigated materials into the proposed wall assemblies: it has been shown that the nascent insulation materials investigated as part of this research could prove to be effective when integrated into thin, high-performance wall assemblies. However, due to supply chain constraints, phenolic foam and silica aerogel could not be sourced to be used in experimental testing. The first step in any future research should be securing the supply of these prospective materials.
- Design of an appropriate cladding and rain-screen system: due to the focus of this research on the thermal performance of the wall assembly, little consideration has been given to moisture control capabilities. A future investigation of high-performance thin wall assemblies should include the incorporation of a suitable cladding system, and one which likely includes a rain screen due to its ability to effectively shed bulk water. As part of this research, answering the question of how thin this rain screen system can be while remaining effective will be an important part of the research.
- Validation of hygric performance with in-situ testing: once wall assemblies have been assembled incorporating high performance insulation materials and a rain screened cladding system, the assemblies should undergo in-situ testing to validate their hygrothermal performance exposing them to real conditions. This type of experiment could be effectively conducted at Carleton University's new CABER facility, which incorporates instrumented cut-outs in the facility's walls for in-situ testing of envelope systems.

- Consideration of interfaces with fenestration and corners in the design of the wall systems: the simple wall assemblies considered in this thesis did not take into account any interfacing envelope components such as windows, doors, and wall corners. The manner in which these elements are framed into the wall assemblies proposed here must be considered for the effective elimination of thermal bridges and gaps through which air and moisture infiltration could take place.
- Consideration of biogenic and other low embodied carbon insulation materials: while the environmental impact of manufacturing the insulation materials considered in this research was taken into consideration in the selection of candidate materials, it was not a priority. With more research being published about the enormous impact of embodied carbon emissions on the overall lifetime emissions of a building, it would be prudent to consider whether the incorporation of less thermally insulative biogenic materials into the building envelope would benefit the overall reduction in emissions of the building. Biogenic materials are naturally derived materials such as hemp or hay which are often a bi-product, and which have a low or negative embodied carbon value.

References

[1] D. Coletto, "What do Canadians think about climate change and climate action?," *Abacus Data*, Oct. 28, 2021. https://abacusdata.ca/climate-change-cop26-canada/ (accessed Jun. 05, 2022).

[2] "2030 EMISSIONS REDUCTION PLAN Canada's Next Steps for Clean Air and a Strong Economy," Gatineau , 2022.

[3] R. Galvez and M. L. MacDonald, "Reducing greenhouse gas emissions from Canada's built environment: Report of the Standing Senate Committee on Energy, the Environment and Natural Resources," *Standing Senate Committee on Energy, the Environment and Natural Resources*, Nov. 2018. https://publications.gc.ca/site/eng/9.864789/publication.html (accessed May 23, 2022).

[4] "Keeping The Heat In - Section 2: How your house works," *Natural Resources Canada*, Apr. 27, 2021. https://www.nrcan.gc.ca/energy-efficiency/homes/make-your-home-more-energy-efficient/keeping-the-heat/section-2-how-your-house-works/15630 (accessed Jul. 13, 2022).

[5] "Durofoam EPS Rigid Insulation 96Inch X 48Inch X 1Inch | The Home Depot Canada," *The Home Depot Canada*, Jun. 2022. https://www.homedepot.ca/product/durofoam-eps-rigid-insulation-96inch-x-48inch-x-1inch/1000116769 (accessed Jun. 02, 2022).

[6] C. Lord, "Cost per square foot of Ottawa-Gatineau housing rising at fastest clip in Canada: Royal LePage," *Ottawa Business Journal*, Aug. 28, 2019. https://www.obj.ca/article/cost-

square-foot-ottawa-gatineau-housing-rising-fastest-clip-canada-royal-lepage (accessed Jun. 02, 2022).

[7] I. Hamilton, H. Kennard, O. Rapf, J. Kockat, and S. Zuhaib, "2021 Global Status Report for Buildings and Construction," Paris, Oct. 2021. Accessed: May 23, 2022. [Online]. Available: https://globalabc.org/resources/publications/2021-global-status-report-buildings-and-construction

[8] "Greenhouse gas sources and sinks in Canada: executive summary 2022 - Canada.ca," Ottawa, 2022. Accessed: May 23, 2022. [Online]. Available: https://www.canada.ca/en/environment-climate-change/services/climate-change/greenhouse-gas-emissions/sources-sinks-executive-summary-2022.html

[9] F. Pomponi, *Embodied carbon in buildings: Measurement, management, and mitigation*. Springer International Publishing, 2018. doi: 10.1007/978-3-319-72796-7.

[10] X. Su, S. Tian, X. Shao, and X. Zhao, "Embodied and operational energy and carbon emissions of passive building in HSCW zone in China: A case study," *Energy Build*, vol. 222, p. 110090, Sep. 2020, doi: 10.1016/J.ENBUILD.2020.110090.

[11] M. C. Barma, R. Saidur, S. M. A. Rahman, A. Allouhi, B. A. Akash, and S. M. Sait, "A review on boilers energy use, energy savings, and emissions reductions," *Renewable and Sustainable Energy Reviews*, vol. 79, pp. 970–983, Nov. 2017, doi: 10.1016/J.RSER.2017.05.187.

[12] U. Berardi and S. Jones, "The efficiency and GHG emissions of air source heat pumps under future climate scenarios across Canada," *Energy Build*, vol. 262, p. 112000, May 2022, doi: 10.1016/J.ENBUILD.2022.112000.

[13] H. Stopps and M. F. Touchie, “Residential smart thermostat use: An exploration of thermostat programming, environmental attitudes, and the influence of smart controls on energy savings,” *Energy Build*, vol. 238, p. 110834, May 2021, doi: 10.1016/J.ENBUILD.2021.110834.

[14] C. Younes, C. A. Shdid, and G. Bitsuamlak, “Air infiltration through building envelopes: A review:,” *https://doi.org/10.1177/1744259111423085*, vol. 35, no. 3, pp. 267–302, Oct. 2011, doi: 10.1177/1744259111423085.

[15] H. R. Trechsel, “1.1 Overview and Introduction,” in *Moisture Analysis and Condensation Control in Building Envelopes*, Philadelphia, PA: ASTM, 2001, pp. 1–3. Accessed: May 26, 2022. [Online]. Available: https://app.knovel.com/hotlink/pdf/id:kt004K8KL8/moisture-analysis-condensation/preface

[16] J. A. Malik and S. Marathe, *Ecological and Health Effects of Building Materials*, 1st ed. Springer International Publishing, 2022. doi: 10.1007/978-3-030-76073-1.

[17] *National Energy Code of Canada for Buildings 2020*, 5th ed. Ottawa: National Research Council of Canada, 2022.

[18] B. Conley, “Thermal Evaluation of Vacuum Insulation Panels within Residential Building Envelopes,” Masters, Carleton University, 2017.

[19] “Details of the R-2000 Standard,” *Natural Resources Canada*, Jul. 01, 2012. https://www.nrcan.gc.ca/energy-efficiency/homes/professional-opportunities/become-energy-efficient-builder/details-the-r-2000-standard/20588 (accessed May 24, 2022).

[20] "About Passive House – Passive House Canada," *Passive House Canada*, 2022. https://www.passivehousecanada.com/about-passive-house/ (accessed May 24, 2022).

[21] "NetZero: future building standards," *Natural Resources Canada*, Jan. 02, 2020. https://www.nrcan.gc.ca/energy-efficiency/energy-efficiency-homes/buying-energy-efficient-new-home/netzero-future-building-standards/20581 (accessed May 24, 2022).

[22] B. John, *Canadian Wood-frame House Construction*, Third. Ottawa: Canada Mortgage and Housing Corporation, 2013.

[23] "CSA O141:05 (R2019) Softwood Lumber," 2019. Accessed: May 26, 2022. [Online]. Available: https://www.csagroup.org/store/product/2701157/

[24] *National Building Code of Canada 2020*, Fifteenth. Ottawa: National Research Council of Canada, 2020. Accessed: May 26, 2022. [Online]. Available: https://nrc.canada.ca/en/certifications-evaluations-standards/codes-canada/codes-canada-publications/national-building-code-canada-2020

[25] "Advanced Framing Construction Guide," Tacoma, WA, 2016. Accessed: May 25, 2022. [Online]. Available: www.CORRIM.org.

[26] Scot. Simpson, *Advanced framing methods : the illustrated guide to complex framing techniques, materials & equipment*. Kingston, MA: R.S. Means Co, 2002.

[27] "Advanced House Framing," *United States Department of Energy*, 2020. https://www.energy.gov/energysaver/advanced-house-framing (accessed May 25, 2022).

[28] J. Kosny, A. Asiz, I. Smith, S. Shrestha, and A. Fallahi, "A review of high R-value wood framed and composite wood wall technologies using advanced insulation techniques," *Energy Build*, vol. 72, pp. 441–456, Apr. 2014, doi: 10.1016/J.ENBUILD.2014.01.004.

[29] C. Campbell, "Durability Characterization of a High Performance Building Envelope with Vacuum Insulation Panels and Energy Recovery Ventilation," Carleton University, Ottawa, Ontario, 2021. doi: 10.22215/ETD/2021-14505.

[30] E. Cuce, P. M. Cuce, C. J. Wood, and S. B. Riffat, "Toward aerogel based thermal superinsulation in buildings: A comprehensive review," *Renewable and Sustainable Energy Reviews*, vol. 34, pp. 273–299, Jun. 2014, doi: 10.1016/J.RSER.2014.03.017.

[31] S. Brideau, "Innovative Insulation Materials Literature Review," Ottawa, ON, 2020.

[32] M. Ismaiel, Y. Chen, C. Cruz-Noguez, and M. Hagel, "Thermal resistance of masonry walls: a literature review on influence factors, evaluation, and improvement:," *https://doi-org.proxy.library.carleton.ca/10.1177/17442591211009549*, vol. 45, no. 4, pp. 528–567, May 2021, doi: 10.1177/17442591211009549.

[33] J. J. del Coz Díaz, P. J. García Nieto, A. M. Rodríguez, A. L. Martínez-Luengas, and C. B. Biempica, "Non-linear thermal analysis of light concrete hollow brick walls by the finite element method and experimental validation," *Appl Therm Eng*, vol. 26, no. 8–9, pp. 777–786, Jun. 2006, doi: 10.1016/J.APPLTHERMALENG.2005.10.012.

[34] M. Stanescu, S. Kajl, and L. Lamarche, "Study of potential nonconformities of a new recreation center building's envelope," *J Phys Conf Ser*, vol. 745, no. 3, Oct. 2016, doi: 10.1088/1742-6596/745/3/032036.

[35] B. Sadowska and P. Bieranowski, “Efficiency of Different Balcony Slab Modernization Method in Retrofitted Multi-Family Buildings,” *Energies 2021, Vol. 14, Page 6666*, vol. 14, no. 20, p. 6666, Oct. 2021, doi: 10.3390/EN14206666.

[36] “ASTM C177-19 Standard Test Method for Steady-State Heat Flux Measurements and Thermal Transmission Properties by Means of the Guarded-Hot-Plate Apparatus,” *ASTM*, 2019. https://www.astm.org/c0177-19.html (accessed May 29, 2022).

[37] *ASTM C1363-19: Standard Test Method for Thermal Performance of Building Materials and Envelope Assemblies by Means of a Hot Box Apparatus*, 2019th ed. West Conshohocken, PA: ASTM International, 2019. Accessed: May 04, 2022. [Online]. Available: https://www.astm.org/c1363-19.html

[38] K. Janampa, O. Cerón, O. Morales, and J. Oré, “Thermal characterization of materials used in rural housing constructions in Ayacucho, Peru,” *J Phys Conf Ser*, vol. 1433, no. 1, Jan. 2020, doi: 10.1088/1742-6596/1433/1/012004.

[39] A. Elkholy and R. Kempers, “An accurate steady-state approach for characterizing the thermal conductivity of Additively manufactured polymer composites,” *Case Studies in Thermal Engineering*, vol. 31, p. 101829, Mar. 2022, doi: 10.1016/J.CSITE.2022.101829.

[40] S. Charca *et al.*, “Assessment of Ichu fibers as non-expensive thermal insulation system for the Andean regions,” *Energy Build*, vol. 108, pp. 55–60, Dec. 2015, doi: 10.1016/J.ENBUILD.2015.08.053.

[41] R. Salgado-Delgado *et al.*, “An Analysis of the Thermal Conductivity of Composite Materials (CPC-30R/Charcoal from Sugarcane Bagasse) Using the Hot Insulated Plate

Technique," *Advances in Materials Science and Engineering*, vol. 2016, 2016, doi: 10.1155/2016/4950576.

[42] A. Ricklefs, "Thermal Conductivity of Cementitious Composites Containing Microencapsulated Phase Change Materials," University of California, Los Angeles, Los Angeles, 2016.

[43] M. E. Somerford, "Modeling and measurements of a novel energy efficient masonry wall unit with significant mass and an integrated thermal barrier - ProQuest," Villanova University, Villanova, PA, 2014. Accessed: May 29, 2022. [Online]. Available: https://www.proquest.com/docview/1845865484?parentSessionId=YcthKypy%2BddL38SDGdxX6z1LQntlc7yEBIOhVLKyVXA%3D&pq-origsite=primo&accountid=9894

[44] V. Kodur, S. Venkatachari, V. A. Matsagar, and S. B. Singh, "Test Methods for Characterizing the Properties of Fiber-Reinforced Polymer Composites at Elevated Temperatures," *Polymers 2022, Vol. 14, Page 1734*, vol. 14, no. 9, p. 1734, Apr. 2022, doi: 10.3390/POLYM14091734.

[45] "ISO - ISO 8302:1991 - Thermal insulation — Determination of steady-state thermal resistance and related properties — Guarded hot plate apparatus," *International Standards Organization*, Aug. 1991. https://www.iso.org/standard/15422.html (accessed May 31, 2022).

[46] C. Baldwin, C. A. Cruickshank, A. Grin, and C. Schumacher, "Design and Development of a Two-Storey Guarded Hot Box and Pressurized Spray Rack," 2022.

[47] A. J. Holstein and D. R. Bohnhoff, "The design and fabrication of a Rotatable Guarded Hot Box (RGHB) capable of static pressure application," in *American Society of Agricultural*

and Biological Engineers Annual International Meeting 2013, ASABE 2013, Jul. 2013, vol. 1, pp. 237–257. doi: 10.13031/AIM.20131578832.

[48] T. v. Moore, C. A. Cruickshank, I. Beausoleil-Morrison, and M. Lacasse, "Thermal evaluation of a highly insulated steel stud wall with vacuum insulation panels using a guarded hot box apparatus:," *https://doi-org.proxy.library.carleton.ca/10.1177/1744259120980030*, vol. 45, no. 3, pp. 303–322, Dec. 2020, doi: 10.1177/1744259120980030.

[49] K. Tarabieh and A. Aboulmagd, "Thermal Performance Evaluation of Common Exterior Residential Wall Types in Egypt," *Buildings 2019, Vol. 9, Page 95*, vol. 9, no. 4, p. 95, Apr. 2019, doi: 10.3390/BUILDINGS9040095.

[50] L. Conti, M. Barbari, and M. Monti, "Steady-State Thermal Properties of Rectangular Straw-Bales (RSB) for Building," *Buildings 2016, Vol. 6, Page 44*, vol. 6, no. 4, p. 44, Oct. 2016, doi: 10.3390/BUILDINGS6040044.

[51] C. Magwood, "Opportunities for Carbon Capture and Storage in Building Materials," Trent University, Peterborough, 2019. Accessed: Mar. 27, 2022. [Online]. Available: https://www.chrismagwood.ca/uploads/1/5/9/3/15931000/magwood_opportunities_for_co2_capture_and_storage_in_building_materials_copy.pdf

[52] A. H. Landrock, "Handbook of plastic foams : types, properties, manufacture, and applications," p. 488, 1995.

[53] C. Mougel, T. Garnier, P. Cassagnau, and N. Sintes-Zydowicz, "Phenolic foams: A review of mechanical properties, fire resistance and new trends in phenol substitution," *Polymer (Guildf)*, vol. 164, pp. 86–117, Feb. 2019, doi: 10.1016/J.POLYMER.2018.12.050.

[54] R. Greenwald, "The aftermath of phenolic foam," *Professional Roofing Magazine*, Jan. 2005. https://www.professionalroofing.net/Articles/The-aftermath-of-phenolic-foam--01-01-2005/572 (accessed Mar. 29, 2022).

[55] "Kooltherm Safety Data Sheet," *Kingspan Insulation LLC*, no. 3. Kingspan Insulation LLC, Atlanta, Apr. 2020. Accessed: Mar. 29, 2022. [Online]. Available: https://ks-kentico-prod-cdn-endpoint.azureedge.net/kingspan-live/kingspanusa/media/kingspan-environmental/kooltherm-safety-data-sheet-2004.pdf?ext=.pdf

[56] S. Q. Zeng, A. J. Hunt, W. Cao, and R. Greif, "Pore Size Distribution and Apparent Gas Thermal Conductivity of Silica Aerogel," *J Heat Transfer*, vol. 116, no. 3, pp. 756–759, Aug. 1994, doi: 10.1115/1.2910933.

[57] Aspen Aerogel, "Spaceloft® Aerogel Blanket Insulation Technical Information," 2019. [Online]. Available: http://www.aerogel.com/_resources/common/images/photogalleries/2/photoalbums/2/images/Spaceloft-Grey-10mm-on-building-site-ready-to-fit.jpg

[58] R. W. Pekala, "Organic aerogels from the polycondensation of resorcinol with formaldehyde," *Journal of Materials Science 1989 24:9*, vol. 24, no. 9, pp. 3221–3227, Sep. 1989, doi: 10.1007/BF01139044.

[59] L. Hu, R. He, H. Lei, and D. Fang, "Carbon Aerogel for Insulation Applications: A Review," *Int J Thermophys*, vol. 40, p. 39, 123AD, doi: 10.1007/s10765-019-2505-5.

[60] M. Wiener, G. Reichenauer, S. Braxmeier, F. Hemberger, and H. P. Ebert, "Carbon Aerogel-Based High-Temperature Thermal Insulation," *International Journal of*

Thermophysics 2009 30:4, vol. 30, no. 4, pp. 1372–1385, Jun. 2009, doi: 10.1007/S10765-009-0595-1.

[61] Z. Yang *et al.*, "Synthesis of monolithic carbon aerogels with high mechanical strength via ambient pressure drying without solvent exchange," *J Mater Sci Technol*, vol. 50, pp. 66–74, Aug. 2020, doi: 10.1016/J.JMST.2020.02.013.

[62] C. Simón-Herrero, A. Romero, F. Dorado, I. Gracia, J. L. Valverde, and L. Sanchez-Silva, "Taylor-made aerogels through a freeze-drying process: economic assessment," *J Solgel Sci Technol*, vol. 89, no. 2, pp. 436–447, Feb. 2019, doi: 10.1007/S10971-018-4873-X/TABLES/10.

[63] D. W. Yarbrough, T. W. Petrie, D. Kinninger, and R. S. Graves, "Thermal Performance of Gas-Filled Panels with Reflective Surfaces Installed in an Attic," Dec. 2007.

[64] S. Shrestha, A. Desjarlais, and J. Atchley, "Thermal Performance Evaluation of Walls with Gas Filled Panel Insulation," Oak Ridge, Tennessee, Oct. 2014. Accessed: Apr. 10, 2022. [Online]. Available: https://info.ornl.gov/sites/publications/files/Pub52624.pdf

[65] G. Garside-Wight, "History of the world in 52 packs | 20. Polystyrene," *Packgaing News*, Dec. 22, 2015. https://www.packagingnews.co.uk/features/comment/history-of-the-world-in-52-packs-20-polystyrene-22-12-2015 (accessed Apr. 10, 2022).

[66] A. Blazejczyk, C. Jastrzebski, and M. Wierzbicki, "Change in Conductive–Radiative Heat Transfer Mechanism Forced by Graphite Microfiller in Expanded Polystyrene Thermal Insulation—Experimental and Simulated Investigations," *Materials 2020, Vol. 13, Page 2626*, vol. 13, no. 11, p. 2626, Jun. 2020, doi: 10.3390/MA13112626.

[67] "BASF Neopor® Plus GPS Above Grade Walls Product Brochure." BASF, Wyandotte, Michigan, 2015. Accessed: Apr. 10, 2022. [Online]. Available: https://neopor.basf.us/files/pdf/Neopor_Plus_GPS_2016_v3.pdf

[68] G. S. Jagdev and P. Mukhopadhyaya, "Temperature-Dependent Thermal Performance of Closed-Cell Foam Insulation Board in Roof Constructions," *Journal of Cold Regions Engineering*, vol. 34, no. 3, p. 04020016, Sep. 2020, doi: 10.1061/(ASCE)CR.1943-5495.0000215.

[69] J. Reignier, A. Sarbu, and V. Barraud, "Spontaneous formation of two-dimensional wrinkles in poly(urethane-isocyanurate) rigid foam boards:," *https://doi-org.proxy.library.carleton.ca/10.1177/0021955X19864396*, vol. 56, no. 3, pp. 297–315, Jul. 2019, doi: 10.1177/0021955X19864396.

[70] "JM Spray Polyurethane Foam (SPF)-Component A (USA and Canada) Safety Data Sheet," Denver, CO, Jul. 2019. Accessed: Apr. 11, 2022. [Online]. Available: https://www.jm.com/content/dam/jm/global/en/MSDS/200000001502_US_EN.pdf

[71] "JM Closed-cell Spray Polyurethane Foam (cc SPF)-Component B (USA) Safety Data Sheet," Denver, CO, Aug. 2019. Accessed: Apr. 11, 2022. [Online]. Available: https://www.jm.com/content/dam/jm/global/en/MSDS/200000000618_US_EN.pdf

[72] "GREAT STUFF™ Window and Door Insulating Foam Sealant Safety Data Sheet," Midland, MI, Nov. 2017. Accessed: Apr. 11, 2022. [Online]. Available: http://stolk.ca/wp-content/uploads/2018/05/Great-Stuff-Window-and-Door-insulating-foam-sealant-090003e8807e9c93.pdf

[73] K. Ghazi Wakili, R. Bundi, and B. Binder, "Effective thermal conductivity of vacuum insulation panels," *Building Research and Information*, vol. 32, no. 4, pp. 293–299, Jul. 2004, doi: 10.1080/0961321042000189644.

[74] H. J. Choi, H. Ahn, G. S. Choi, J. S. Kang, and J. H. Huh, "Analysis of long-term change in the thermal resistance of extruded insulation materials through accelerated tests," *Applied Sciences (Switzerland)*, vol. 11, no. 19, Oct. 2021, doi: 10.3390/APP11199354.

[75] D. Schroer, M. Hudack, M. Soderquist, and I. Beulich, "Rigid Polymeric Foam Boardstock Technical Assessment," 2012. Accessed: Apr. 12, 2022. [Online]. Available: https://app.knovel.com/hotlink/toc/id:kpO0NINE21/antec-2012-plastics-annual/antec-2012-plastics-annual

[76] "Kooltherm Premium Performance Rigid Thermoset Insulation," *Kingspan USA*, 2022. https://www.kingspan.com/us/en-us/product-groups/insulation/insulation-boards/kooltherm (accessed Apr. 12, 2022).

[77] "Open Versus Closed Cell Phenolic Foams," *Kingspan New Zealand*, Sep. 10, 2018. https://www.kingspan.com/nz/en-nz/products/insulation/knowledge-base/2019/open-versus-closed-cell-phenolic-foams (accessed Apr. 12, 2022).

[78] K. Nocentini, P. Achard, and P. Biwole, "Hygro-thermal properties of silica aerogel blankets dried using microwave heating for building thermal insulation," *Energy Build*, vol. 158, pp. 14–22, Jan. 2018, doi: 10.1016/J.ENBUILD.2017.10.024.

[79] S. Iswar, W. J. Malfait, S. Balog, F. Winnefeld, M. Lattuada, and M. M. Koebel, "Effect of aging on silica aerogel properties," *Microporous and Mesoporous Materials*, vol. 241, pp. 293–302, Mar. 2017, doi: 10.1016/J.MICROMESO.2016.11.037.

[80] R. Nosrati and U. Berardi, “Long-term performance of aerogel-enhanced materials,” *Energy Procedia*, vol. 132, pp. 303–308, 2017, doi: 10.1016/J.EGYPRO.2017.09.733.

[81] C. Chen and L. Hu, “Super Elastic and Thermally Insulating Carbon Aerogel: Go Tubular Like Polar Bear Hair,” *Matter*, vol. 1, no. 1, pp. 36–38, Jul. 2019, doi: 10.1016/J.MATT.2019.06.012.

[82] “Graphite Polystyrene (GPS) Rigid Insulation,” 2016.

[83] “Performance You Can Rely On: Smart Insulation by Neopor Plus GPS,” *BASF*, 2015. https://neopor.basf.us/files/pdf/Neopor_Plus_GPS_2016_v3.pdf (accessed Apr. 12, 2022).

[84] D. Belanger and U. Berardi, “The Impact of Aging on the Effective Thermal Conductivity of Foam Insulation: A Simulation Investigation Using Laboratory Characterization Data,” May 2018.

[85] “Owens Corning FOAMULAR C-300 XPS Insulation 24-inch x 96-inch x 2-inch Ship Lap Edge,” *The Home Depot Canada*. https://www.homedepot.ca/product/owens-corning-foamular-c-300-extruded-polystyrene-rigid-insulation-24-inch-x-96-inch-x-2-inch-ship-lap-edge/1000155124 (accessed Apr. 13, 2022).

[86] “DUROSPAN GPS R10 96-inch x 48-inch x 2.13-inch GPS Insulation Board ,” *The Home Depot Canada*. https://www.homedepot.ca/product/durospan-gps-r10-insulation-96x48x2-13/1001211235 (accessed Apr. 13, 2022).

[87] “IKO 1-in x 4-ft x 8-ft Polyisocyanurate Insulated Sheathing,” *Lowe’s Canada*. https://www.lowes.ca/product/foam-board-insulation/iko-1-in-x-4-ft-x-8-ft-polyisocyanurate-insulated-sheathing-337106 (accessed Apr. 13, 2022).

[88] “Spray Foam Insulation Cost in 2021,” *EcoStar Insulation Canada*. https://www.ecostarinsulation.ca/blog/spray-foam-insulation-cost (accessed Apr. 13, 2022).

[89] “Process Data Set: Vacupor® NT-B2-S Environmental Product Declaration,” Aug. 25, 2020. https://www.oekobaudat.de/OEKOBAU.DAT/datasetdetail/process.xhtml?uuid=2f301b5d-917e-4ca8-8f65-cb9f15064541&version=00.01.000 (accessed Apr. 17, 2022).

[90] G. R. Martin and T. P. Gloria, “Foamular XPS Insulation Environmental Product Declaration,” Toledo, OH, 2018.

[91] H. Peters and A. Röder, “Kingspan Kooltherm K5 Environmental Product Declaration,” Berlin, 2019.

[92] C. Hill, “Spaceloft Aerogel Insulation Environmental Product Declaration,” Northborough, MA, 2015.

[93] J. Oorbeck and J. Geibig, “Neopor® Plus Graphite Polystyrene Insulation Environmental Product Declaration,” Florham Park, NJ, 2018.

[94] “Polyurethane (PU) board: Foam without facing Environmental Product Declaration,” Brussels, Belgium, 2014.

[95] D. A. Kontogeorgos, G. K. Semitelos, I. D. Mandilaras, and M. A. Founti, “Experimental investigation of the fire resistance of multi-layer drywall systems incorporating Vacuum Insulation Panels and Phase Change Materials,” *Fire Saf J*, vol. 81, pp. 8–16, Apr. 2016, doi: 10.1016/J.FIRESAF.2016.01.012.

[96] “GreenGuard®/GreenGuard® LG XPS Insulation Board Safety Data Sheet,” Atlanta, GA, 2021.

[97] “Decabromodiphenyl ethane (DBDPE) - information sheet,” *Government of Canada*, Jun. 28, 2019. https://www.canada.ca/en/health-canada/services/chemical-substances/fact-sheets/chemicals-glance/decabromodiphenyl-ethane.html (accessed Apr. 17, 2022).

[98] M. Frederiksen, K. Vorkamp, J. B. Nielsen, L. S. Sørensen, T. F. Webster, and M. Vazakas, “Human exposure to novel flame retardants - from materials to humans,” Aug. 2014. Accessed: Apr. 17, 2022. [Online]. Available: https://vbn.aau.dk/en/publications/human-exposure-to-novel-flame-retardants-from-materials-to-humans

[99] “Aspen Aerogels Spaceloft® Safety Data Sheet,” Northborough, MA, 2015.

[100] “Technical Guidance Document: Spaceloft Aerogel Blanket Insulation,” Northborough, MA, 2015.

[101] “NEOPOR KF2300 Safety Data Sheet,” Florham Park, NJ, 2017.

[102] “ISO-HT Polyisocyanurate Safety Data Sheet (SDS),” *DYPLAST PRODUCTS, LLC*, 2015. https://www.dyplastproducts.com/msds-isoht (accessed Apr. 17, 2022).

[103] “Code Requirements - R Values,” *Canadian Wood Council*, 2017. https://cwc.ca/en/design-tools/effective-r-calculator/code-requirements/ (accessed Apr. 19, 2022).

[104] “Let-In 1x4 Shear Bracing - GreenBuildingAdvisor,” *Green Building Advisor*, 2021. https://www.greenbuildingadvisor.com/cad/detail/let-in-1x4-shear-bracing (accessed Jul. 13, 2022).

[105] "Tables for Calculating Effective Thermal Resistance of Opaque Assemblies," *Natural Resources Canada*, Feb. 23, 2016. https://www.nrcan.gc.ca/energy/efficiency/housing/new-homes/energy-starr-new-homes-standard/tables-calculating-effective-thermal-resistance-opaque-assemblies/14176 (accessed Apr. 21, 2022).

[106] S. W. Churchill and H. H. S. Chu, "Correlating equations for laminar and turbulent free convection from a vertical plate," *Int J Heat Mass Transf*, vol. 18, no. 11, pp. 1323–1329, Nov. 1975, doi: 10.1016/0017-9310(75)90243-4.

[107] R. Mitchell *et al.*, "THERM 6.3 / WINDOW 6.3 NFRC Simulation Manual," Berkley, Jul. 2013. Accessed: Apr. 25, 2022. [Online]. Available: http://windows.lbl.gov/software/software.html

[108] Thomas. Blomberg, "Heat conduction in two and three dimensions: computer modelling of building physics applications," Lund University, Lund, 1996. Accessed: Apr. 26, 2022. [Online]. Available: https://portal.research.lu.se/en/publications/heat-conduction-in-two-and-three-dimensions-computer-modelling-of

[109] S. D. Gatland, A. N. Karagiozis, and S. Glass, "ANSI/ASHRAE Addendum e to ANSI/ASHRAE Standard 160-2009 Criteria for Moisture-Control Design Analysis in Buildings ," Atlanta, Nov. 2016. Accessed: Apr. 28, 2022. [Online]. Available: www.ashrae.org

[110] A. Hukka and H. A. Viitanen, "A mathematical model of mould growth on wooden material," *Wood Sci Technol*, vol. 33, no. 6, pp. 475–485, 1999, doi: 10.1007/S002260050131.

[111] "Weather Data Center," *The American Society of Heating, Refrigerating and Air-Conditioning Engineers*, 2022. https://www.ashrae.org/technical-resources/bookstore/weather-data-center (accessed Jul. 13, 2022).

[112] C. Baldwin, C. A. Cruickshank, M. Schiedel, and B. Conley, "Comparison of Steady-state and In-situ Testing of High Thermal Resistance Walls Incorporating Vacuum Insulation Panels," *Energy Procedia*, vol. 78, pp. 3246–3251, Nov. 2015, doi: 10.1016/J.EGYPRO.2015.11.690.

Appendix A: Isothermal Planes Method

The isothermal planes method is a simple approach for the thermal resistance evaluation of wall assemblies by simplification to a one-dimensional thermal circuit. In this approach, each wall layer's thermal resistance is added together. Homogeneous layers are simply added, whereas layers which are not homogeneous – that is, the layer contains materials of dissimilar thermal properties – must be combined in parallel. This approach is illustrated below for the rigid exterior insulation concept.

The following diagram lists and colour codes the individual layers in the wall concept.

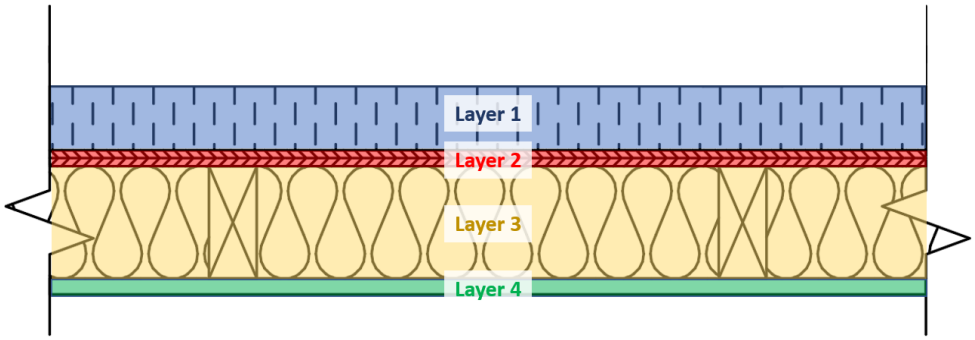

Figure A-1: Layers Present in an Isothermal Planes Method Evaluation

The layers are as follows:

- **Layer 1**: 6.35 cm (2.5-in) of phenolic foam insulation with a thermal resistivity of 52.0 m·K/W
- **Layer 2**: 1.27 cm (1/2-in) of plywood sheathing with a thermal resistivity of 8.7 m·K/W
- **Layer 3**: 8.89 cm (3.5-in) of studs (8.7 m·K/W) and batt insulation (24.3 m·K/W). The stud spacing is 40.64 cm (16-in) so there is one 3.81 cm (1.5-in) wide stud for every 40.64 cm length, with the rest occupied by batt insulation, so the cross-sectional area ratio of the stud is 0.094.

- **Layer 4**: 1.27 cm (1/2-in) of gypsum drywall with a thermal resistivity of 6.2 m·K/W

The overall effective thermal resistance of the wall based on the isothermal planes method is thus:

$$R_{eff} = R_1 + R_2 + R_3 + R_4 \qquad (A\text{-}1)$$

$$R_{eff} = r_1 * l_1 + r_2 * l_2 + \frac{l_3}{\frac{A_{stud}}{r_{batt}} + \frac{A_{batt}}{r_{batt}}} + r_4 * l_4$$

$$R_{eff} = 52 * 0.0635 + 8.2 * 0.0127 + \frac{0.0889}{\frac{0.094}{8.7} + \frac{0.906}{24.3}} + 6.2 * 0.0127$$

$$R_{eff} = 5.33\ m \cdot K/W \quad (R - 30.28)$$

The same approach is used for the calculation of the other concepts.

Appendix B: THERM Temperature Gradients

The following are screen captures of the temperature gradient graphs produced by LBNL THERM for the modelled wall assemblies, providing a better understanding of the potential thermal bridges through the structural members of each wall. Each model incorporated the boundary conditions presented in Table 5-2.

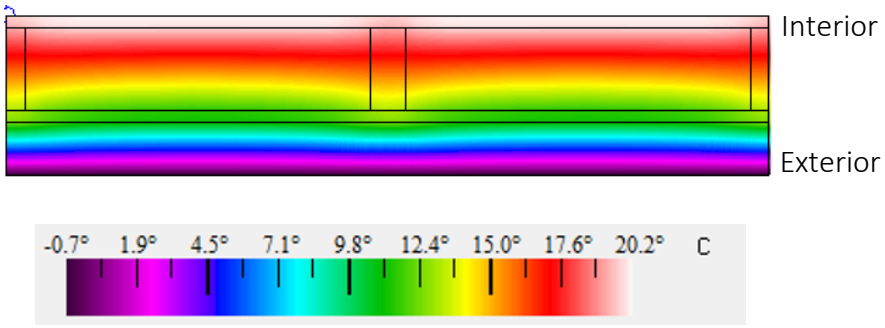

Figure B-1: Rigid Exterior Insulation Concept Temperature Gradient

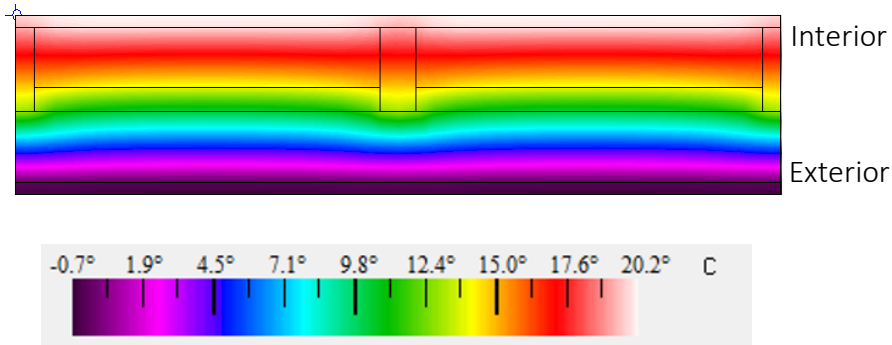

Figure B-2: Rigid Insulation with Stud Grooves Concept Temperature Gradient

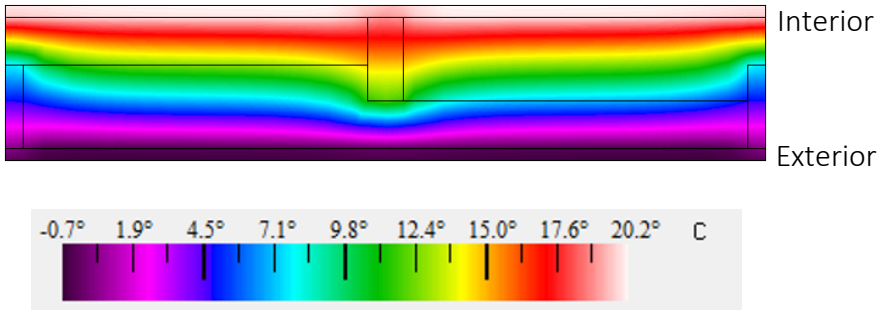

Figure B-3: Offset-framed Wall with L-shaped Insulation Concept Temperature Gradient

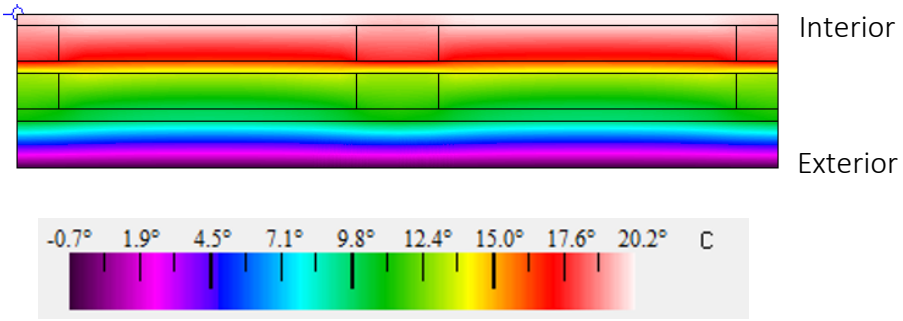

Figure B-4: Continuous Aerogel Insulation Concept Temperature Gradient

Appendix C: WUFI Pro Inputs

The table below provides a summary of the common layers across the thickness of the walls in the WUFI Pro 7 simulations.

Table C-1: Layer Properties for WUFI Simulation

Layer Width (m)	Layer Description
0.0105	Composite Wood Siding with cladding rain penetration of 1% of rain load
0.01	Air Layer 10 mm without additional moisture capacity, 20 ACH with left
0.001	Delta VENT-S WRB
0.003125	OSB; Rain Penetration Moisture Source on exterior element; 0.01% rain load
0.00625	OSB
0.003125	OSB
0.005	Air Layer 5 mm without additional moisture capacity, 10 ACH with left
0.005	Air Layer 5 mm without additional moisture capacity, 10 ACH with right
0.089	Low Density Glass Fiber Batt Insulation
0.001	PE-Membrane (Poly; 0.07 perm)
0.0125	Gypsum Board (USA)

The following table presents additional settings common to all simulations.

Table C-2: Additional WUFI Settings

Parameter	Description
Grid	300
Orientation	Based on highest driving rain sum using Climate Analysis
Exterior surface	Heat resistance: 0.03 m^2K/W
Interior surface	Heat resistance: 0.12 m^2K/W, latex paint sd-value: 0.7
Initial moisture	Typical build-in in each layer
Initial temperature	0 degrees
Calculation period	3 years (2021-01-01 to 2024-01-01)
Outdoor climate	ASHRAE Year 2
Indoor climate	ASHRAE 160, Heating only, 21 degree heating setpoint, 2 bedrooms